Iowa State University
Digital Repository

Retrospective Theses and Dissertations

Iowa State University Capstones, Theses and Dissertations

1986

Pulsed Amperometric Detection of sulfur compounds at noble metal electrodes in aqueous solutions

Theresa Z. Polta
Iowa State University

Follow this and additional works at: https://lib.dr.iastate.edu/rtd

Part of the Analytical Chemistry Commons

Recommended Citation

Polta, Theresa Z., "Pulsed Amperometric Detection of sulfur compounds at noble metal electrodes in aqueous solutions" (1986). *Retrospective Theses and Dissertations*. 8290.
https://lib.dr.iastate.edu/rtd/8290

This Dissertation is brought to you for free and open access by the Iowa State University Capstones, Theses and Dissertations at Iowa State University Digital Repository. It has been accepted for inclusion in Retrospective Theses and Dissertations by an authorized administrator of Iowa State University Digital Repository. For more information, please contact digirep@iastate.edu.

المنارة للاستشارات

www.manaraa.com

INFORMATION TO USERS

While the most advanced technology has been used to photograph and reproduce this manuscript, the quality of the reproduction is heavily dependent upon the quality of the material submitted. For example:

- Manuscript pages may have indistinct print. In such cases, the best available copy has been filmed.
- Manuscripts may not always be complete. In such cases, a note will indicate that it is not possible to obtain missing pages.
- Copyrighted material may have been removed from the manuscript. In such cases, a note will indicate the deletion.

Oversize materials (e.g., maps, drawings, and charts) are photographed by sectioning the original, beginning at the upper left-hand corner and continuing from left to right in equal sections with small overlaps. Each oversize page is also filmed as one exposure and is available, for an additional charge, as a standard 35mm slide or as a 17"x 23" black and white photographic print.

Most photographs reproduce acceptably on positive microfilm or microfiche but lack the clarity on xerographic copies made from the microfilm. For an additional charge, 35mm slides of 6"x 9" black and white photographic prints are available for any photographs or illustrations that cannot be reproduced satisfactorily by xerography.

8703749

Polta, Theresa Z.

PULSED AMPEROMETRIC DETECTION OF SULFUR COMPOUNDS AT NOBLE METAL ELECTRODES IN AQUEOUS SOLUTIONS

Iowa State University PH.D. 1986

University
Microfilms
International 300 N. Zeeb Road, Ann Arbor, MI 48106

Pulsed Amperometric Detection of sulfur compounds at noble metal electrodes in aqueous solutions

by

Theresa Z. Polta

A Dissertation Submitted to the
Graduate Faculty in Partial Fulfillment of the
Requirements for the Degree of
DOCTOR OF PHILOSOPHY

Department: Chemistry
Major: Analytical Chemistry

Approved:

Signature was redacted for privacy.

In Charge of Major Work

Signature was redacted for privacy.

For the Major Department

Signature was redacted for privacy.

For the Graduate College

Iowa State University
Ames, Iowa

1986

TABLE OF CONTENTS

I. INTRODUCTION 1

II. LITERATURE REVIEW 3

A. Electrochemical Oxidation of Low Molecular Weight Sulfur Compounds 3

1. Detection at platinum electrodes 3

2. Detection at carbon electrodes 17

3. Detection at mercury electrodes 21

4. Detection at gold electrodes 23

B. Electrochemical Oxidation of Boron Polyhedral Anions 27

C. High Performance Liquid Chromatography of Selected Sulfur Compounds 29

D. Pulsed Amperometric Detection 32

III. EXPERIMENTAL 37

A. Chemicals 37

B. Instrumentation 37

1. Voltammetric studies 37
a. Electrodes, rotator and recorder 37
b. Potentiostats 38

2. Flow-injection 38
a. Electrodes 38
b. Injection system, potentiostat and recorder 41

3. High performance liquid chromatography 44

IV. PULSED AMPEROMETRIC DETECTION OF SULFUR COMPOUNDS AT PLATINUM ELECTRODES IN ALKALINE SOLUTION 46

A. Cyclic Voltammetry 46

B. Pulsed Amperometric Detection 52

C. Flow-injection Analysis 58

V. THE DEPENDENCE OF RESPONSE ON ADSORPTION TIME FOR PULSED AMPEROMETRIC DETECTION OF SULFUR COMPOUNDS 66

A. Theory 66

1. Adsorption with no concentration polarization 66

2. Adsorption with concentration polarization 69

B. Adsorption Equilibrium Constant 71

C. Variation of Adsorption Time 74

D. Analytical Calibration in PAD 83

VI. PULSED AMPEROMETRIC DETECTION OF INORGANIC SULFUR COMPOUNDS AT GOLD ELECTRODES IN ALKALINE SOLUTION 87

A. Cyclic Voltammetry 87

B. Calibration 94

C. Liquid Chromatography 94

VII. PULSED AMPEROMETRIC DETECTION OF ORGANIC SULFUR COMPOUNDS AT GOLD ELECTRODES IN AQUEOUS SOLUTIONS 103

A. Cyclic Voltammetry 103

B. Pulsed Amperometric Detection 108

C. Dependence of Response on Adsorption Time 114

D. Flow-Injection Analysis 121

E. Liquid Chromatography 121

VIII. PULSED AMPEROMETRIC DETECTION OF SULFUR CONTAINING BORON POLYHEDRALS AT GOLD ELECTRODES IN AQUEOUS SOLUTIONS 141

A. Introduction 141

B. Cyclic Voltammetry 144

C. Calibration 152

D. Liquid Chromatography 152

IX. CONCLUSIONS 158

X. FUTURE RESEARCH 160

XI. BIBLIOGRAPHY 162

XII. ACKNOWLEDGEMENTS 175

XIII. APPENDIX 177

LIST OF FIGURES

Figure III-1. Dionex flow-through cell 39

Figure III-2. Au flow-through cell 42

Figure IV-1. Current-potential curves for thiourea at a Pt RDE by cyclic voltammetry in 0.25 M NaOH 48

Figure IV-2. Current-time curves for thiourea at a Pt RDE in 0.25 M NaOH 53

Figure IV-3. Current-potential curves for thiourea at Pt by pulsed voltammetry in 0.25 M NaOH 56

Figure IV-4. Detection peaks for thiourea in 0.25 M NaOH by FI/PAD 59

Figure IV-5. Calibration curves (I_p vs. C) for thiourea in 0.25 M NaOH by FI/PAD 61

Figure IV-6. Calibration curves ($1/I_p$ vs. 1/C) for thiourea in 0.25 M NaOH by FI/PAD 64

Figure V-1. Calibration data for thiourea in 0.25 M NaOH by FI/PAD 72

Figure V-2. Dependence of response for thiourea in 0.25 M NaOH on t_{ads} 75

Figure V-3. Plot of log ($-I_p/\mu A$) vs. log (t_{ads}/ms) for regions A and B of Figure V-2 77

Figure V-4. Numerical solutions in data from Figure V-2 81

Figure V-5. Plots of log ($-I_p/\mu A$) vs. log (C^b/M) for thiourea in 0.25 M NaOH 84

Figure VI-1. Current-potential curves for thiosulfate at a Au RDE by cyclic voltammetry in 0.25 M NaOH 88

Figure VI-2. Current-potential curves for sulfide at a Au RDE by cyclic voltammetry in 0.25 M NaOH 91

Figure VI-3. Chromatogram of sulfide, sulfite and thiosulfate 97

Figure VI-4. Chromatogram of sulfide, sulfite and thiosulfate using PAD 99

Figure VI-5. Calibration curves (I_p vs. C^b) for sulfide, sulfite and thiosulfate by HPLC/PAD 101

Figure VII-1. Current-potential curves for thiourea at a Au RDE by cyclic voltammetry in 0.25 M NaOH 105

Figure VII-2. Current-time curves for thiourea at a Au RDE in 0.25 M NaOH 109

Figure VII-3. Current-potential curves for thiourea at Au by pulsed voltammetry in 0.25 M NaOH 112

Figure VII-4. Dependence of current response for thiourea in 0.25 M NaOH on t_{ads} 115

Figure VII-5. Dependence of fractional surface coverage for thiourea in 0.25 M NaOH on t_{ads} 118

Figure VII-6. Detection peaks for thiourea in 0.25 M NaOH by FI/PAD 122

Figure VII-7. Chromatogram of thioureas and thioacetamide using PAD 125

Figure VII-8. Chromatogram of thiosemicarbazide and thionicotinamide using PAD 128

Figure VII-9. Chromatogram of thiophenes using PAD 130

Figure VII-10. Calibration curves (I_p vs. C^b) for thiophenes using HPLC with PAD 134

Figure VII-11. Chromatogram of dithiocarbamates using PAD 137

Figure VII-12. Calibration curves (I_p vs. C^b) for dithiocarbamates using HPLC with PAD 139

Figure VIII-1. Current-potential curves for $B_{12}H_{11}SH^{2-}$ at a Au RDE by cyclic voltammetry in NH4PF6 adjusted to neutral pH 145

Figure VIII-2. Current-potential curves for $B_{12}H_{11}SSH_{11}B_{12}^{4-}$ at a Au RDE by cyclic voltammetry in NH_4PF_6 adjusted to neutral pH 147

Figure VIII-3. Current-potential curves for $B_{12}H_{11}S(O)SH_{11}B_{12}^{4-}$ at a Au RDE by cyclic voltammetry in NH_4PF_6 adjusted to neutral pH 149

Figure VIII-4. Calibration curves (I_p vs. C^b) for sulfur containing boron polyhedrals in NH_4PF_6, adjusted to neutral pH, by FI/PAD 153

Figure VIII-5. Chromatogram of sulfur containing boron polyhedrals using PAD 156

LIST OF TABLES

Table II-1. Thiophene Structures 19

Table II-2. Boron Structures 28

Table III-1. Pine Electrodes 37

Table IV-1. Representative sulfur compounds detected by PAD in alkaline media 47

Table VII-1. Representative organic sulfur compounds detected by PAD in alkaline media 104

Table VII-2. Metal ions complexed by the diethyldithiocarbamate anion 133

Table VII-3. Metal ions complexed by dithiocarbamates 133

Table VIII-1. Structures of sulfur containing boron polyhedrals 143

I. INTRODUCTION

During the last two decades, the need for inexpensive, economical fuel cells produced a strong interest in the electrochemical oxidation of organic substances. These studies were motivated by the lack of understanding of oxidation pathways for organic compounds at solid electrodes. Many organic materials were studied extensively, with the notable exception of those containing sulfur. Some reviews (1,2) on the electrochemical oxidation of organic compounds were published which contain no references to the oxidation of organic compounds containing sulfur atoms. Other reviews (3,4) have been published which contain only short sections devoted to this topic. Recently, however, several reviews (5,6) of electrochemical oxidation of organic compounds have been published which recognize the importance of the literature on the oxidation of sulfur containing substances and contain many pages on this subject.

The loss of activity for noble-metal electrodes due to adsorbed carbonaceous radicals and polymeric films has been observed for most organic compounds, with the most severe loss of activity observed for sulfur compounds (7). To alleviate this problem, Fahidy et al. (8,9) devised solid electrodes with continuous reactivation of the anode surface through the use of wiper-blades. In addition to the above method, periodic polarity-reversal techniques have long been known to condition the electrode surface and reactivate it after passivation has occurred.

The intent of this work is to show that Pulsed Amperometric Detection (PAD) can be successfully applied for the electroanalytical determinations of sulfur containing compounds at noble metal electrodes in aqueous solutions. This detection technique will then be incorporated with flow-injection (FI) and high performance liquid chromatography (HPLC) techniques in order to show its suitability for monitoring effluent streams containing the compounds of interest.

II. LITERATURE REVIEW

A. Electrochemical Oxidation of Low Molecular Weight Sulfur Compounds

1. Detection at platinum electrodes

The first reports of anodic oxidation of simple organic sulfides at platinum (Pt) were made by Nicholson (10,11) in the mid-1950s. She demonstrated that alkyl sulfides are electrochemically active and can be irreversibly oxidized at 0.8 - 1.0 V on a platinum working electrode in methanolic HCl. It was noted that reproducible current-voltage (I-E) curves were obtained only after the electrode potential had been cycled between the limits for anodic and cathodic solvent decomposition for several minutes prior to each recorded scan. Although aliphatic sulfides gave anodic currents suitable for analytical quantitation, the current due to oxidation of chloride (Cl^-) obscured any peak for oxidation of aryl sulfides.

A voltammetric procedure for the estimation of aliphatic sulfides also was described by Drushel and Miller (12,13). They studied the sulfur compounds found in petroleum fractions, at stationary platinum wire electrodes preconditioned with an ac voltage operating at 1000 Hz prior to the recording of each I-E curve. Cyclic and noncyclic alkyl sulfides and alkyl aryl sulfides were quantitatively determined based on the voltammetric measurements.

Houghton and Humffray investigated the anodic oxidation of diaryl sulfides and determined that single-sweep voltammetry was a valid technique for electroanalysis in acid media, provided halide ions were absent. It was shown (14,15) that controlled-potential oxidation of diphenyl sulfide at a platinum anode in the presence of perchlorate, sulfate or chloride ions produces diphenyl sulfoxide in near quantitative yield. Dibenzothiophene was investigated under similar conditions (16) and conversion to the 5-oxide was shown to be quantitative. Imberger and Humffray (17) completed the study of aryl sulfides with the anodic oxidation of thianthrene. At 1.6 V in the presence of perchlorate ion, thianthrene gives a mixture of products consisting of the _cis_-dioxide, _trans_-dioxide, sulfone, trioxide and tetraoxide.

After these initial studies, interest turned to the electrochemical reactions taking place on platinum electrodes covered with adsorbed sulfur or sulfur dioxide. Seo and Sawyer (18,19) developed a voltammetric method for the determination of total sulfite in sulfuric acid solutions using activated platinum electrodes. In addition, they postulated that two oxidative processes occur: first, a purely electrochemical electron-transfer process which occurs at potentials less positive than required for oxide formation; and second, a chemical reaction between anodically formed oxide and the sulfite species which occurs in the potential region for oxide formation.

In addition to the direct electrochemical detection of sulfur on platinum, the electrocatalytic effect of chemisorbed sulfur has also been examined. Binder, Koehling and Sandstede (20-26) studied the effect of sulfur on the electro-oxidation of some organic compounds. They found that a complete coverage of the surface of a platinum electrode with sulfur considerably increases the activity of the electrode towards the oxidation of carbon monoxide. However, in the anodic oxidation of formic acid a maximal increase of the stationary current was obtained when only one third of the electrode surface was covered with sulfur. At complete coverage of the electrode surface with sulfur, the electro-oxidation of formic acid was suppressed.

A study of the kinetics of adsorption and oxidation of sulfur at platinum electrodes in aqueous solutions was then begun by Weber and Loucka (27) and further investigated by Loucka (28-31). They proposed that during the adsorption of sulfur, surface atoms were removed from the platinum crystal lattice, exposing a sub-surface layer upon which a reactive oxide forms. This oxide was then concluded to participate in the oxidation of elementary sulfur to sulfur(VI). Najdeker and Bishop (32) reviewed the evidence presented by Loucka and suggested that the formation of platinum(IV) sulfide provided a better basis for interpreting the electrochemical processes on platinum in aqueous solutions containing hydrogen sulfide. This theory was seemingly verified by Ramasubramanian (33) using electron diffraction. He confirmed the presence of PtS in the anodic films which resulted at sufficiently positive potentials (>1.3 V) in sulfuric acid solutions saturated with H_2S.

Another theory, however, was suggested by Jayaram et al. (34), and Contractor and Lal (35-37) to describe the processes which occur at the electrode surface upon adsorption of sulfur. They studied both adsorbed sulfur and sulfur dioxide on platinum and proposed that sulfur is chemisorbed in two forms of a sulfoxide on the electrode surface. These two forms of adsorbed sulfur should be distinguishable by the number of platinum sites occupied per sulfur atom. The formation of an adsorbed sulfur layer from SO_2 was suggested to occur through the following reactions:

$$SO_2 + 2H^+ + 2e^- \longrightarrow \underset{**}{SO} + H_2O \qquad [1]$$

$$SO_2 + 2H^+ + 2e^- \longrightarrow \underset{*}{SO} + H_2O \qquad [2]$$

$$\underset{**}{SO} + 2H^+ + 2e^- \longrightarrow \underset{**}{S} + H_2O \qquad [3]$$

$$\underset{*}{SO} + 2H^+ + 2e^- \longrightarrow \underset{*}{S} + H_2O \qquad [4]$$

$$\underset{**}{S} + SO_2 + 4H^+ + 4e^- \longrightarrow \underset{**}{S_2} + 2H_2O \qquad [5]$$

$$\underset{*}{S} + SO_2 + 4H^+ + 4e^- \longrightarrow \underset{*}{S}_2 + 2H_2O \qquad [6]$$

with species formed in reactions [1] and [2] being represented as:

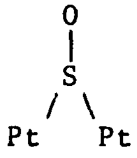

**

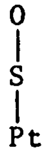

*

The electrochemical oxidation of sulfur dioxide on platinum electrodes was also taken up by Comtat and Mahenc (38). These authors showed that two oxidation waves existed, both apparently diffusion limited, the first of which was attributed to a purely electrochemical step of the redox type involving two electrons, and the second being a reaction in which adsorbed oxygen on platinum participates. It was suggested, however, by Appleby and Pichon (39), and Audry and Voinov (40), that the oxidation of SO_2 proceeds through the intermediate formation of dithionic acid:

$$2SO_2 + 2H_2O \longrightarrow H_2S_2O_6 + 2H^+ + 2e^- \qquad [7]$$

The basis for this assumption was the bimolecular order of the reaction in concentrated sulfuric acid. Kazarinov (41) and Tarasevich et al. (42) refuted this theory with radioisotopic and voltammetric studies of SO_2 on platinum in sulfuric acid. They found that at all pH values, SO_2 electro-oxidation proceeds to H_2SO_4 without intermediate formation of dithionic acid.

Szklarczyk, Czerwinski and Sobkowski (43) summarized the above work on chemisorbed sulfur on platinum and continued to investigate the electrode processes of sulfur dioxide on platinum electrodes by potentiodynamic and radiometric methods. They concluded that the product of SO_2 adsorption is sulfur and that it is oxidized stepwise to sulfate ions during anodic polarization. No mechanism was proposed to substantiate this claim.

Recently, Spotnitz et al. (44-46) studied the behavior of sulfur dioxide in sulfuric acid solutions at a platinum rotating disk electrode. It was observed that cycling the potential in these solutions between ca. -0.10 and 1.2 V (vs. SCE) resulted in activation of the electrode so that diffusion-controlled SO_2 oxidation currents could be obtained in the double layer region of platinum ($E = 0.3$ to 0.6 V). Without activation, SO_2 oxidation proceeds noticeably only in the potential region of surface oxide formation. The formation of sulfur oxides through oxidation of adsorbed sulfur and the formation of platinum oxides were noted to complicate the voltammetric behavior of the system.

The electrochemical oxidation of cysteine and related compounds has also been investigated systematically. Davis and Bianco (47) showed the necessity of a special ac voltage pretreatment to obtain reproducible I-E curves and they concluded that the main detection process was a one electron oxidation to form the disulfide, cystine. However, the electrode reaction was found to be strongly suppressed by the oxide film (PtO) formed on the electrode surface.

The common sulfur amino acids were also studied by several Czechoslovakian researchers (48-52) and the following conclusions were made: first, neither cysteine nor cystine change their oxidation state upon adsorption at a platinum electrode; second, there are two adsorbed species for cysteine-one strongly adsorbed, the other one weakly adsorbed; third, compared with the adsorption of cysteine or cystine, the adsorption of glutathione is weaker; fourth, the oxidation of dissolved cysteine takes place via the weakly adsorbed species; fifth, the overall oxidation of cysteine involves the transfer of one electron, while the detailed mechanism requires an oxidation by splitting off two electrons followed by a subsequent ion-substrate dimerization reaction; and lastly, the final oxidation product of both adsorbed cysteine and cystine was proposed to be cysteic acid, while glutathione is oxidized only to the dimerization product. Recently, Reddy and Krishnan (53,54) confirmed these findings.

Kuz'mina and Songina (55) studied the oxidation of thiourea at a rotating platinum electrode in solutions of oxygen containing acids and in deoxygenated hydrochloric acid in order to develop a voltammetric method for the determination of thiourea. They proposed that the oxidation was stepwise, with the electrode oxidation step first, followed by a further oxidation with the participation of oxygen.

The coulometric oxidation of thiourea and related compounds was studied at constant potential by Santhanam and Krishnan (56,57). It was found that on platinum electrodes in acid media the oxidation of thiourea involved a reversible one electron process, but that in basic solution no coulometric determination could be made due to passivation of the electrode surface. Other compounds investigated included phenylthiourea and thioglycollic acid, which were studied only at low pH values. For phenylthiourea, the oxidation process was shown to involve a single electron per molecule of reactant with the product being the disulfide. The oxidation of thioglycollic acid, however, was found to proceed as a two electron process, probably with a thionyl sulfoxide as the product.

The above study was extended by Reddy and Krishnan in an attempt to elucidate the mechanism of oxidation for thiourea (58,59) and phenylthiourea (60). They proposed the overall oxidation reaction for thiourea to be

$$2(NH_2)_2CS \longrightarrow H_2NC(NH)SSC(NH)NH_2 + 2H^+ + 2e^- \qquad [8]$$

with the rate determining step being the formation of a free radical, followed by the combination of two free radicals to form formamidine disulfide. Unlike the conclusions of Santhanam and Krishnan, however, these authors proposed that the oxidation of thiourea on platinum is an irreversible process. On the other hand, all of the results reported by Santhanam and Krishnan on the electrochemical oxidation of phenylthiourea were verified by Reddy and Krishnan using cyclic voltammetry, chronoamperometry and potentiostatic steady-state techniques.

Other investigations into the mechanism and products of oxidation of thiourea and related compounds were conducted during the early and mid-1970s. Gorbachev et al. (61) confirmed the overall reaction scheme to be that which was proposed by Reddy and Krishnan, but these authors suggested the rate limiting step to be the recombination of the adsorbed radicals to form formamidine disulfide. Maslii and Lupenko (62) studied the oxidation of thiourea on a platinum electrode in sulfuric acid over a wide range of potentials and determined that over the entire potential range, thiourea was oxidized with the formation of formamidine disulfide. Astruc et al. (63) were able to oxidize thiourea in non-aqueous solutions on a platinum electrode to the dithioformamidine salt. A related compound, dimethylolthiourea, was investigated by Sorokin (64). The oxidation of this compound was found to involve one electron and the rate was controlled by adsorption as well as diffusion.

Recently, Franklin and Iwunze (65) found that it was possible to electrochemically oxidize thiourea on platinum electrodes in strongly basic solutions provided a cationic surfactant (Hyamine 2389) was added to the aqueous solutions to form micelles. The Hyamine solubilized the product of the oxidation and prevented the electrode from becoming passivated. The oxidation was shown to be a one electron, irreversible, diffusion-controlled process producing formamidine disulfide. However, it was noted that the pH of the surfactant film on the anode was apparently not the pH of the bulk solution.

Other organic sulfur compounds which have received considerable attention include the diethyldithiocarbamate anion [I]

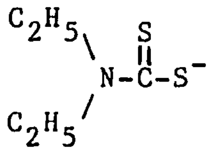

[I]

and its metal complexes. Usatenko and Tulyupa (66) were the first to study any of these compounds on platinum and established only that the oxidation of sodium diethyldithiocarbamate proceeds in two steps, the first being a one electron oxidation. This two step oxidation reaction was confirmed by Bessarabova et al. (67) and a mechanism proposed. They suggested that the first stage in the oxidation of [I] was its conversion to tetraethylthiuram disulfide [II]

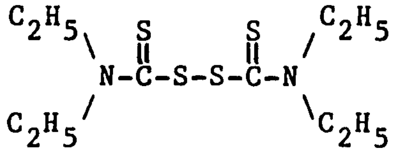

[II]

and that the second stage involved further oxidation to oxygen containing products, including sulfates, with the participation of oxygen adsorbed on the platinum electrode. The rate of the first stage was found to be diffusion-limited while the rate of the second stage was limited by the direct reaction of [I] and its intermediate oxidation products with adsorbed oxygen.

Usatenko and Galushko (68) continued the investigations and verified that the products of the first oxidation step of diethyldithiocarbamate is tetraethylthiuram disulfide, which results from the dimerization of the oxidation primary product. They also confirmed by infra-red spectra, the final presence of bis(diethylcarbamoyl) disulfide [III]

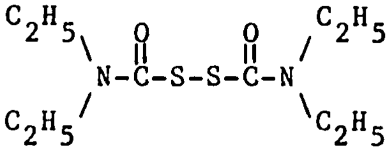

[III]

and SO_4^{2-}. Another study of the products of oxidation of [I] on platinum was made by Scrimager and DeHayes (69). These authors investigated the electrochemical behavior of the compound in acetonitrile and found the products obtained through successive oxidation of [I] to be [II] and the 3,5-bis(N,N-diethyliminum) trithiolane-1,2,4 dication [IV],

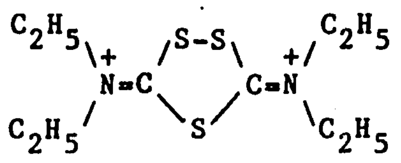

[IV]

although the stability of the latter compound was found to be limited and its reactivity was not explored.

Labuda et al. (70,71) characterized the voltammetric behavior of Cr(III) diethyldithiocarbamates as well as [I], [II], tetramethylthiuram monosulfide and other related compounds. It was again confirmed that the product of diethyldithiocarbamate oxidation is tetraethylthiuram disulfide. In addition, the further oxidation of [II] and the oxidation of tetramethylthiuram monosulfide were both shown to lead to the formation of derivatives of the trithiolane dication.

Unlike thiourea and the diethyldithiocarbamate anion, the electro-oxidation of dimethylsulfoxide (DMSO) has received little attention. Sobkowski and Szklarczyk (72) attempted to fill this void in their study of the adsorption and electrode reactions of DMSO. They determined that the adsorbed dimethylsulfoxide is reduced in two steps to dimethylsulfide in the hydrogen range of potentials and oxidized to dimethylsulfone above 0.6 V in sulfuric acid solution. The latter product was found to be desorbed from the electrode surface.

In addition to the numerous organic sulfur compounds whose electrochemical behaviors have been characterized by voltammetric methods, several inorganic compounds containing sulfur have been the subject of studies performed on platinum electrodes. The electro-oxidation of thiocyanate (SCN^-) on platinum in neutral and acidic aqueous media was first investigated by Songina and Pavlova in the early 1960s (73). They proposed that the oxidation of SCN^- proceeds in two steps: first, with the formation of thiocyanogen $(SCN)_2$, followed probably by a further chemical reaction between the product of the electrode process and the solvent to form sulfate.

In the early 1970s this subject again was taken up and an extensive series of reports were published (74-78). The anodic oxidation of SCN^- was examined under molten conditions and in solutions of DMSO and acetonitrile. It was determined that the anodic film formed at platinum electrodes upon oxidation of molten SCN^- was the polymer $(SCN)_x$, which caused passivation of the electrode surface. In DMSO and acetonitrile, the oxidation of SCN^- was shown to produce the SCN radical which stimulated dimerization to yield $(SCN)_2$. At this same time, Belyi et al. (79) carefully studied the electro-oxidation of SCN^- at a stationary platinum electrode at low temperatures in an unnamed solvent. The analysis of their results confirmed that SCN^- oxidation is a one step, irreversible process involving one electron per molecule of reactant. It was also noted that the simultaneous oxidation at the anode of SCN^- with the complex $[(SCN)_3]^-$ was possible.

Other inorganic sulfur compounds have been examined on platinum. Kuz'mina and Songina (80) studied the oxidation of sulfite (SO_3^{2-}), sulfide (S^{2-}) and thiosulfate ($S_2O_3^{2-}$) in oxygenated acid solutions. Yokosuka et al. (81,82) more closely examined the oxidation of thiosulfate and determined that during the oxidation of $S_2O_3^{2-}$ in alkaline solutions, SO_3^{2-} and trithionate were formed as intermediates before complete oxidation to SO_4^{2-} occurred. In neutral solutions, $S_2O_3^{2-}$ was converted to SO_4^{2-}, $S_2O_6^{2-}$, SO_3^{2-}, $S_3O_6^{2-}$ and $S_4O_6^{2-}$. The latter three intermediates were oxidized further and only SOH^{2-} and $S_2O_6^{2-}$ finally remained in solution.

The study of the oxidation of sulfide was extended by Kapusta et al. (83). They found that sulfide oxidation in alkaline solution results in the formation of a surface layer containing platinum (IV) sulfide and sulfur, which passivates the electrode. It was noted also that oxide formation is inhibited in sulfide solutions because of the competing adsorption of S^{2-} and OH^-, and that removal of the oxide film, by chemical dissolution in concentrated sulfide solutions, results in further sulfide oxidation during the negative potential scan.

Finally, the electrochemistry of polysulfide ions on platinum in dimethylacetamide (DMA) has been investigated by Paris and Plichon (84,85). Their study reported the stability of S_8^{2-} and $S_3^{\cdot -}$ polysulfide ions in electron pair donor solvents and concluded that S_3^{2-} and S_4^{2-} ions are more basic than S_8^{2-} in DMA, based on changes in voltammograms during the acidification of the solutions.

2. Detection at carbon electrodes

Although the largest number of electrochemical investigations of low molecular weight sulfur compounds has taken place for platinum electrodes, several examinations have also been taken up for carbon (C) electrodes. Zakharov et al. (86) examined the voltammetric behavior of thiourea at a graphite electrode and found that only the oxidation to its disulfide product is possible. The absence of evidence for the further oxidation of the disulfide to various oxygen containing products was explained by the very slight amounts of oxygen known to adsorb to graphite under anodic polarization, thus making oxygen containing oxidation products less likely to occur.

The oxidation of thiourea was also studied by Kirchnerova and Purdy (87,88) at glassy carbon electrodes in aqueous solutions containing acetonitrile. They found that the electro-oxidation of thiourea is a pH dependent, multistep process accomplished with adsorption. The first step was proposed to involve a one electron transfer to form a short-lived radical ion $[(NH_2)_2\text{-C-S}\cdot]^+$ which rapidly dimerized to C,C'-dithioformamidinum ion. Further oxidation steps were suggested involving not only electron transfer, but also hydration equilibria and H^+ and OH^- transfer. In strongly acidic solutions, the product of highest oxidation state appeared to be the diprotonated formamidine sulfonic acid, while in solutions of low acidity (pH 4-6), it appeared the final product was formamidine sulfinic acid.

Thiosemicarbazide and some related compounds have been studied by Lugovoi and Chernova (89) and Hofbauerova et al. (90,91). It was determined that the electrochemical oxidation at a graphite electrode in aqueous solution proceeds in two steps: first, in a four electron oxidation, thiocyanate and N_2 are formed, then in a second step, thiocyanate is oxidized to cyanide (CN^-) and H_2SO_4 by exchanging eight electrons.

The electrochemical oxidation of thiophene and its common derivatives (see Table II-1 for structures) on carbon electrodes has been the subject of an extensive investigation by Janda and Srogl et al. The series began with the oxidation of thiophene [V], 2-methylthiophene, 3-methylthiophene, and 2,5-dimethylthiophene (92). Next (93), it was shown

Table II-1. Thiophene Structures

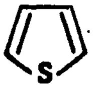

[V]

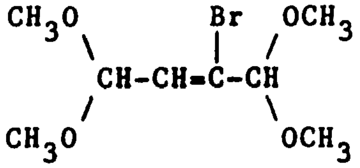

$$(CH_3O)_2CH-CH=C(Br)-CH(OCH_3)_2$$

[VI]

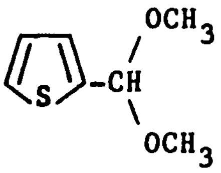

[VII]

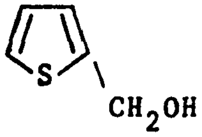

[VIII]

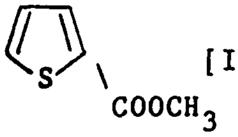

[IX]

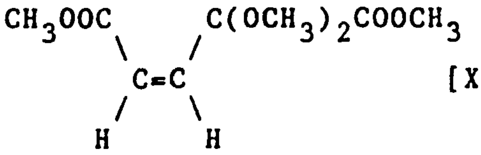

$$CH_3OOC-CH=CH-C(OCH_3)_2COOCH_3$$

[X]

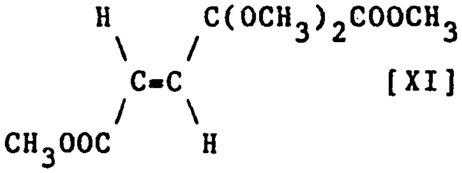

$$CH_3OOC-CH=CH-C(OCH_3)_2COOCH_3$$

[XI]

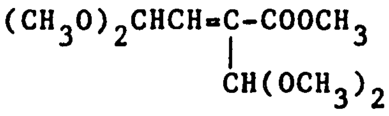

$$(CH_3O)_2CHCH=C(CH(OCH_3)_2)-COOCH_3$$

[XII]

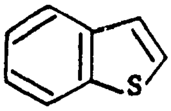

[XIII]

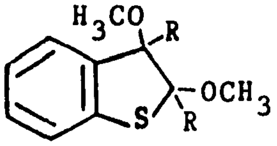

[XIV]

that the electrolytic oxidation of 2,5-dibromothiophene resulted in the formation of methylfumarate, while 3-bromothiophene produced a mixture of products among which the bis-(dimethyl acetal) of bromobutenedial [VI] was the main component. The third report of the series (94) revealed that the dimethyl acetal of 2-thiophencarboxaldehyde [VII] was the main product of the oxidation of 2-thenyl alcohol [VIII]. Next (95), the oxidation of methyl-2-thiophene carboxylate [IX] on a graphite electrode was shown to give _cis_- and _trans_-1,3-bismethoxycarbonyl-3,3-dimethyl propene [X,XI], while methyl-3-thiophenecarboxylate gave exclusively 1,1,4,4-tetramethoxy-2-methoxycarbonyl-2-butene [XII] as its oxidation product. Finally (96), it was shown that the electro-oxidation of benzothiophene [XIII], 3-methylbenzothiophene and 2,3-dimethylbenzothiophene yields the corresponding 2,3-dimethoxy-2,3-dihydrobenzothiophenes [XIV].

Recently, Armstrong et al. (97-100) undertook an interesting study of the effect of electrode orientation upon the anodic behavior of the carbon-polysulfide interphase. They concluded that passivation of the electrode occurs more readily for an electrode positioned vertically downwards. The sulfur, formed as spherical globules in the liquid state upon oxidation of the solution, does not wet the electrode surface; thus, for an electrode placed vertically upwards, globules are able to rise from the anode as a direct consequence of the density difference between sulfur and the polysulfide melt.

3. Detection at mercury electrodes

Despite the work done at solid electrodes, mercury (Hg) electrodes are still the most commonly used for electroanalytical determinations of sulfur containing compounds (101). The electrochemistry of cysteine/cystine was studied by Stankovich and Bard (102) at a hanging Hg-drop electrode by cyclic voltammetry and at a Hg-pool electrode by coulometry. They proposed a mechanism for cystine involving reduction of an adsorbed monolayer to form cysteine and also that oxidation of cysteine involves formation of an adsorbed organomercury species, $Hg(RS)_2$, which is reversible.

The application of high performance liquid chromatography (HPLC) with electrochemical detection to the quantitation of biologically relevant sulfhydryl substances was first described by Rabenstein and Saetre (103) using a mercury based detector. Although their initial report was limited to standard solutions, they subsequently determined glutathione in whole blood and cysteine and homocysteine in plasma (104). These compounds were also studied by Eggli and Asper (105) using HPLC and flow injection (FI) analysis; and by Demaster et al. (106) using cation-exchange HPLC.

The most recent development in mercury based detectors for thiols and disulfides has been the introduction of a thin-layer, dual, mercury-amalgam electrode by Bioanalytical Systems, Inc. (107). The first electrode reduces disulfides to their corresponding thiols, the second electrode then detects the thiols formed at the first electrode as well as other thiols in the sample. By utilizing the dual electrode detector in conjunction with HPLC (108), Lunte and Kissinger have determined that thiols and disulfides can be detected in any biological sample, including tissue samples which contain large amounts of glutathione or other endogenous thiols (109-111).

Thiourea and related compounds have also been characterized on mercury electrodes. Kolevatova and Kuznetsov (112) examined thiourea at a dropping mercury electrode (DME) and proposed a one electron oxidation mechanism which is independent of acidity. Other related thioureas were investigated by Hanekamp et al. (113) and Lawrence et al. (114). They found that, for the compounds studied, the DME detector is significantly inferior to the glassy carbon detector with regard to sensitivity; however, in a comparison of selectivity and surface passivation problems, the DME proved to be greatly advantageous. In addition, King, Kolby, and Price (115) studied the oxidation of thioacetamide at Hg-pool electrodes. Their results confirmed the postulation that a Hg(II)-thioacetamide complex forms similar to that formed upon oxidation of cysteine.

Inorganic sulfur compounds have also been investigated on mercury electrodes. The polarographic determinations of sulfide and polysulfide ions in alkaline media were carried out by Kovacova and Zezula (116). The anions studied all yielded an analogous two electron anodic wave, which was found to be dependent on the concentration of the depolarizer and on the pH. For a complete review of the literature covering the polargraphic determination of inorganic sulfur species see Uddin (117).

4. Detection at gold electrodes

Of the noble metals, gold (Au) is the most convenient for studying electrochemical processes such as the oxidation of dissolved sulfur compounds, because there is an extensive potential range over which there is no significant background current from surface oxide formation. However, detailed studies of the reactions of sulfur species on this metal are particularly sparse, probably because sulfur deposited on gold does not display electrocatalytic activity, such as that found when sulfur is deposited on platinum.

The oxidation of sulfur dioxide in sulfuric acid solutions was investigated by Samec and Weber (118,119) at stationary and rotating gold disk electrodes. They proposed an oxidation mechanism involving rapid reaction of H_2O with adsorbed SO_2 to give HSO_4^- and noted that the oxidation is accelerated by an unidentified reduced species formed on the negative scan.

Wierse, Lohrengel and Schultze (120) investigated the reactions of sulfur formed by oxidation of sulfide and polysulfide ions in alkaline solutions. They concluded that the adsorption of sulfide ions on gold is limited only by diffusion and the sulfur formed upon oxidation is restricted to sub-monolayer quantities. In a related study, Van Huong et al. (121) found that sulfur, deposited from the gas phase onto gold, is stabilized by adsorption on the electrode surface over a wide potential range in neutral solution and suggested the following oxidation mechanism:

$$\mathrm{Au{-}S_{ads} + 2H_2O \longrightarrow Au + SO_2 + 4H^+ + 4e^-} \qquad [9]$$

Recently, a thorough investigation of the deposition and reactions of sulfur on gold electrodes was undertaken by Hamilton and Woods (122). They reported sub-monolayer coverage by sulfur at underpotentials and multilayers of adsorbed sulfur at more positive potentials. They postulated polysulfides as intermediate products in the reaction producing sulfur and its reverse reaction, with S_2^{2-} as the predominant species. Sulfur was found to be completely oxidized to sulfate, although the reaction was inhibited by the presence of a layer of adsorbed sulfur.

Another inorganic sulfur containing anion was studied by

Martins et al. (123,124). They examined the electrochemistry of thiocyanate at gold electrodes in acetonitrile and DMSO solutions. In DMSO, within a relatively limited potential range, the main electrode process was determined to be:

$$3\ SCN^- \longrightarrow (SCN)_3^- + 2e^- \qquad [10]$$

and the kinetics were found to be controlled by both diffusion and adsorption. Unlike the above results, in acetonitrile, the primary electrochemical reaction was the anodic dissolution of the gold electrode. The thiocyanate anion was also investigated in aqueous perchloric acid solution by Itabashi (125). This author explained the electro-oxidation of SCN^- on gold by the following sequence of reactions:

$$SCN^- \longrightarrow SCN\cdot + e^- \qquad [11]$$

$$SCN\cdot + SCN^- \longrightarrow (SCN)_2^{\overline{\cdot}} \qquad [12]$$

$$2(SCN)_2^{\overline{\cdot}} \longrightarrow (SCN)_3^- + SCN^- \qquad [13]$$

The yield of the trithiocyanate anion was found to increase with decreasing pH, thus suggesting the formation of a molecule such as $H(SCN)_3$ to stabilize the final oxidation product.

Recently, Moscardo-Levelut and Plichon (126,127) studied the electrochemical behavior of sulfide, polysulfide, and the sulfur oxyanions at gold electrodes in aqueous sodium hydroxide solutions. The oxidation of sulfide was found to proceed in two steps: the first leading to S_2^{2-}, S_3^{2-} and molecular sulfur, and the second further oxidizing these intermediates to SO_3^{2-}. It was noted that, with the exception of S_2^{2-} and S_3^{2-}, no other polysulfide anions were discovered under these conditions. In addition, it was reported that sulfate and sulfite are not electroactive on gold in basic solutions and that thiosulfate can be oxidized, but not reduced under these conditions.

In addition to the examinations of the previously discussed inorganic sulfur compounds, a few studies of the electro-oxidation of sulfur containing organic compounds have been reported. Koryta and Pradac (128) extended their investigations of the electrochemical behavior of the common sulfur amino acids with the study of cystine at a gold electrode. In comparison to platinum, they found the rate of adsorption of cystine at a gold electrode to be larger and the quantity of adsorbed material to be smaller. The principal oxidation product was cysteic acid and a mechanism involving participation of surface oxide was proposed. The sulfur containing amino acids were also studied by Reynaud, Malfoy and Canesson (129), and Safronov et al. (130), in order to gain a preliminary understanding of the electrochemical behavior of protein components.

Finally, Zakharov et al. (131) investigated the electro-oxidition of thiourea on a gold electrode in sulfuric acid solutions. Two anodic processes were observed: first, the diffusion controlled oxidation of thiourea, followed by a further oxidation, having diffusion and adsorption character, to various oxygen containing products. This two step mechanism was also found to explain the oxidation of diethyldithiocarbamate on gold electrodes (132).

B. Electrochemical Oxidation of Boron Polyhedral Anions

Polarographic data have been reported for several $B_nH_n^{2-}$ polyhedral anions (133-135) (see Table II-2 for structures) and some halogenated derivatives of the B_{10} and B_{12} cages (136) as a criterion of their comparative oxidative stabilities. The order of oxidative stability was determined to be $B_7 < B_6 < B_9 < B_8 < B_{11} < B_{10} < B_{12}$. All of these studies were for the anions in aqueous solution. In addition, halogenation of the B_n cage was found to increase the oxidative stability while introduction of hydroxyl tended to decrease the oxidative stability of the anions.

The electrochemical oxidation of $B_{12}H_{12}^{2-}$ and its thiol derivative are of particular interest. Voltammetry of $[(C_2H_5)_4N]_2B_{12}H_{12}$ at a rotating platinum electrode in acetonitrile has been investigated by Wiersema and Middaugh (137,138). They found that the product of the one electron

Table II-2. Boron Structures

n	Structure	n	Structure
6	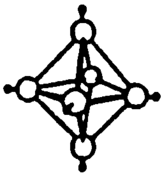	10	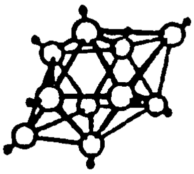
7	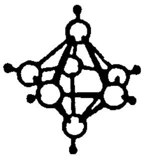	11	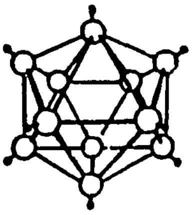
8	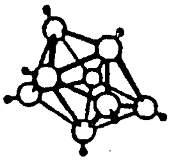	12	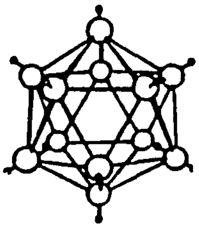
9	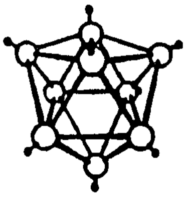		

oxidation of $B_{12}H_{12}^{2-}$ is $B_{24}H_{23}^{3-}$ and the reaction can be represented by

$$2B_{12}H_{12}^{2-} \longrightarrow B_{24}H_{23}^{3-} + H^+ + 2e^- \qquad [14]$$

The structure of the dimeric product was formulated to consist of two B_{12} polyhedra joined by a bridging hydrogen, and was found to be resistant to further oxidation without degradation. Studies of the electro-oxidation of $B_{12}H_{12}SH^{2-}$ are unknown prior to this work.

For a complete review of the electrochemistry of boron compounds, see the recent compilation by Morris, Gysling and Reed (139).

C. High Performance Liquid Chromatography of Selected Sulfur Compounds

The use of gas chromatography (GC) for the determination of organic sulfur compounds has been limited by the lack of volatility and thermal stability of the species of interest. Liquid chromatography in its traditional forms (column, thin-layer, and paper) has long been known as an effective tool in the determination of such compounds (140), but it is generally limited because of long analysis time and/or low sensitivity. However, since the advent of high performance liquid chromatography (HPLC), renewed interest in the analytical separation and quantitation of sulfur compounds has occurred.

In addition to the studies previously reviewed in this work, several analytical separation schemes have been proposed for different classes of sulfur compounds, which do not involve electrochemical detection. Cox and Przyjazny (141) developed separation procedures for several groups of sulfur compounds including: thiols, sulfides, disulfides, sulfones, isothiocyanates, thioamides and thioureas. From their work, it was concluded that gas chromatography is a superior method for the analysis of alkyl and cycloalkyl thiols and sulfides, as well as low molecular weight disulfides. Liquid chromatography was found to be more suitable for the determination of aromatic thiols, sulfides, and disulfides, as well as thioamides and thioureas. Both methods were roughly equivalent in the determination of sulfones. In addition, those compounds for which liquid chromatographic analysis was superior could generally be detected below the ppm range.

The separation of a mixture of thioureas and thioacetamide was accomplished by Hashimoto using salting-out chromatography (142). This author demonstrated that thiourea, ethylenethiourea, 1,3-dimethyl-2-thiourea, 1-allyl-2-thiourea, 1,3-diethylthiourea and thioacetamide could be separated in ca. 40 minutes under the appropriate conditions. Detection limits for these compounds were reported to be in the 10 ng/100µL range. Kobayashi et al. (143) also investigated a separation procedure for these compounds and devised a reversed-phase system which separated the thioureas only, in ca. 45 minutes. Detection limits under 0.05 ppm were reported for all the thioureas studied.

Reverse phase chromatographic separations of nonionic sulfur compounds were also carried out by Mockel et al. (144). Examples of successful separations were reported for elemental sulfur homocycles, polysulfanes, aliphatic thiols and dithiols, and aliphatic polysulfides.

Werkhoven-Goewie et al. (145) applied the principle of ligand-exchange, based on a reaction with the palladium(II)-calcein complex, for the separation and detection of thiols, thioketones, thioethers and disulfides. Specific results were reported for a synthetic mixture of thioureas, as well as the sulfur containing amino acids. Detection limits were in the 0.5-1.0 ng/100μL range, with linearity observed over 2-3 orders of magnitude of concentration.

The separation of organic sulfides was accomplished by Bossle et al. (146,147) using pre-column derivatization in conjunction with HPLC, in addition to direct detection following chromatographic separation. One chromatogram was reported for the complete analysis of three derivatized sulfides in less than 15 minutes. The direct detection was reported only for standard solutions and biological samples containing 2,2'-thiodiethanol.

Gustafsson et al. (148,149) devised a separation scheme for fungicidal dithiocarbamates, which involved an extensive pre-column work-up to form the methyl esters of these compounds followed by HPLC analysis. Examples were reported for standard solutions and extracts of six different food crops. All the compounds had detection limits of < 0.05 ppm. For a complete review of chromatographic techniques for pesticide analysis see Cochrane (150).

Finally, an analytical system was developed by Story (151) which allows the determination of individual inorganic sulfur species in mixtures containing any combination of sulfide, sulfite, thiosulfate, sulfate, trithionate, tetrathionate, pentathionate and hexathionate. The complicated procedure required post-column chemical treatment to convert all the sulfur species to sulfate, which was eventually determined spectrophotometrically after chelation with Fe(III). The sensitivity of the detector was found to be proportional to the number of sulfur atoms present in the original anion and detection limits ca. 10 ppm were reported.

D. Pulsed Amperometric Detection

Hughes, Meshi and Johnson (152) observed that the surface activity of platinum electrodes was restored by alternate anodic and cathodic polarizations of the electrode, and they incorporated this pretreatment into a triple-step potential waveform. This Pulsed Amperometric Detection (PAD) technique involves the measurement of the analytical signal at a precisely controlled delay time (t_d) following application of the detection potential, E_1. Next, a positive potential pulse to E_2 is applied, at a value in the vicinity of anodic oxygen evolution, to achieve oxidative cleaning of the electrode surface. The subsequent negative step to E_3, at a value in the vicinity of cathodic hydrogen evolution, results in the rapid removal of the surface oxide that is formed while at E_2. In many cases, adsorption of analyte also occurs at E_3. The potential waveform has a frequency of ca. < 1 Hz. This allow the technique to be employed in conjunction with FI and HPLC analyses with sufficient time resolution to accurately describe peak shapes.

PAD has been utilized by several authors for the detection of simple alcohols, polyalcohols and carbohydrates. As mentioned above, Hughes, Meschi and Johnson introduced the technique and reported the first successful examples of detection. They illustrated that it was possible to maintain uniform levels of electrode activity during the anodic detection of methanol, ethanol, ethylene glycol and formic acid at platinum electrodes in aqueous acid solutions. Hughes and Johnson extended this initial study to the detection of polyalcohols and carbohydrates in standard solutions (153) and the analysis of beverages (154) and other food products (155) following separations by HPLC. Detection limits of ca. 0.1-1 ppm were reported for monosaccharides.

The application of PAD at gold electrodes for the detection of carbohydrates was reported by Edwards and Haak (156), and Rocklin and Pohl (157). They illustrated the capabilities of the technique with a separation of eleven carbohydrates in less than fifteen minutes. Detection limits as low as 30 ppb for sugar alcohols and monosaccharides, and ca. 0.1 ppm for oligosaccharides were reported.

Recently, a comparison of the pulsed amperometric detection of carbohydrates at gold and platinum electrodes was conducted by Neuburger and Johnson (158). They concluded that gold electrodes have the advantage of high sensitivity and lower detection limits in comparison to platinum electrodes. Detection limits were claimed to be decreased by ca. 5 times, for glucose, fructose, sorbitol and sucrose detected at a gold electrode, although no data were presented to substantiate this claim. These authors have also proposed a two-step potential waveform for PAD of carbohydrates at gold electrodes (159). Sensitivities and detection limits were found to be approximately equivalent to the previously discussed three-step methods. For a review of the direct electrochemical detection of all carbohydrates, see Johnson (160).

Aliphatic amines, including essential amino acids, have been reported by Polta and Johnson (161) to be detectable at platinum electrodes in alkaline media using PAD. A representative chromatogram was shown for the separation of seven amino acids by HPLC in ca. fifteen minutes. Detection limits were at the ppm level. The mechanism of oxidation was concluded to involve electrocatalytic oxygen transfer, and hydroxylamines were speculated as being the initial products of the electrode reaction. It was noted that the analytical response was dependent upon the adsorption isotherm of the amino acid being detected; hence, linear calibration plots of current vs. concentration were obtained only at low surface coverages of analyte. Aminoglycosides were also detected by these authors at platinum electrodes (162) and the response was concluded to correspond to the oxidation of the amine group and not the alcohol groups.

Rocklin (163) has reported that formaldehyde, acetaldehyde, propionaldehyde, butyraldehyde and formic acid can be determined in a single analysis by ion chromatography with electrochemical detection by oxidation using PAD at a platinum electrode. The separation was accomplished in ca. twenty minutes and detection limits ranged from 1 to 3 ppm. It was noted that the presense of methanol and ethanol interfere with the analysis.

In addition to the electroactive adsorbates discussed here thus far, adsorbed electroinactive species have also been detected using PAD at platinum electrodes. Polta and Johnson (164) illustrated this technique using chloride and cyanide. They determined that the adsorption of the anions alters the rate of surface oxide formation, thus enabling an indirect detection of the electroinactive species by monitoring the current due to oxide formation on the electrode surface. Sensitivity was found to be high and calibration curves were consistant with adsorption control according to the Langmuir isotherm.

Recently, Thomas and Sturrock (165) described the reverse-phase chromatographic separation of carbamate pesticides with PAD at a platinum electrode. In addition, Ohsawa et al. (166) have applied the technique to the determination of xylitol in human serum and saliva following separation by an ion chromatograph. For complete reviews of pulsed amperometric detection, see Austin et al. (167), Johnson et al. (168), and Johnson and Polta (169).

III. EXPERIMENTAL

A. Chemicals

All chemicals were reagent grade. Water was distilled, deionized and filtered through an activated carbon column. All eluents for the HPLC system were passed through a 0.45-μm filter prior to use. Dissolved oxygen was removed from solutions in voltammetric studies at rotated electrodes by saturation with nitrogen.

B. Instrumentation

1. Voltammetric studies

a. Electrodes, rotator and recorder The rotating disk and ring-disk electrodes (RDE and RRDE) (Pine Instrument Co., Grove City, PA) are listed in Table III-1.

Table III-1. Pine Electrodes

Electrode Number	Model	Type	Electrode Material	Area (cm^2)
I	AFDT06	RRDE	Pt,Pt	0.459, 0.059
II	AFMD10	RDE	Pt	0.010
III	DD20	RDE	Au	0.458
IV	AFMD10	RDE	Au	0.010

The disk of electrode I and electrode III were used to obtain current-potential (I-E) curves by cyclic voltammetry.

The ring of electrode I and electrode IV were used to obtain I-E curves by pulsed voltammetry. Current-time (I-t) curves were obtained using electrodes II and IV. The rotator was model PIR (Pine Instrument Co.). The recorder used for I-E curves was a RE0074 X-Y recorder (EG&G, Princeton Applied Research, Princeton, NJ).

b. Potentiostats Potentiostatic control for cyclic, linear scan voltammetry, for all compounds studied, except the sulfur containing boron polyhedrals, was achieved by a model 173 potentiostat equipped with a model 175 universal programmer (EG&G, Princeton Applied Research). A model RDE3 potentiostat (Pine Instrument Co.) was used for cyclic voltammetry of the sulfur containing boron polyhedrals. Potentiostatic control for the pulsed voltammetry was achieved by a UEM Pulsed Amperometric Detector (Dionex Corp., Sunnyvale, CA). A miniture saturated calomel electrode (SCE) served as the reference electrode and all potentials are reported for voltammetric studies as volts (V) vs. SCE.

2. Flow-injection

a. Electrodes Detection at Pt was achieved at a flow-through cell (Dionex Corp.) which consisted of a Pt disk working electrode (0.008 cm^2), a carbon counter electrode, and a silver-silver chloride reference electrode (SSCE) in a sandwich-type arrangement (Figure III-1). Detection at Au

Figure III-1. Dionex flow-through cell

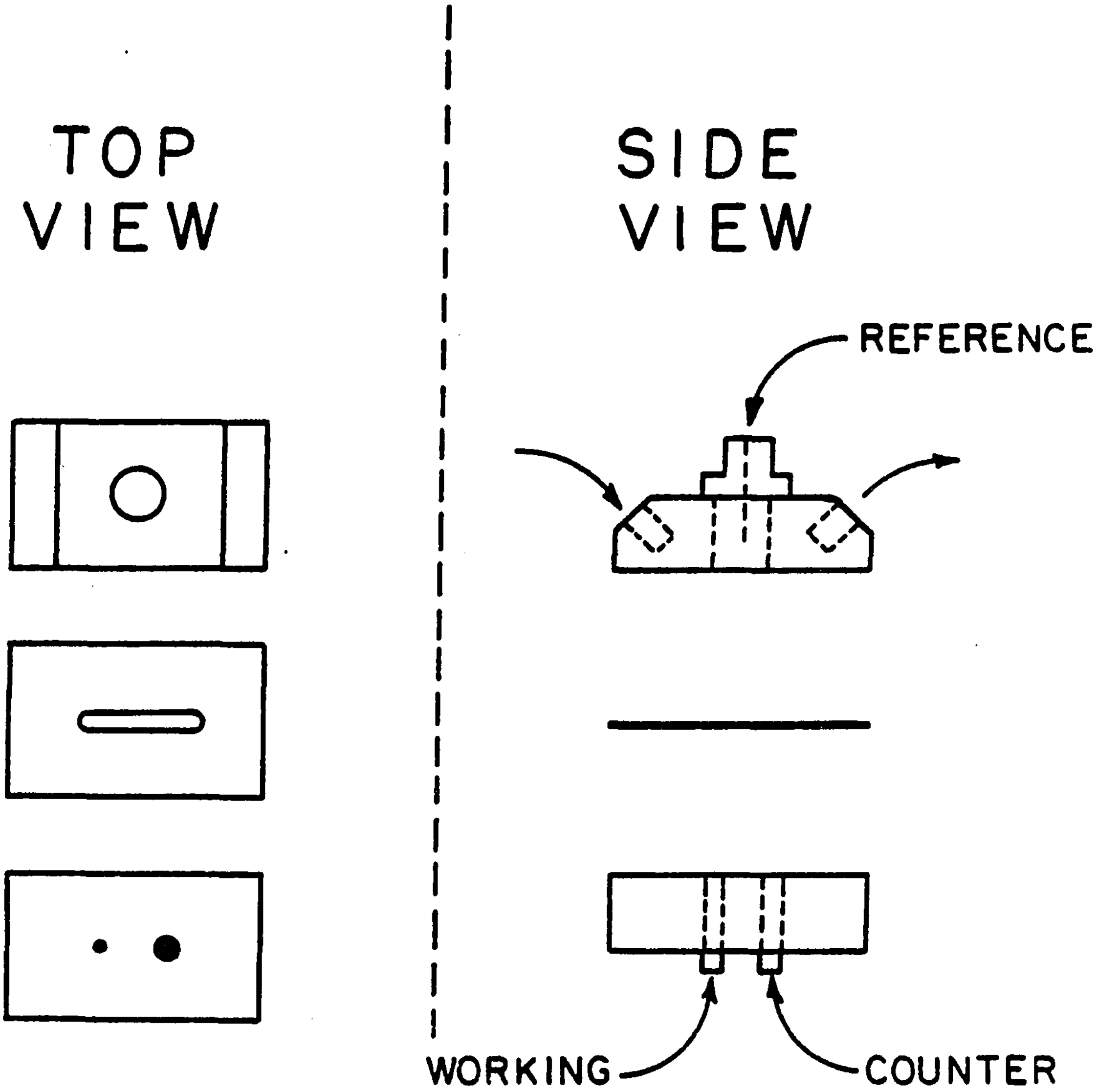
TOP VIEW
SIDE VIEW
REFERENCE
WORKING
COUNTER

was achieved at a flow-through cell designed by D. C. Johnson and constructed with help by the machine shop of the Department of Chemistry, Iowa State University (Figure III-2). The Au wire was fitted into an appropriate size of Teflon tubing and sealed into place in the body of the cell by a plastic, tapered screw. The wire was allowed to extend ca. 0.5 mm beyond the end of the tapered screw, into the effluent stream. The cell was immersed in a beaker filled with supporting electrolyte containing the reference electrode and a Pt-wire counter electrode.

b. Injection system, potentiostat and recorder The flow-injection apparatus was based on a model SHS-200 sample handling system (Fiatron Systems, Inc., Glendale, WI), which incorporates a multichannel peristaltic pump with a microprocessor-controlled sample injection valve. Potentiostatic control of the flow-through electrode was achieved by the UEM Pulsed Amperometric Detector. Data were recorded using a model 250-1 strip-chart recorder (Curken, Inc., Lincoln, NE). Potentials for flow-injection detection at Pt are reported in V vs. SSCE. Potentials for FI detection at Au are reported in V vs. SCE. The dispersion coefficient, i.e., $\kappa = C_p/C^b$, for the FI system was determined to be 0.090, using anodic detection of I^- in 0.5 M H_2SO_4 at constant potential.

Figure III-2. Au flow-through cell

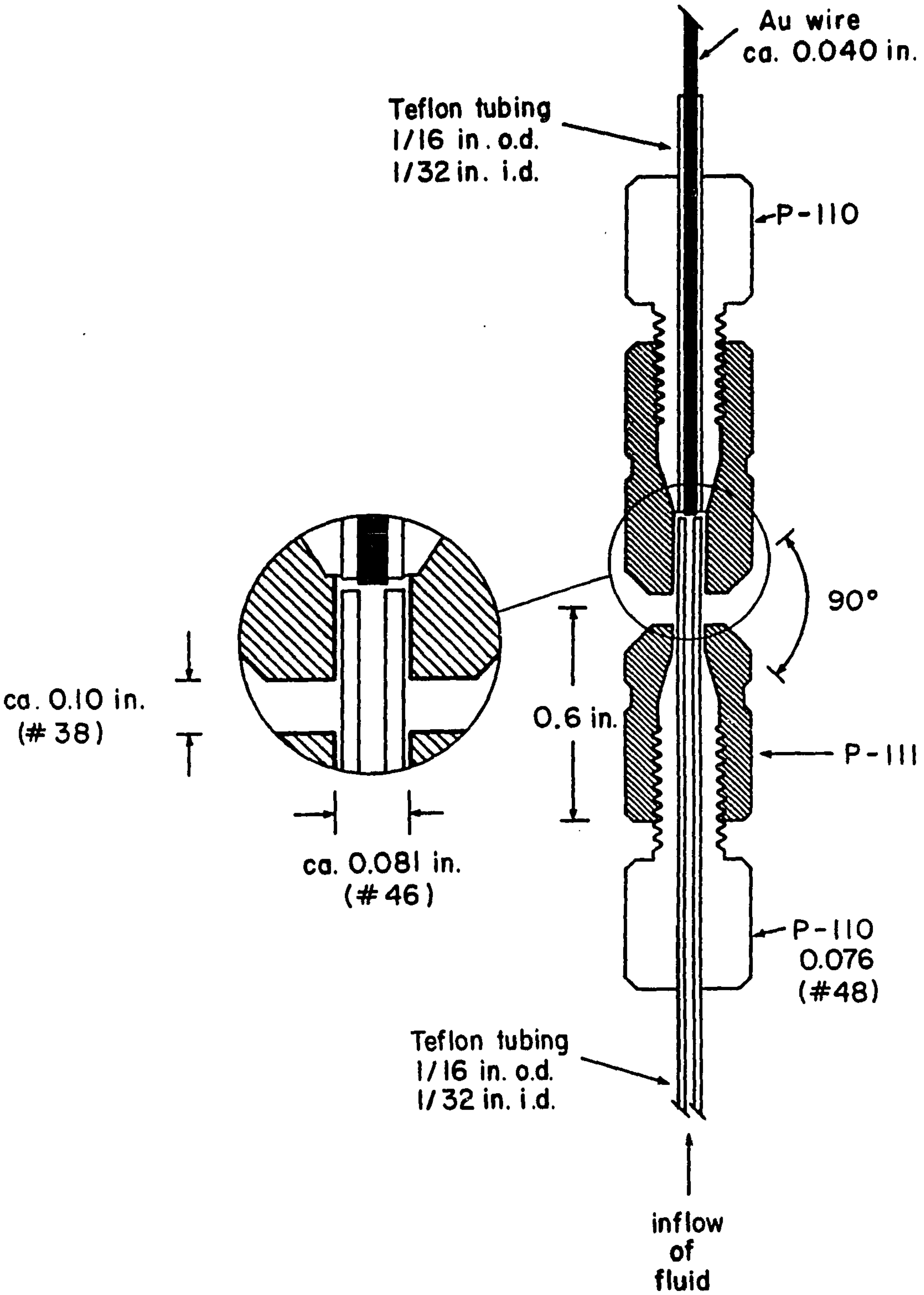
Au wire
ca. 0.040 in.
Teflon tubing
1/16 in. o.d.
1/32 in. i.d.
P-110
90°
ca. 0.10 in.
(# 38)
0.6 in.
P-111
ca. 0.081 in.
(# 46)
P-110
0.076
(#48)
Teflon tubing
1/16 in. o.d.
1/32 in. i.d.
inflow
of
fluid

3. High performance liquid chromatography

The liquid chromatograph was assembled similarly to that described by Hughes (170). Flow of the eluent solution was maintained by a Milton Roy model CK Mini-pump (Laboratory Data Control, Riviera Beach, FL) with dual pistons operating 180 degrees out of phase. The Teflon tubing connecting the eluent reservoir and the pump was 0.11-in. i.d. x 1/8-in. o.d.; all other tubing was Teflon with dimensions 0.012-in. i.d. x 0.062-in. o.d. Connections were made with Omnifit fittings. The sample injection valve was a Rheodyne model 2125 (Larry Bell and Associates, Minneapolis, MN) with a 50-μL sample loop.

An AG6 anion exchange guard column (P/N 35392, Dionex Corp.) in series with an AS6 anion exchange separator column (P/N 35391, Dionex Corp.) was used to separate inorganic sulfur compounds and thioureas. Separation of thiophenes, as well as thiosemicarbazide and thionicotinamide, was achieved with an MPIC-NG1 neutral polystyrene guard column (P/N 35320, Dionex Corp.) in series with an MPIC-NS1 neutral polystyrene separator column (P/N 35321, Dionex Corp.). Dithiocarbamates and sulfur containing boron polyhedrals were separated using a DEAE anion exchange column (Anspec Co., Inc., Ann Arbor, MI).

Amperometric detection was achieved at the Au flow-through cell potentiostated by the UEM Pulsed Amperometric

Detector. Chromatograms were recorded using the Curken strip chart recorder. All potentials for chromatographic detection at Au are reported in V vs. SCE.

IV. PULSED AMPEROMETRIC DETECTION OF SULFUR COMPOUNDS AT PLATINUM ELECTRODES IN ALKALINE SOLUTION

A. Cyclic Voltammetry

The voltammetric response of several sulfur compounds was obtained for preliminary characterization using cyclic voltammetry in 0.25 M NaOH. Aqueous base was chosen as the electrolyte to keep the volatile compounds studed in the ionic form, and because further work was anticipated using anion-exchange chromatography with NaOH as the eluent. Anodic response was observed for numerous inorganic and organic sulfur compounds as given in Table IV-1. The voltammmetric response appeared surprisingly similar for these compounds and thiourea was chosen as a representative compound for further study due to its low volatility and relatively low toxicity. A typical I-E curve for thiourea at a platinum electrode is shown in Figure IV-1. The cathodic peaks for the negative scan in the region -0.6 to -0.9 V in the absence of thiourea correspond to the production of adsorbed hydrogen atoms. Evolution of $H_2(g)$ occurs at $E <$ -0.9 V. The anodic peaks observed on the positive scan in the same potential region correspond to oxidation of adsorbed hydrogen atoms. The anodic wave at $E >$ -0.3 V and the cathodic peak at -0.3 V in the absence of thiourea are caused by surface oxide formation and reduction, respectively. Evolution of $O_2(g)$ occurs at $E >$ 0.6 V in this media.

Table IV-1. Representative sulfur compounds detected by PAD in alkaline media

Classification	Structure	Examples Studied
Inorganic		SCN^-
		$S_2O_3^{2-}$
		S^{2-}
		CS_2
Organic:		
thiol	R-SH	$R = C_2H_5$
thioamide	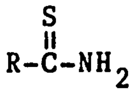 $R-C(=S)-NH_2$	$R = NH_2$ (thiourea) $R = CH_3$ (thioacetamide)
thiocarbamate	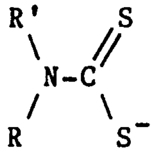	$R = R' = C_2H_5$
sulfoxide	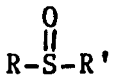 $R-S(=O)-R'$	$R = R' = CH_3$(DMSO)

Figure IV-1. Current-potential curves for thiourea at a Pt RDE by cyclic voltammetry in 0.25 M NaOH

Conditions: ϕ = 6.0 V min^{-1}, W = 94 rad s^{-1}

Concentrations: (a) 0.00 mM, (b) 1.00 mM

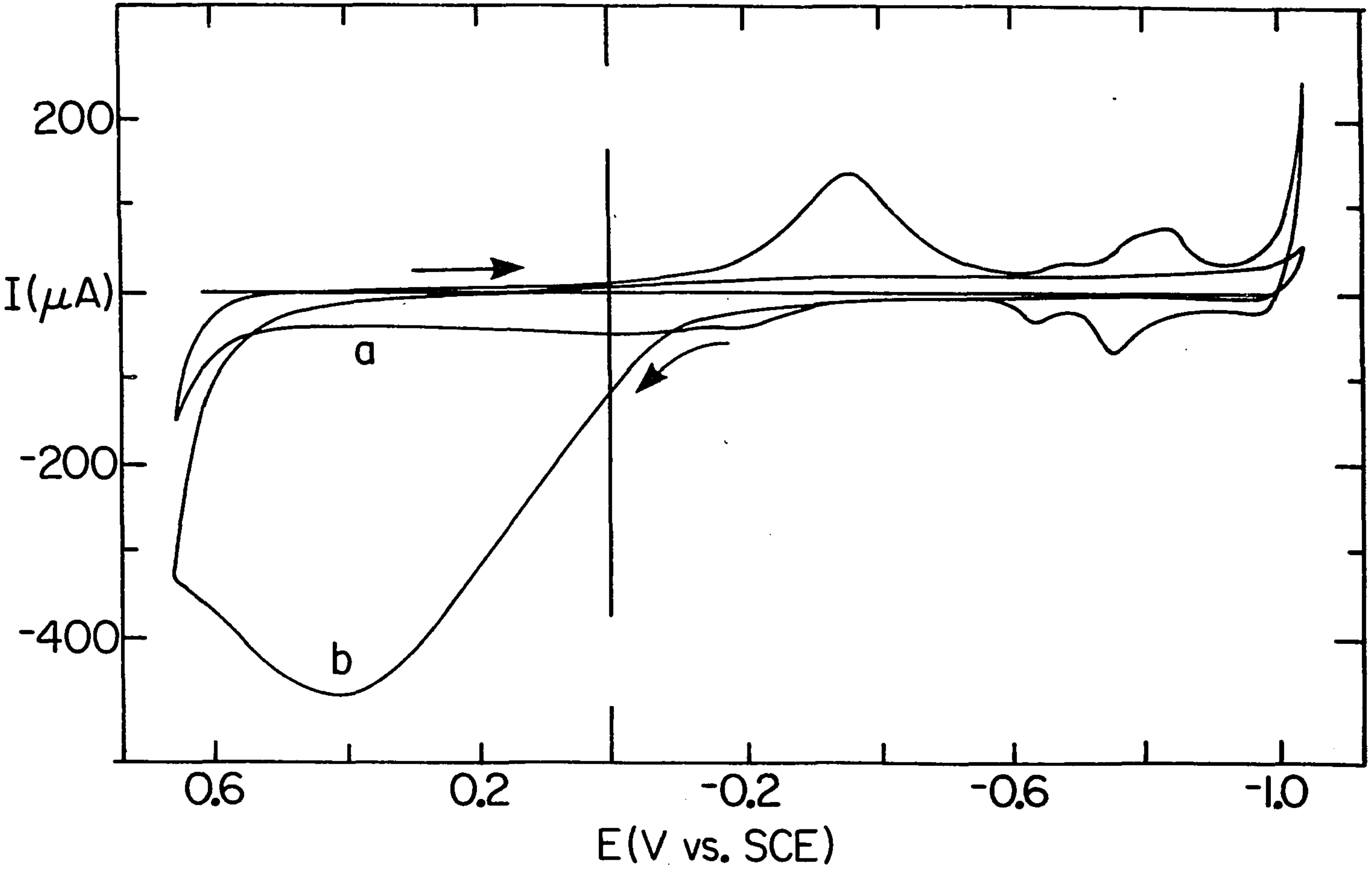
200
I(μA)
-200
-400
a
b
0.6
0.2
-0.2
-0.6
-1.0
E(V vs. SCE)

In the presence of thiourea, the cathodic and anodic processes for adsorbed hydrogen are completely suppressed, indicating that thiourea is adsorbed at the electrode surface under these conditions to such an extent that no free Pt sites are available for hydrogen adsorption. Oxidation of thiourea produces an anodic wave on the positive potential scan in the region -0.1 to 0.6 V. The oxidation is severely inhibited by the surface oxide formed during the positive scan, as noted by the dramatic decrease in current upon reversal of the scan at 0.6 V. Yet, if a surface oxide is formed during the positive scan with thiourea present, a reduction peak for the oxide at -0.3 V is expected on the negative scan (see residual curve for absence of thiourea). No oxide reduction peak is observed in the presence of thiourea, however. A possible explanation for the lack of an oxide reduction peak is that, simultaneous to oxide reduction, an anodic process for thiourea is occurring and the net effect ($I_{anod} + I_{cath}$) is that only a small cathodic current is obtained in the region where the large cathodic oxide peak is expected.

The FI/PAD system was applied to investigate the possibility of an anodic process for thiourea in the region -0.2 to -0.6 V. The waveform applied was: E_1 (300 ms) varied in the region of interest, E_2 = 0.70 V (100 ms) to oxidatively clean the electrode surface, and E_3 = -1.00 V

(800 ms) to reduce the Pt surface and allow adsorption of analyte. When this waveform was executed, anodic peaks were detected for thiourea. A mechanism consistent with these results and the literature is the one electron oxidation of thiourea to its corresponding formamidine disulfide at E_3 in the region of platinum oxide reduction, i.e., $E < -0.4$ V. It is concluded that the adsorbed disulfide is the species which has been responsible for previous observations of serious loss of electrode activity. Exhaustive electrolysis, at a large Pt-gauze electrode with E = 0.6 V for five hours, yielded enough SO_4^{2-} to be readily detected as insoluble $BaSO_4$ following addition of $Ba(NO_3)_2$. It is concluded on this basis that the adsorbed disulfide is oxidized to urea and sulfate by a surface oxide catalyzed process on the positive scan for $E > 0.1$ V.

The FI/PAD experiment was repeated with DMSO and no anodic process was detected in the potential region -0.1 to -0.9 V, although the adsorption of DMSO is evident from I-E curves by suppression of the hydrogen peaks at the Pt electrode. These results are consistent with the conclusions for thiourea, as no dimer containing a sulfur-sulfur bond can easily be formed from DMSO.

The anodic current for thiourea in the region -0.1 to 0.6 V was found to be dependent on the rate of potential scan. A plot of current vs. scan rate was approximately linear with a zero intercept, indicating that the oxidation is strictly a surface-controlled process. However, the current was found also to be slightly dependent on rotation speed. Thus, we conclude that mass transport, as well as adsorption, is a factor in determining the anodic response for thiourea; however, the rate of oxidation of the transported thiourea is controlled by the rate of surface oxide generation and, hence, is a linear function of scan rate.

B. Pulsed Amperometric Detection

Amperometric detection of thiourea at a constant electrode potential is not successful for analytical quantitation because of rapid fouling of the electrode surface by the proposed dimerization product for $E < -0.1$ V, as well as the formation of PtO for $E > -0.1$ V. The anodic current response with and without thiourea is shown as a function of time in Figure IV-2 (Curves a and b). Literature (167) reports that the rapid decay of current as shown is either due to oxide formation, with desorption of an electroinactive adsorbate, or oxide formation with oxide-catalyzed oxidative desorption of an electroactive adsorbate. It is concluded that the second process is the more likely explanation. Also shown in Figure IV-2 (Curves c and d) is the current response of the electrode upon application of PAD with and without thiourea. It is easily noted that the signal response

Figure IV-2. Current-time curves for thiourea at a Pt RDE in 0.25 M NaOH

Conditions: W = 94 rad sec^{-1}

Concentrations (mM): (a,c) 0.0 (b,d) 0.50

DC detection: (a,b) E = 0.60 V vs. SCE

Pulse detection: (c,d) E_1 = 0.60 V (300 ms),
E_2 = -1.00 V (800 ms),
E_3 = 0.70 V (50 ms)

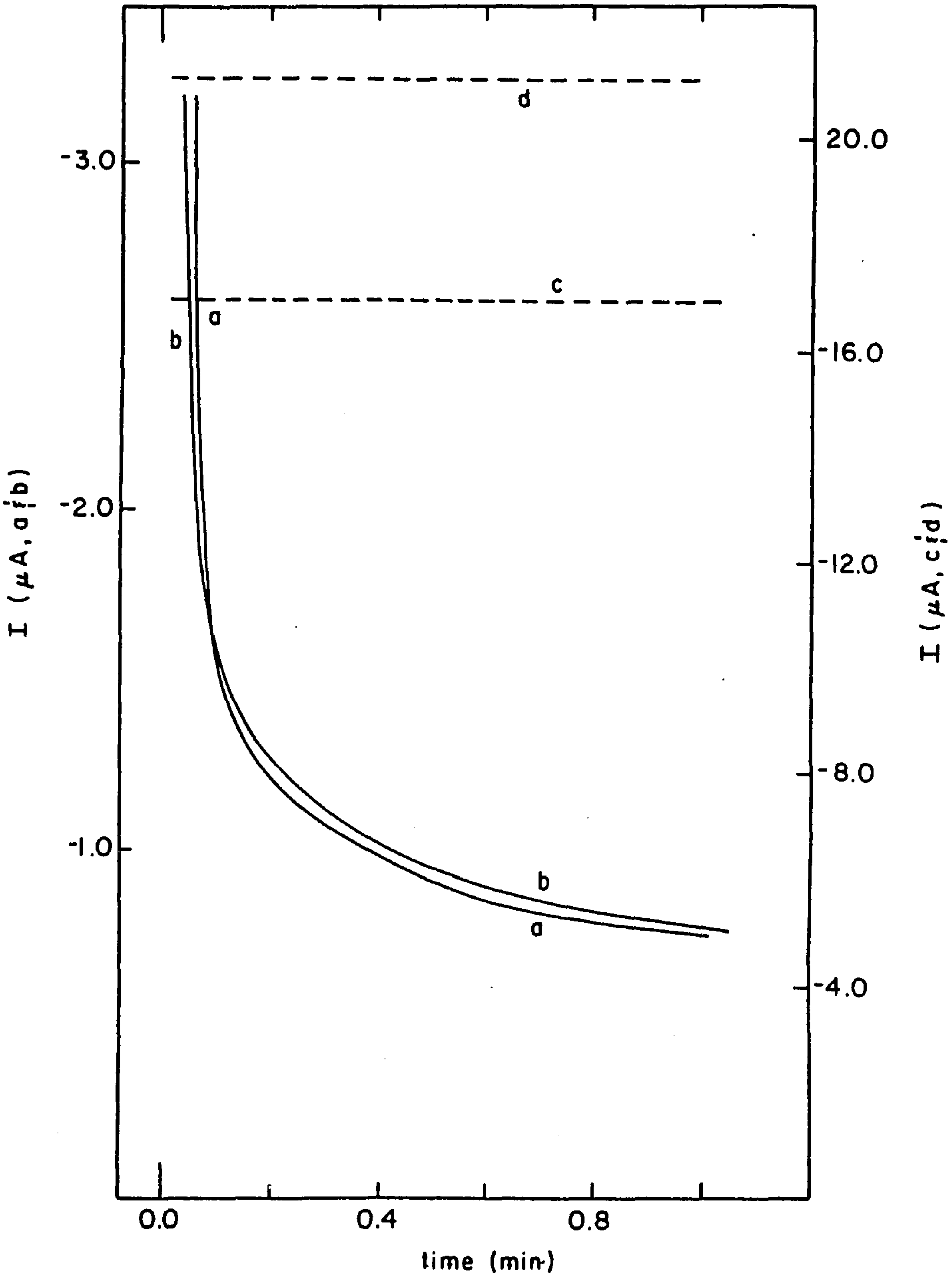
d
c
a
b
b
a
-3.0
-2.0
-1.0
20.0
-16.0
-12.0
-8.0
-4.0
0.0
0.4
0.8
time (min)
I (μA, a & b)
I (μA, c & d)

is steady in both cases. The analytical significance of a steady background signal obtained with PAD is that the anodic current signal for the analyte can be amplified and the constant background electronically offset.

The selection of an appropriate potential waveform for maximum sensitivity for thiourea with PAD was made on the basis of the I-E curve in Figure IV-1. E_2 was chosen corresponding to the region of oxide reduction and analyte adsorption. E_3 was chosen greater than E_1 to decrease the background current measured at E_1, as the rate of oxide formation at E_3 is greater than at E_1. A suitable value for E_1 was determined from hydrodynamic voltammagrams shown in Figure IV-3. The anodic signal was measured for 50 ms after a delay period of 300 ms to allow the background currents to decay to a reasonably small value before sampling the faradaic signal for the oxidation of adsorbed thiourea. Upon comparison of the cyclic and pulsed voltammetric curves, it is noted that the largest difference between the anodic signal with and without thiourea occurs at 0.6 V for the pulsed experiment, unlike the cyclic experiment where the maximum occurs at ca. 0.4 V. These results confirm the necessity of performing the FI/PAD experiment to optimize the design of the waveform for maximum sensitivity.

Figure IV-3. Current-potential curves for thiourea at Pt by pulsed voltammetry in 0.25 M NaOH

Conditions: E_1 varied (300 ms),
E_2 = -1.00 V (800 ms),
E_3 = 0.70 V (50 ms);
$W = 94$ rad sec^{-1}

Concentrations (mM): (•) 0.0, (X) 1.0

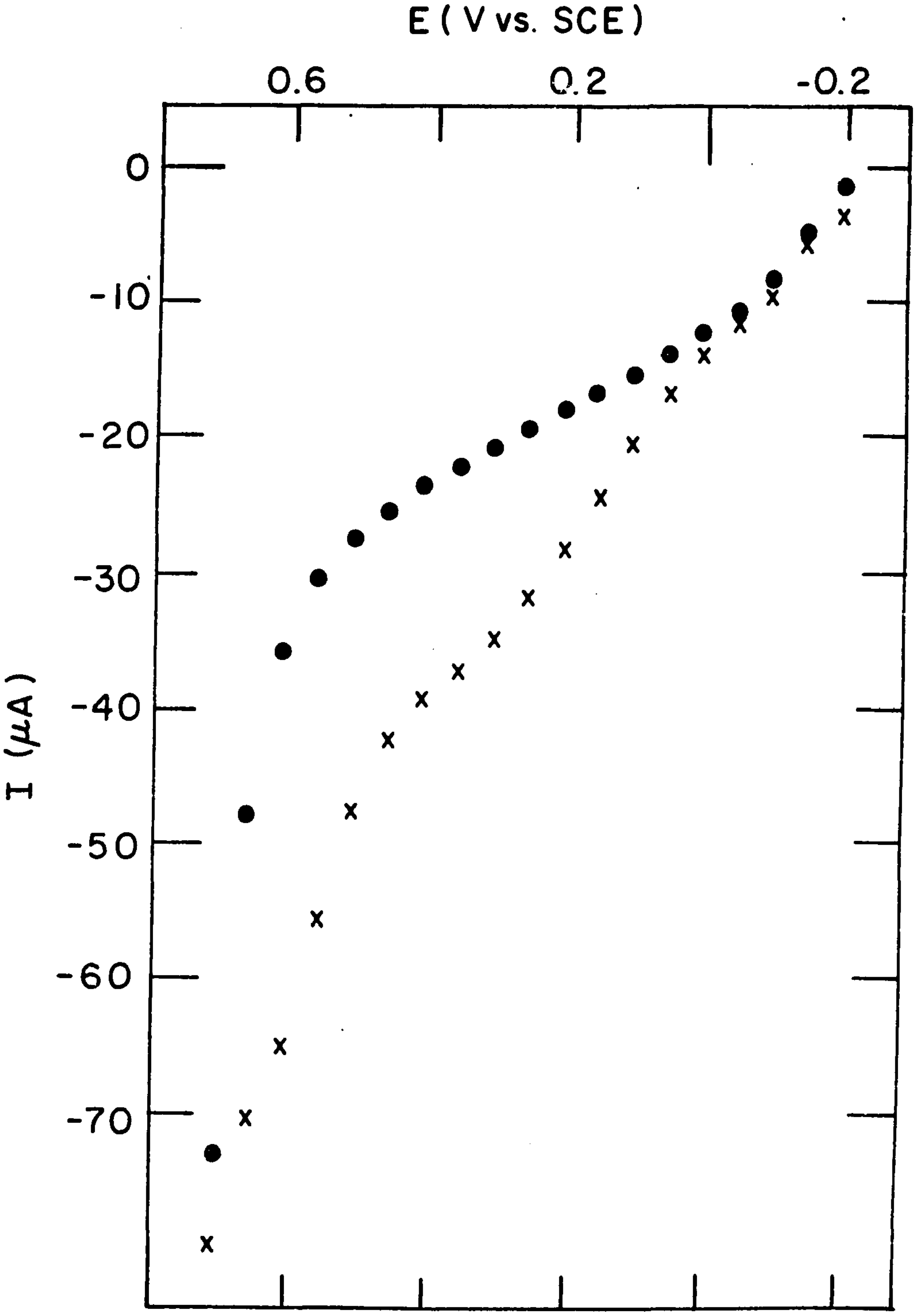
E (V vs. SCE)
0.6
0.2
-0.2
I (μA)
0
-10
-20
-30
-40
-50
-60
-70

C. Flow-injection Analysis

Application of the waveform with $E_1 = 0.6$ V (300 ms), $E_2 = -1.00$ V (800 ms), and $E_3 = 0.7$ V (50 ms), for FI detection of thiourea, gave reproducible peaks (rsd < 3% for 10 injections) with an anodic peak current found to be linear with concentration for 0.10 - 0.50 mM, as shown in Figure IV-4. The detection limit for thiourea using the PAD waveform in this FI system is 0.38 ppm (i.e., 17 ng in the 45-μL sample). For reference, three injections of 0.50 mM thiourea were also made for a constant electrode potential of 0.60 V. After three injections, no detectable peaks were observed.

Calibration plots for thiourea (I_p vs. C^b) are shown in Figure IV-5 for adsorption time values of 200, 1000 and 8500 ms. The response is approximately linear for very dilute solutions and/or low values of t_{ads}, e.g., $C^b < 0.60$ mM for $t_{ads} = 1000$ ms. However, curvature can be severe at high C^b and large t_{ads}, as shown by Curve c for $t_{ads} = 8500$ ms. This behavior was anticipated because all previous studies using PAD have reported similar nonlinear response at high concentrations of analyte. Nonlinear calibration curves previously have been attributed to a response mechanism whereby the anodic peak signal (I_p) is proportional to the peak surface coverage (θ_p) by adsorbed analyte. The Langmuir isotherm

Figure IV-4. Detection peaks for thiourea in 0.25 M NaOH by FI/PAD

Pulsed detection: (a-f) E_1 = 0.60 V (300 ms),
E_2 = -1.00 V (800 ms),
E_3 = 0.70 V (50 ms);
V_f = 0.67 mL min^{-1}; V_s = 45 µL

DC detection: (α) E = 0.60 V; V_f = 0.60 mL min^{-1};
V_s = 40 µL

Concentration: given in figure as mM

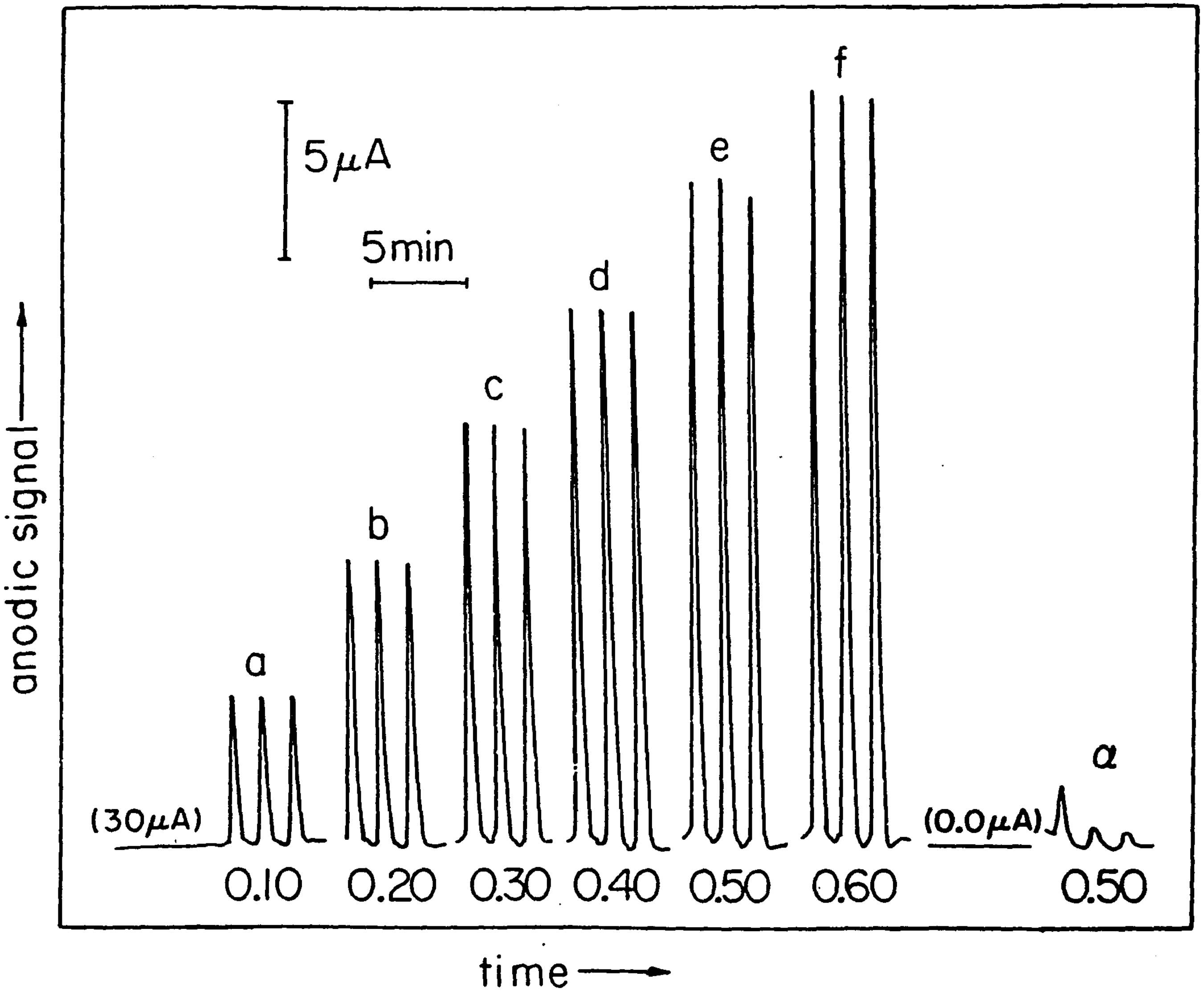
5 μA
5 min
anodic signal
a
b
c
d
e
f
α
(30 μA)
(0.0 μA)
0.10
0.20
0.30
0.40
0.50
0.60
0.50
time

Figure IV-5. Calibration curves (I_p vs. C) for thiourea in 0.25 M NaOH by FI/PAD

Conditions: V_f = 0.65 mL min^{-1}, V_s = 43 µL

Waveform:

(A) E_1 = 0.60 V (300 ms), E_2 = -1.00 V (8500 ms),
E_3 = 0.70 V (50 ms);
(B) E_1 = 0.60 V (300 ms), E_2 = -1.00 V (1000 ms),
E_3 = 0.70 V (50 ms);
(C) E_1 = 0.60 V (300 ms), E_2 = -1.00 V (200 ms),
E_3 = 0.70 V (50 ms)

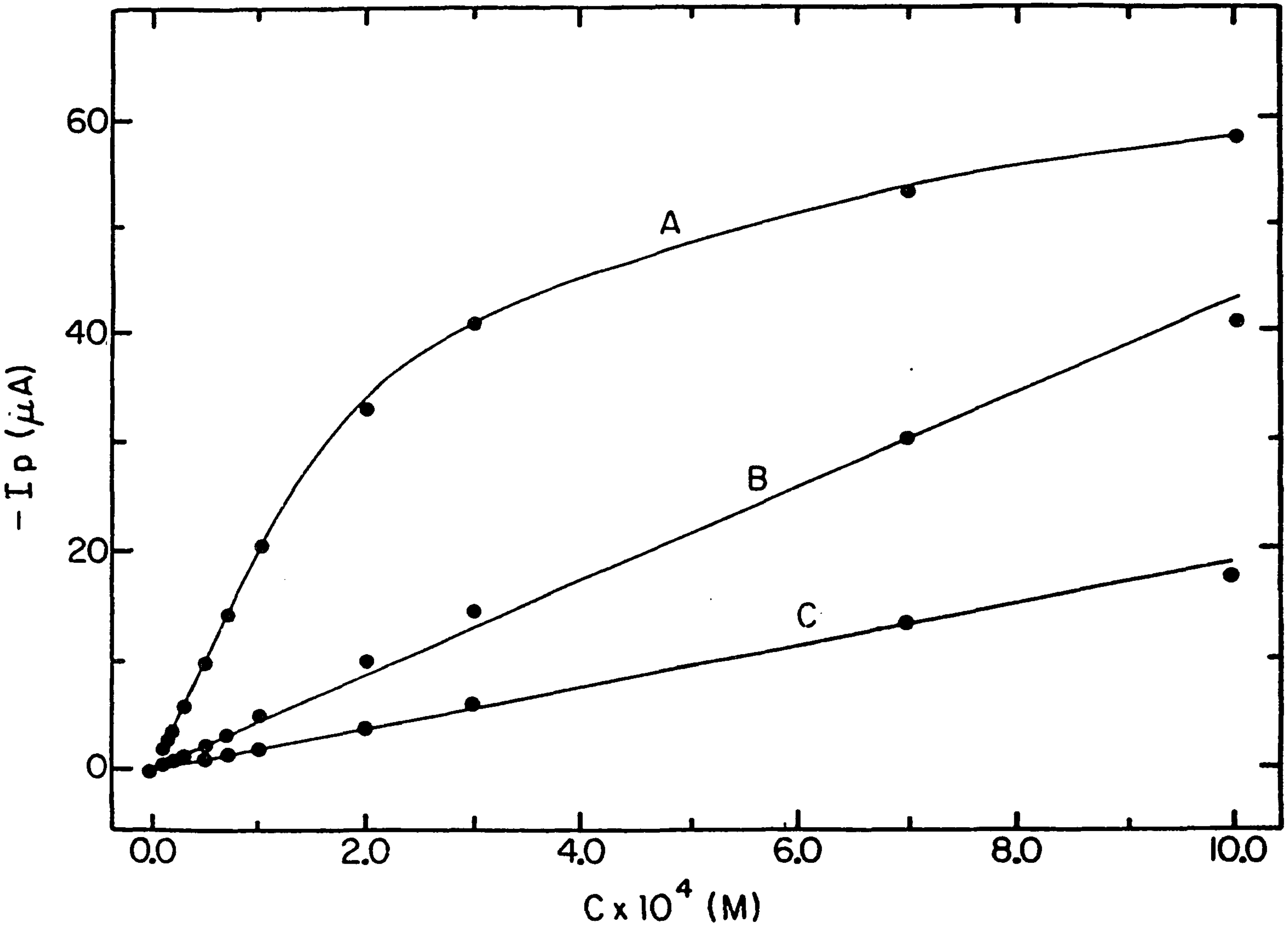

60
40
20
0
− I p (μA)
A
B
C
0.0
2.0
4.0
6.0
8.0
10.0
C x 10^4 (M)

describes this behavior for low values of θ_p and is stated as

$$\theta_p = I_p/I_{p,max} = KC_p/(1 + KC_p) \qquad [1]$$

where K is the equilibrium constant for the adsorption and $I_p = I_{p,max}$ at $\theta_p = 1.0$. The value of C_p in the FI system can be related to the bulk concentration (C^b) of the sample injected by the dispersion coefficient (κ) according to

$$\kappa = C_p/C^b \qquad [2]$$

Hence, Eq. 3 is rewritten as

$$\theta_p = I_p/I_{p,max} = K'C^b/(1 + K'C^b) \qquad [3]$$

where $K' = K\kappa$, the dispersed adsorption equilibrium constant for the FI system. For $\theta_p << 1$ (i.e., small C^b or small t_{ads}), $K'C^b << 1$ and Eq. 3 can be simplified to

$$\theta_p = I_p/I_{p,max} = K'C^b \qquad [4]$$

Thus, at short adsorption times, plots of I_p vs. C^b should be linear; however, for large t_{ads} and large C^b, response must be linearized by plotting $1/I_p$ vs. $1/C^b$. These conclusions seem to be supported by the data for thiourea shown in Figures IV-5 and IV-6.

Figure IV-6. Calibration curves ($1/I_p$ vs. $1/C$) for thiourea in 0.25 M NaOH by FI/PAD

Conditions: $V_f = 0.65$ mL min^{-1}, $V_s = 43$ µL

Waveform:

(A) $E_1 = 0.60$ V (300 ms), $E_2 = -1.00$ V (8500 ms), $E_3 = 0.70$ V (50 ms);
(B) $E_1 = 0.60$ V (300 ms), $E_2 = -1.00$ V (1000 ms), $E_3 = 0.70$ V (50 ms);
(C) $E_1 = 0.60$ V (300 ms), $E_2 = -1.00$ V (200 ms), $E_3 = 0.70$ V (50 ms)

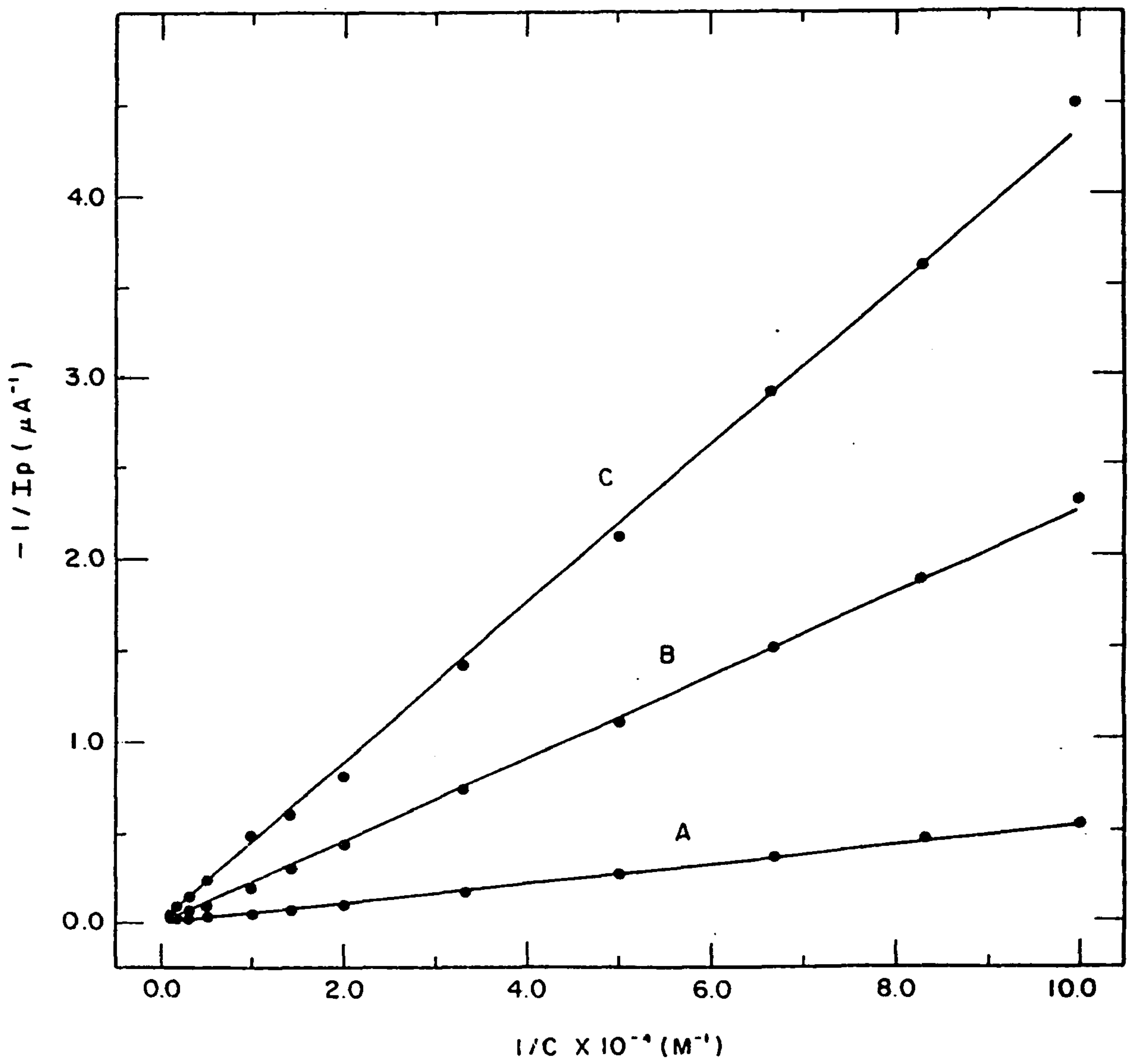

- 1 / Ip (μA⁻¹)
0.0
1.0
2.0
3.0
4.0
C
B
A
0.0
2.0
4.0
6.0
8.0
10.0
1/C X 10⁻⁴ (M⁻¹)

V. THE DEPENDENCE OF RESPONSE ON ADSORPTION TIME FOR PULSED AMPEROMETRIC DETECTION OF SULFUR COMPOUNDS

A. Theory

The reaction which occurs during the adsorption period of the triple-step waveform is represented by

$$S\text{-}H_2O + A \underset{k_{-1}}{\overset{k_1}{\rightleftharpoons}} S\text{-}A + H_2O \qquad [1]$$

where S is a surface adsorption site, A is dissolved analyte at the electrode surface, $S\text{-}H_2O$ is adsorbed water, S-A is adsorbed analyte, and k_1 and k_{-1} are the rate constants for adsorption and desorption, respectively. The net rate of adsorption is given by

$$\dot{\theta}_A = d\theta_A/dt = k_1\theta_{H_2O}C_A{}^s - k_{-1}\theta_A \qquad [2]$$

where θ_A is the fractional surface coverage of adsorbed analyte and $C_A{}^s$ is the concentration of A at the electrode surface. Since $\theta_{H_2O} + \theta_A = 1$, Eq. 2 is rewritten as

$$\dot{\theta}_A = k_1C_A{}^s(1 - \theta_A) - k_{-1}\theta_A \qquad [3]$$

1. Adsorption with no concentration polarization

In the absence of concentration polarization, i.e., very slow adsorption kinetics, the surface and bulk concentrations of A are approximately equal, i.e., $C_A{}^s = C_A{}^b$, and

$$\dot{\theta}_A = k_1 C_A{}^b - (k_1 C_A{}^b + k_{-1})\theta_A \qquad [4]$$

This is a first order differential equation which has the solution

$$\theta_A(t) = [k_1 C_A{}^b/(k_1 C_A{}^b + k_{-1})] + z\cdot\exp\{-(k_1 C_A{}^b + k_{-1})t\} \qquad [5]$$

where z is the integration constant to be determined.

The initial condition for $\theta_A(t)$ in the adsorption period is $\theta_A(0) = 0$. Therefore,

$$z = -k_1 C_A{}^b/(k_1 C_A{}^b + k_{-1}) \qquad [6]$$

and Eq. 5 becomes

$$\theta_A(t) = [k_1 C_A{}^b/(k_1 C_A{}^b + k_{-1})]\cdot[1 - \exp\{-(k_1 C_A{}^b + k_{-1})t\}] \qquad [7]$$

For $t \cong 0$,

$$\exp\{-(k_1 C_A{}^b + k_{-1})t \cong 1 - (k_1 C_A{}^b + k_{-1})t \qquad [8]$$

and so,

$$\theta_A(t) = k_1 C_A{}^b t \qquad [9]$$

For PAD in a flow-injection system (FI/PAD), the peak value of $\theta_A(t)$, i.e., $\theta_p(t)$, is assumed to be equal to the value $I_p/I_{p,max}$ determined in the detection period, where $I_{p,max}$ corresponds to I_p for $\theta_p = 1.0$. Furthermore, for FI/PAD, the value of $C_A{}^b$ in Eqs. 4-9 corresponds to the peak concentration (C_p) which is related to the bulk concentration of the sample injected (C^b) by the dispersion coefficient (κ) of the FI system as defined by

$$\kappa = C_p/C^b \qquad [10]$$

Hence, Eq. 9 is rewritten as

$$\theta_p(t) = I_p/I_{p,max} = k_1\kappa C^b t \qquad [11]$$

Therefore, according to Eq. 11, a plot of I_p vs. C^b, for a specified value of t, is expected to be linear; so too is a plot of I_p vs. t for a constant value of C^b.

For t -> ∞, the boundary condition is in effect, i.e., $\dot{\theta}_A = 0$, and from Eq. 4 we write

$$\lim_{t \to \infty} \theta_A(t) = \frac{k_1 C_A{}^b}{k_1 C_A{}^b + k_{-1}} \qquad [12]$$

which is equivalent to the Langmuir adsorption isotherm

$$\theta_A(\infty) = \frac{K C_A{}^b}{1 + K C_A{}^b} \qquad [13]$$

where $K = k_1/k_{-1}$ is the equilibrium constant for adsorption. Assuming again for FI/PAD that $\theta_p(t) = I_p/I_{p,max}$, the reciprocal of Eq. 13 can be written as

$$\frac{1}{I_p} = \frac{1}{I_{p,max}}\left[1 + \frac{1}{K\kappa C^b}\right] \qquad [14]$$

Hence, whether by Eq. 11 for small t, or Eq. 14 for large t, plots of $1/I_p$ vs. $1/C^b$ are expected to be linear but with different slopes. The intercepts of the plots are expected to be zero for small t and nonzero for large t.

2. Adsorption with concentration polarization

For fast adsorption kinetics, $C_A{}^s << C_A{}^b$ and $\dot{\theta}_A$ for small t is controlled ultimately by the rate of mass transport. The adsorption flux is defined as $\Gamma_o\dot{\theta}_A$, where Γ_o is the maximum molar surface coverage for the adsorbate. The mass transport flux is defined as $k_{mt}(C_A{}^b - C_A{}^s)$, where k_{mt} is the rate of mass transport. Therefore,

$$C_A{}^s = C_A{}^b - (\Gamma_o/k_{mt})\dot{\theta}_A \qquad [15]$$

and Eqs. 3 and 15 are combined to give

$$(1 + \Gamma_o k_1/k_{mt})\dot{\theta}_A + [k_1 C_A{}^b + k_{-1} - (\Gamma_o k_1/k_{mt})\dot{\theta}_A]\theta_A - k_1 C_A{}^b = 0 \qquad [16]$$

The exact solution to Eq. 16, as derived in the appendix of this dissertation for a constant k_{mt}, is

$$\{1+[k_1 k_{-1}\Gamma_o/k_{mt}(k_1 C_A{}^b+k_{-1})]\}\cdot\ln|1-[1+(k_{-1}/k_1 C_A{}^b)]\theta_A| - \Gamma_o k_1\theta_A/k_{mt} = -(k_1 C_A{}^b+k_{-1})t \qquad [17]$$

This equation holds for the initial condition of the adsorption period, assuming k_{mt} is a constant, and the unique solution for the limit at $t = 0$ can be obtained as follows: For very small t, $\theta_A << \theta_{H_2O}$ and Eq. 16 is simplified to

$$(1 + \Gamma_o k_1/k_{mt})\dot{\theta}_A = k_1 C_A{}^b \qquad [18]$$

Since $k_1 >> 0$ under these conditions,

$$\dot{\theta}_A \cong k_{mt} C_A{}^b / \Gamma_o \qquad [19]$$

Integration for constant k_{mt} yields

$$\theta_A(t) = (k_{mt}/\Gamma_o) C_A{}^b t \qquad [20]$$

and, for FI/PAD,

$$\theta_p(t) = I_p/I_{p,max} = (k_{mt}/\Gamma_o)\kappa C^b t \qquad [21]$$

which is analogous with the result given by Eq. 11 for response controlled by slow adsorption kinetics. For a time-dependent k_{mt}, the case of mass transport-limited response is given by

$$\theta_p(t) = I_p/I_{p,max} = (\kappa C^b/\Gamma_o)\int k_{mt} dt \qquad [22]$$

For $t \to \infty$, the adsorption process approaches equilibrium; hence, $\dot{\theta}_A \to 0$ and Eq. 16 becomes

$$(k_1 C_A{}^b + k_{-1})\theta_A = k_1 C_A{}^b \qquad [23]$$

which is equivalent to Eq. 12. Since Eq. 16 has been shown to satisfy the boundary conditions for the adsorption period, values for k_1, k_{-1} and Γ_0 can be evaluated by a mathematical fit of Eq. 17 to experimental data.

B. Adsorption Equilibrium Constant

The response of PAD for thoiurea at $t_{ads} = 8500$ ms was shown in Figures IV-5 and IV-6 and is reproduced here in Figure V-1. The plot of I_p vs. C^b is readily observed to be nonlinear for $C^b > 1 \times 10^{-4}$ M, and in Chapter IV it was suggested that linearization of the data could be achieved by plotting $1/I_p$ vs. $1/C^b$. However, careful examination of the plot of $1/I_p$ vs. $1/C^b$ in Figure V-1 reveals two linear segments. For the region $1 \times 10^5\ M^{-1} > 1/C^b > 1 \times 10^4\ M^{-1}$, the data are linear ($r^2 = 0.991$, $s_{xy} = 6.0 \times 10^{-3}$) with a slope of $5.42 \times 10^{-6}\ \mu A^{-1}\ M^{-1}$ and an intercept of $-0.004\ \mu A^{-1}$, which is virtually zero, as expected for mass transport-limited adsorption (Eq. 21). For the region $1 \times 10^4\ M^{-1} > 1/C^b > 1 \times 10^3\ M^{-1}$, the plot of $1/I_p$ vs. $1/C^b$ also is linear ($r^2 = 0.9943$, $s_{xy} = 2.2 \times 10^{-4}$) with a slope of $3.20 \times 10^{-6}\ \mu A^{-1}\ M^{-1}$ and an intercept of $0.0140\ \mu A^{-1}$, which is concluded to correspond to the isotherm-limited response (Eq. 14). From this intercept, we calculate $I_{p,max} = 71.4$ µA; from the slope, $K\kappa = 4.4 \times 10^3\ M^{-1}$ and, since $\kappa = 0.90$, $K = 4.9 \times 10^4\ M^{-1}$.

Figure V-1. Calibration data for thiourea in 0.25 M NaOH by FI/PAD
Data taken from Curve A in Figure IV-5

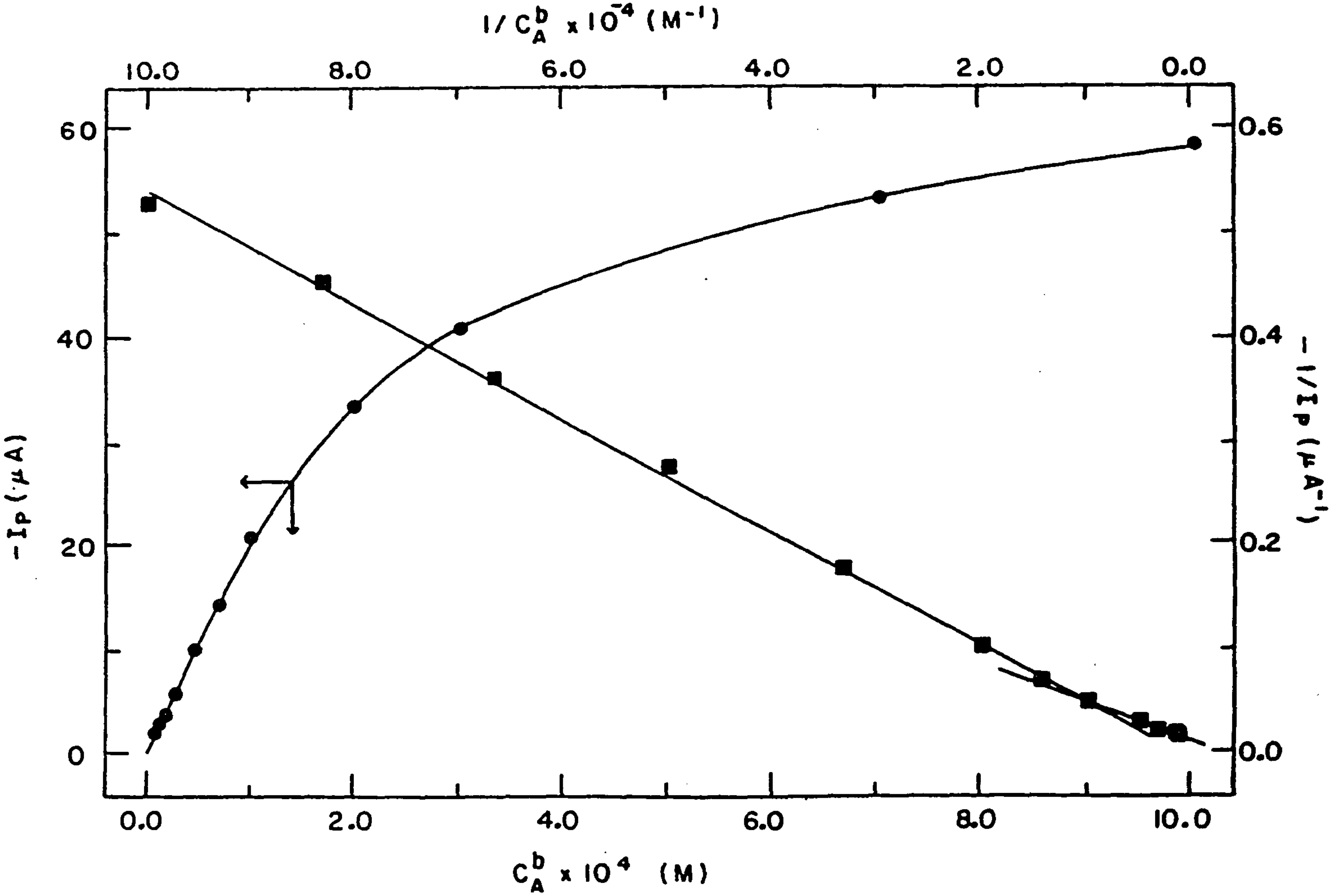

$1/C_A^b \times 10^{-4}$ (M^{-1})
10.0
8.0
6.0
4.0
2.0
0.0
60
40
20
0
$-I_p$ (μA)
0.6
0.4
0.2
0.0
$-1/I_p$ (μA^{-1})
0.0
2.0
4.0
6.0
8.0
10.0
$C_A^b \times 10^4$ (M)

C. Variation of Adsorption Time

To further understand the adsorption behavior of thiourea on Pt, values of I_p were obtained as a function of t_{ads} in the range 100 - 10,000 ms for $C^b = 1.0 \times 10^{-4}$ M; the results are shown in Figure V-2. Electrode response increased rapidly from a region of nonlinear time dependence for $t_{ads} <$ ca. 1000 ms (designated region A), to a linear region (designated B) for ca. 1000 ms $< t_{ads} <$ ca. 3000 ms. The negative deviation from a linear time dependence for $t_{ads} >$ ca. 3000 ms is concluded to be the result of transition from a mass transport-controlled response to isotherm-control. Values of I_p for $t_{ads} <$ ca. 100 ms were often erratic, probably due to slow potentiostatic response.

For a constant mass transport rate (k_{mt}), as assumed in the derivation of Eq. 21, I_p is expected to be a linear function of t_{ads}. This assumption is definitely inappropriate for small t_{ads}, where k_{mt} is given by $(D/\pi t)^{1/2}$. Hence, Eq. 19 for small t is integrated over the period t_{ads} to yield for FI/PAD

$$I_p/I_{p,max} = \theta_p(t) = (2\kappa C^b/\Gamma_o)(Dt_{ads}/\pi)^{1/2} \qquad [24]$$

The slope of the plot of $\log(-I_p)$ vs. $\log(t_{ads})$ in Figure V-3 is 0.50 in region A, in agreement with Eq. 24. At ca. 1.0 s, a break occurs in the log-log plot, and the slope of the plot for region B is 0.80, less than the value of 1.0 expected for

Figure V-2. Dependence of response for thiourea in 0.25 M NaOH on t_{ads}

Conditions: $C^b = 1.0 \times 10^{-4}$ M thiourea, $V_s = 43\ \mu L$,
$V_f = 0.65$ mL min^{-1}

Waveform: $E_1 = 0.60$ V (300 ms), $E_2 = -1.00$ V ($t_2 = t_{ads}$),
$E_3 = 0.70$ V (50 ms)

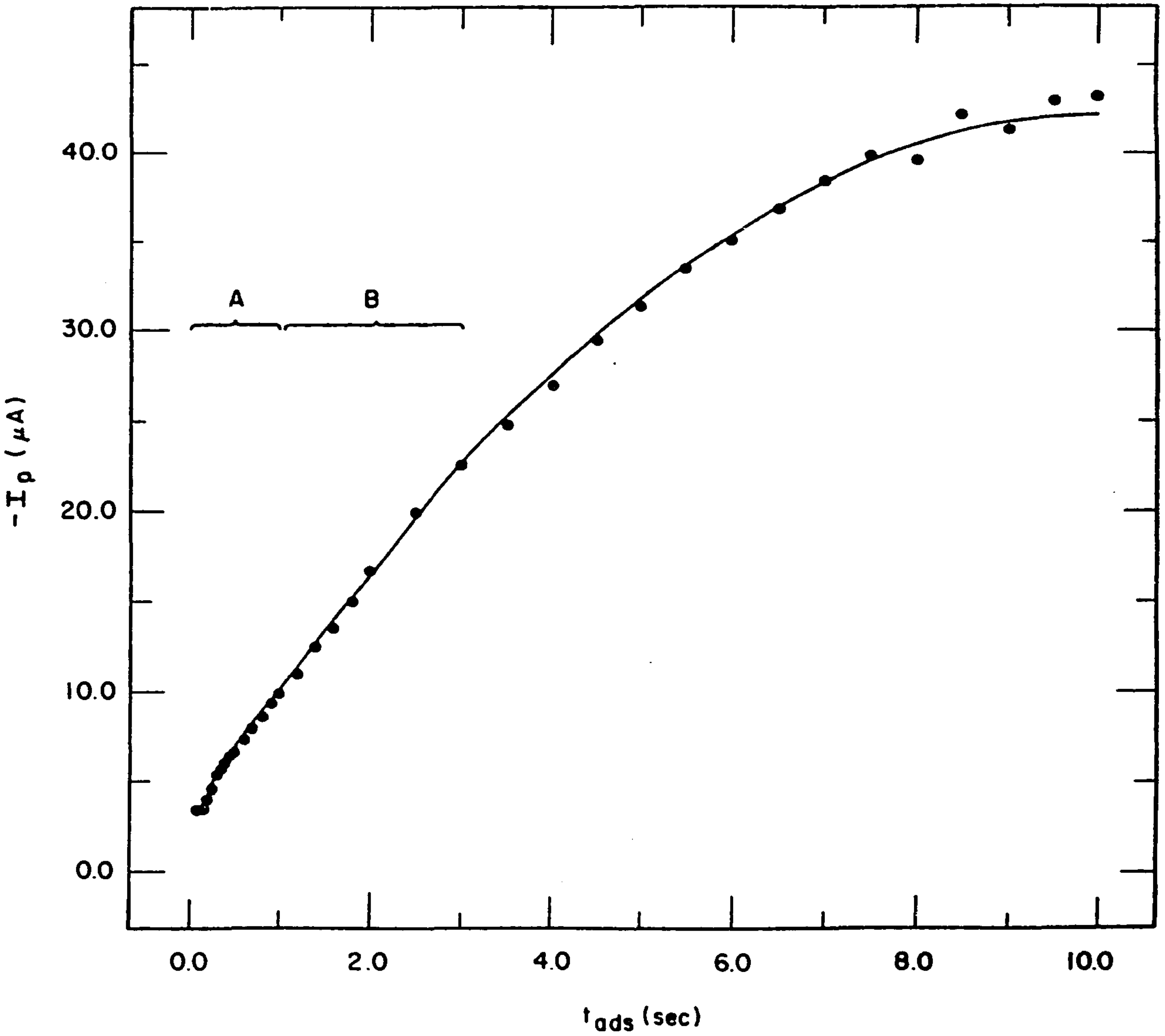

A
B
40.0
30.0
20.0
10.0
0.0
$-I_p$ (μA)
0.0
2.0
4.0
6.0
8.0
10.0
t_{ads} (sec)

Figure V-3. Plot of log ($-I_p/\mu A$) vs. log (t_{ads}/ms) for regions A and B of Figure V-2

Slopes: (A) 0.50, (B) 0.80

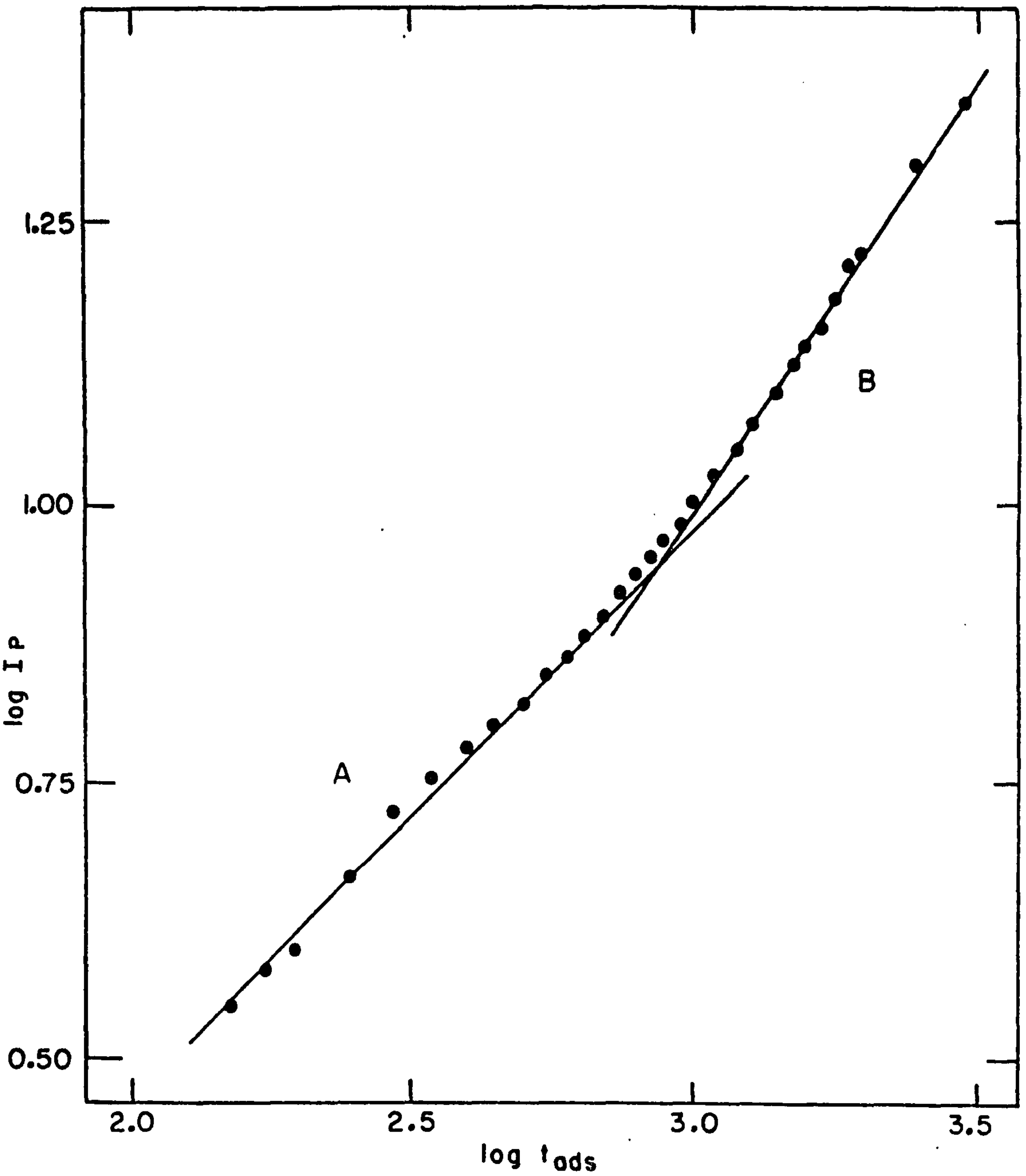
1.25
1.00
0.75
0.50
log I P
A
B
2.0
2.5
3.0
3.5
log tads

constant k_{mt} from Eq. 21. The fact that the observed slope in region B is less than unity is concluded to be a consequence of the transition from pure transport control (region A) to mixed transport-isotherm control (region B and beyond).

Thus far, it has been assumed that $\theta_p(t)$ for the adsorbed analyte at the end of the adsorption period is indicated by the ratio $I_p/I_{p,max}$ determined in the detection period. This assumption cannot be tested rigorously by electroanalytical means without an independent measurement of θ_A. However, the assumption necessitates the independence of $I_p/I_{p,max}$ on variation of the delay time (t_d) in the detection period, which is easily tested. Values of I_p were obtained as a function of t_d for 5.0×10^{-4} M thiourea using $t_{ads} = 100$ and 8500 ms. For $t_{ads} = 100$ ms, I_p is transport limited; for $t_{ads} = 8500$ ms, $I_p = I_{p,max}$ for this concentration. Values of $I_p/I_{p,max}$ corresponded to $\theta_p = 0.69 \pm 0.05$ and were independent of t_d. These results are concluded to add validity to the assumption $\theta_p(t) = I_p/I_{p,max}$.

With confidence gained from the above results, the data in Figure V-2 was subjected to further analysis. In order to evaluate the rate constants k_1 and k_{-1} in Eq. 1, and the maximum surface coverage by the analyte, Γ_θ in Eq. 21, values of $\theta_p(t)$ were generated by dividing values of I_p from Figure V-2 by $I_{p,max} = 71.4$ µA. The desired parameters were then estimated using a cubic spline approximation (171) and the results were verified by numerically solving Eq. 17 and plotting the recalulated $\Theta_p(t)$ as a function of t_{ads} using these calculated constants. The result of this mathematical fitting routine is shown in Figure V-4. The solid line represents the smooth curve obtained by applying the cubic spline approximation to the designated, equally-spaced data points (+), in the region $t_{ads} > 1000$ ms. C^b was 1.0×10^{-4} M (1×10^{-7} mol cm^{-3}) and k_{mt} was assumed equal to the value $(D/\pi t)^{1/2}$ at t = 1000 ms; using $D = 1 \times 10^{-5}$ cm^2 s^{-1}, k_{mt} = 1.8×10^{-3} cm s^{-1}. The results of the cubic spline approximation are $k_1 = 4.0 \times 10^4$ M^{-1} s^{-1} and $k_{-1} = 1.9$ s^{-1}; hence K = $k_1/k_{-1} = 2.1 \times 10^4$ M^{-1}, as compared to the value 4.9×10^4 M^{-1} obtained from the plot of $1/I_p$ vs. $1/C^b$ for $t_{ads} = 8500$ ms. The calculated value of Γ_o is 1.3×10^{-10} mol cm^{-2}. The density of surface sites on a polycrystalline Pt electrode is estimated to be 3.0×10^{15} atoms cm^{-2}, calculated from the density of the metal and an assumed surface roughness factor of 2. Hence, for thiourea, we estimate that each adsorbed molecule occupies ca. 40 surface Pt atoms, seemingly an excessive estimate. The numeric solution to Eq. 17 is represented by the dashed line in Figure V-4, and it is readily apparent that there exists a high correlation between the experimental data and the numerical solution, thereby lending credibility to the proposed mathematical model.

Figure V-4. Numerical solutions in data from Figure V-2

$\theta = -I_p/71.4\ \mu A$

(+) data chosen from Fig. V-2 at regular intervals of t_{ads}
(-) results of cubic spline approximation
(---) numerical results calculated using k_1, k_{-1}, and Γ_o obtained by cubic spline approximation

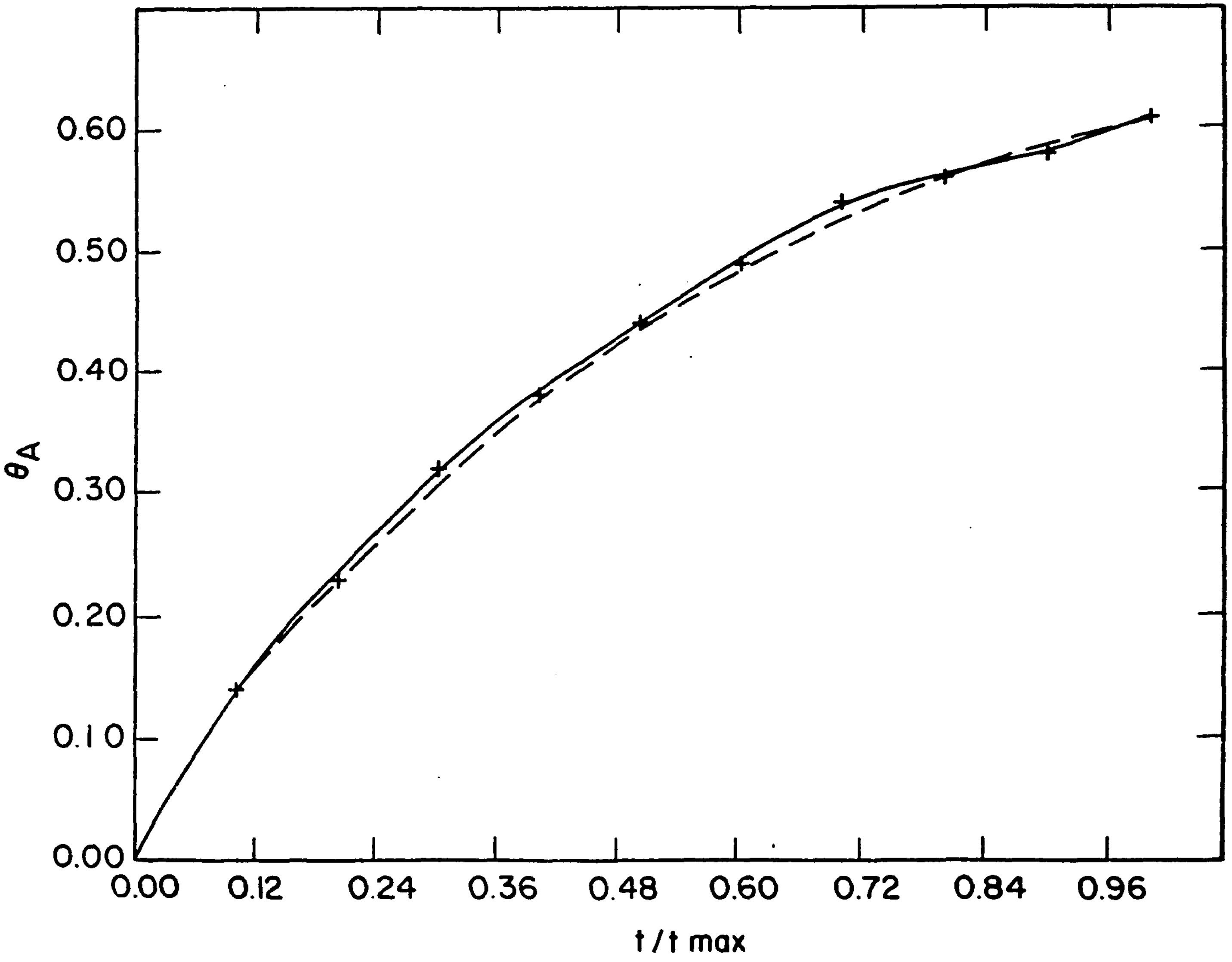
0.60
0.50
0.40
0.30
0.20
0.10
0.00
θ_A
0.00
0.12
0.24
0.36
0.48
0.60
0.72
0.84
0.96
t / t max

D. Analytical Calibration in PAD

Because linear calibration plots are preferred for amperometric detection in flow-injection and liquid chromatographic systems, linear plots of I_p vs. C^b are desirable. Typically, for tests of linearity of response over two or more decades of concentration, log-log plots of I_p vs. C^b are examined and the slope of such plots are expected to be unity. The log-log plots for detection of thiourea by PAD in the FI system at t_{ads} = 200, 1000, and 8500 ms are shown in Figure V-5. The linear approximations shown were calculated by linear regression for 1.0×10^{-5} M < C^b < 1.0×10^{-4} M, where mass transport control is most likely. The calculated slopes are: (A) 0.986, (B) 1.048 and (C) 1.046. Reference lines of slope = 1.0 are included in Figure V-5 for visual comparison. Shown also (curve D) is the predicted isotherm-limited response (i.e., for $t_{ads} = \infty$) calculated from Eq. 14 using $K\kappa = 4.4 \times 10^3$ M^{-1}. The value of $\log(-I_{p,max})$ is represented also in the figure. Based on these results, it is concluded that PAD response for thiourea at Pt electrodes is mass-transport controlled for $I_p/I_{p,max}$ < ca. $0.2\ K\kappa C^b/(1 + K\kappa C^b)$.

The interdependence of amperometric response on $K\kappa$ and t_{ads} can be seen qualitatively with the aid of Figure V-5. Assume, for this example, that the adsorption energy of the analyte is significantly less than for thiourea such that $K\kappa$

Figure V-5. Plots of log $(-I_p/\mu A)$ vs. log (C^b/M) for thiourea in 0.25 M NaOH

Data from Figure IV-5

Curves: (A) t_{ads} = 200 ms
(B) t_{ads} = 1000 ms
(C) t_{ads} = 8500 ms
(D) predicted response for t --> ∞ ,
i.e., isotherm-limited response

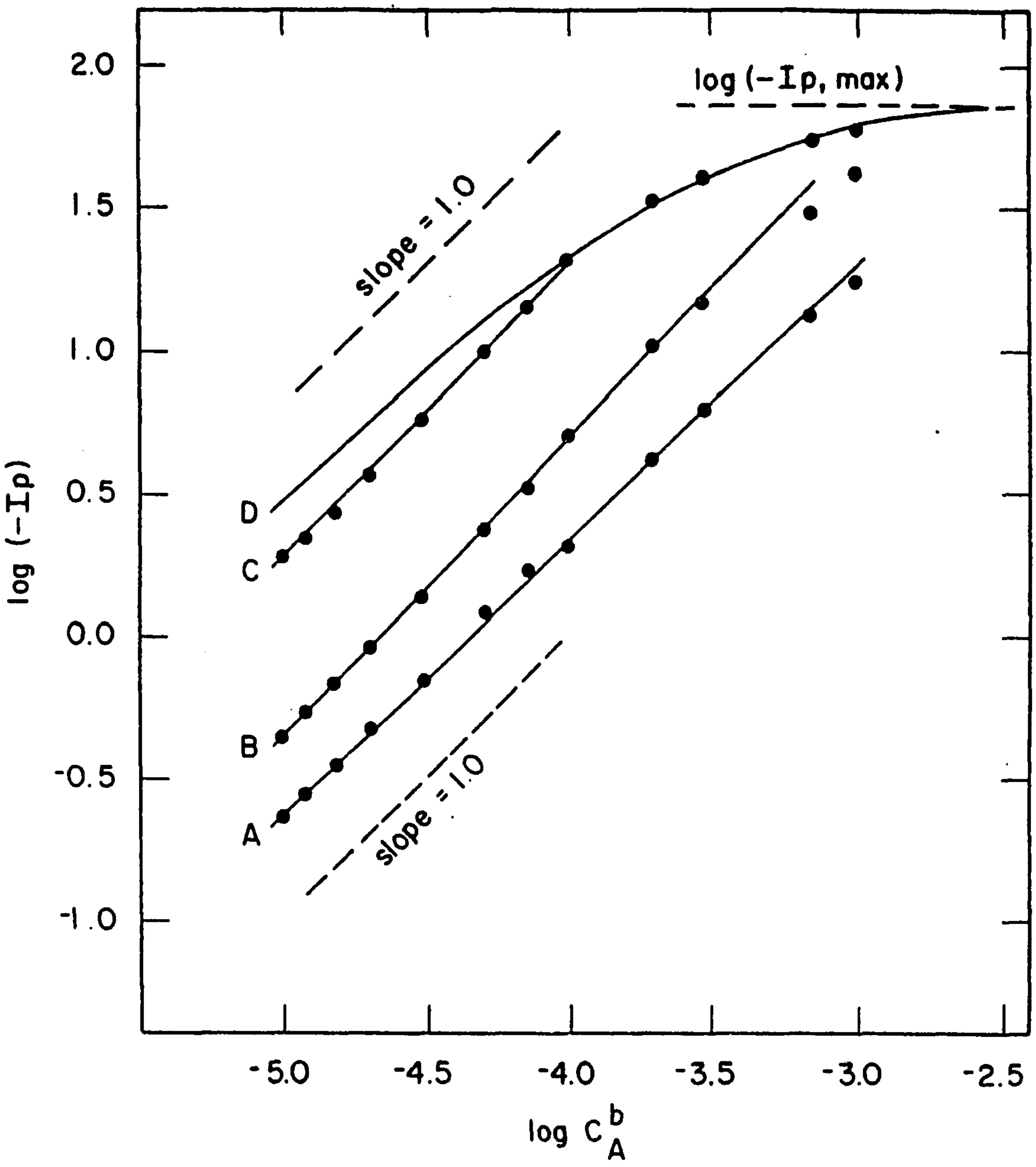
log (−Ip, max)
slope = 1.0
slope = 1.0
D
C
B
A
log (−Ip)
2.0
1.5
1.0
0.5
0.0
-0.5
-1.0
-5.0
-4.5
-4.0
-3.5
-3.0
-2.5
log C_A^b

is decreased by a factor of 10 to 4.4×10^2 M^{-1}. Presume also that $I_{p,max}$ remains unchanged from that indicated in Figure V-5 for thiourea. Hence the isotherm-limited response at $C^b = 1 \times 10^{-5}$ M is decreased approximately by a factor of 10 (i.e., $\log(-I_p)$ = ca. -0.5 at $\log(C^b) = -5.0$). Therefore, isotherm-limited response in this case is expected for t_{ads} = 200 ms, whereas for thiourea, the isotherm-limited response is not observed even at t_{ads} = 8500 ms for $C^b = 1.0 \times 10^{-5}$ M. The values of K for adsorption of carbohydrates and amines are generally much less than for thiourea and increased response is not usually obtained for t_{ads} > ca. 200 ms for many of these compounds. The practical consequence to calibration for compounds with small K is that response is frequently under mixed control by mass transport and the adsorption isotherm even for very dilute solutions.

VI. PULSED AMPEROMETRIC DETECTION OF INORGANIC SULFUR COMPOUNDS AT GOLD ELECTRODES IN ALKALINE SOLUTION

A. Cyclic Voltammetry

The voltammetric response of thiocyanate (SCN^-), carbon disulfide (CS_2) and sulfite (SO_3^{2-}) at gold electrodes in 0.25 M NaOH is illustrated adequately by the I-E curve for thiosulfate ($S_2O_3^{2-}$) obtained for a cyclic, linear scan of potential as shown in Figure VI-1. The residual response of the electrode (curve a) obtained in the absence of $S_2O_3^{2-}$ is characterized by an anodic wave during the positive scan for $E > -0.2$ V, which corresponds to the formation of the surface oxide layer (172). Rapid evolution of $O_2(g)$ occurs for $E > 0.7$ V. The oxide layer is reduced on the negative potential scan to produce the peak at 0.05 V. Evolution of $H_2(g)$ occurs at $E < -1.45$ V. Upon addition of $S_2O_3^{2-}$, oxidation of the analyte produces an anodic current peak at $E = 0.45$ V on the positive potential scan (curve b), with the peak current found to increase as a nonlinear function of the bulk concentration of the analyte (C^b). There is, however, virtually no evidence for oxidation of $S_2O_3^{2-}$ on the subsequent negative scan in the region $E = 0.6$ to 0.3 V. The cathodic currents observed in the region $E = -1.0$ to -1.45 V are probably due to the reduction of SO_3^{2-} and trithionate, formed as intermediates during the oxidation of $S_2O_3^{2-}$.

Figure VI-1. Current-potential curves for thiosulfate at a Au RDE by cyclic voltammetry in 0.25 M NaOH

Conditions: $\phi = 6.0\ \mathrm{V\ min^{-1}}$, $W = 94\ \mathrm{rad\ s^{-1}}$

Concentrations: (a) 0.00 mM, (b) 0.10 mM

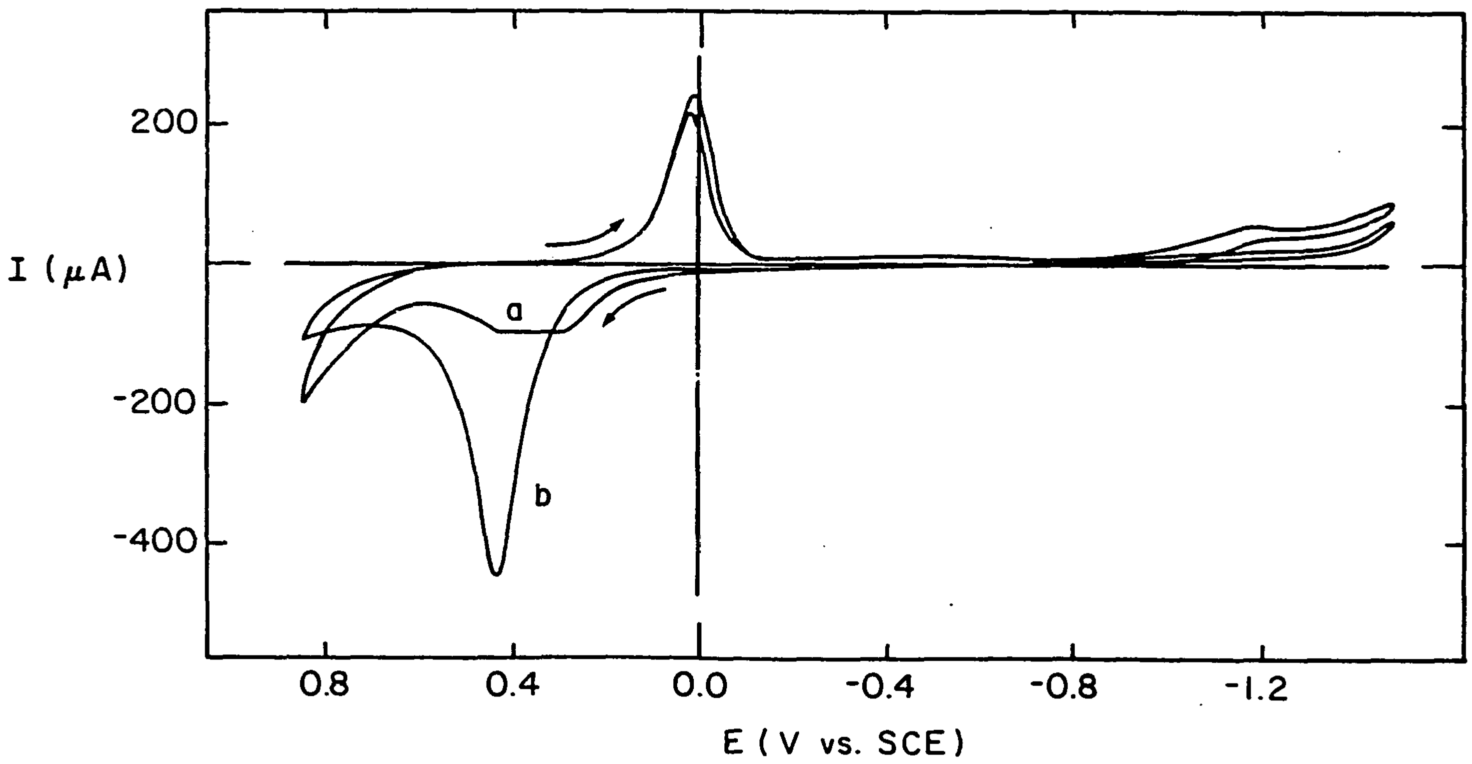
200
I (μA)
-200
-400
a
b
0.8
0.4
0.0
-0.4
-0.8
-1.2
E (V vs. SCE)

The anodic current peak for thiosulfate obtained on the positive potential scan was determined to vary in height as a linear function of potential scan rate and to be virtually independent of the rotational velocity of the RDE. Such behavior is consistent with the conclusion that the oxidation is a surface-controlled reaction. Furthermore, the oxide film produced on the positive potential scan to 0.85 V prevents further detection of $S_2O_3^{2-}$ on the negative potential scan.

The unique voltammetric response of sulfide (S^{2-}) at gold electrodes in 0.25 M NaOH is illustrated by the I-E curves shown in Figure VI-2. The residual response is again represented as curve a. In the presence of sulfide, oxidation of the analyte produces an anodic wave on the positive potential scan in the region E = -0.3 to 0.9 V (curves b - f). Not only does the current increase as a nonlinear function of bulk concentration of sulfide, but also the potential at which the anodic current peak occurs shifts with additions of sulfide.

The shape of the anodic wave indicates that the oxidation of S^{2-} occurs in at least two steps. The anodic current peak which occurs at ca. - 0.2 V on the positive potential scan is concluded to be the result of the initial oxidation of sulfide to form a surface film containing polysulfides and/or molecular sulfur. This gold sulfide film is known to

Figure VI-2. Current-potential curves for sulfide at a Au RDE by cyclic voltammetry in 0.25 M NaOH

Conditions: $\emptyset$ = 6.0 V min^{-1}, W = 94 rad s^{-1}

Concentrations (mM): (a) 0.00, (b) 0.10,
(c) 0.20, (d) 0.30,
(e) 0.40, (f) 0.50

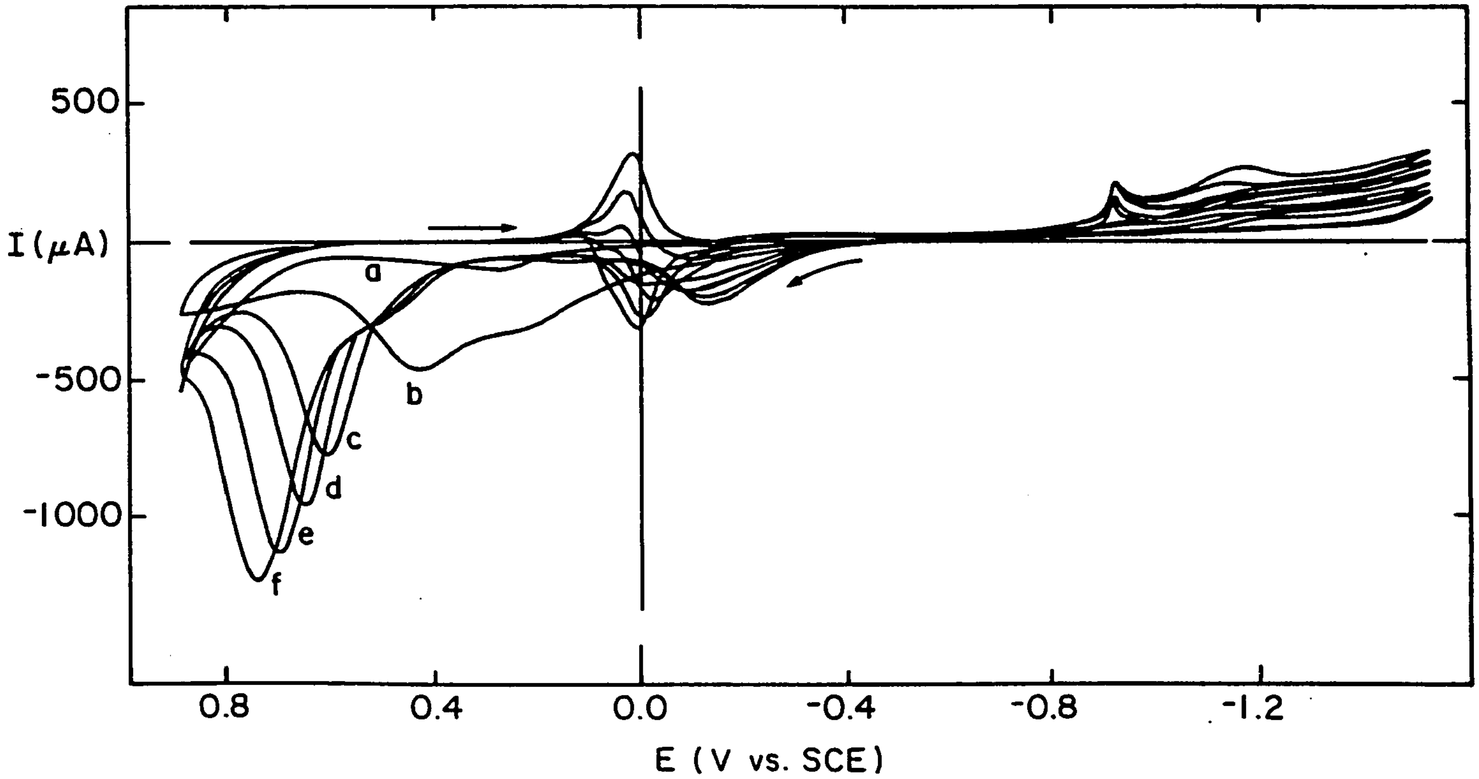
500
I (μA)
-500
-1000
a
b
c
d
e
f
0.8
0.4
0.0
-0.4
-0.8
-1.2
E (V vs. SCE)

inhibit the formation of gold oxides; thus, the wave immediately preceding the main anodic current peak is suggested to be the delayed formation of surface oxide. The main anodic current peak is the result of the further oxidation of sulfide to sulfur oxyanions. The shifting of the peak towards higher potentials with increasing sulfide concentration is understandable in that larger amounts of sulfide present in solution result in the formation of more gold sulfide film, upon initial oxidation (E = 0.0 to -0.2 V). It follows that the larger amount of gold sulfide formed is more inhibiting toward surface oxide formation and the subsequent oxidation of sulfide to sulfur oxyanions (E > 0.0 V); thus, the potential of the maximum rate of reaction shifts toward more positive values.

During the negative potential scan, an anodic current peak is observed at 0.0 V. Sulfide oxidation is known not to occur on oxide covered surfaces and, indeed, no anodic current is observed for E = 0.85 to 0.1 V. Reduction of the oxide film beginning at 0.1 V, however, generates bare gold sites upon which oxidation of sulfide to gold sulfide film again occurs. Continuing the negative potential scan results in the reduction of the sulfide film back to S^{2-} in the region E = -0.9 to -1.45 V.

B. Calibration

Calibration plots were obtained for thiosulfate, thiocyanate and sulfide using FI and PAD. The waveform applied at the gold flow-through electrode was $E_1 = 0.50$ V (300 ms), $E_2 = 0.80$ V (10 ms) and $E_3 = -0.75$ V (500 ms). I_p vs. C^b plots were linear for $C^b < 0.10$ mM for all three inorganic species ($r^2 = 0.9966$ ($S_2O_3^{2-}$); 0.9934 (SCN^-); 0.9979 (S^{2-})), but deviated significantly from linearity at higher concentrations. This behavior is the same as that observed for the detection of alcohols, carbohydrates, and amino acids by PAD, and is concluded to be the consequence of a reaction mechanism in which only adsorbed species are detected (see Chapter V). Hence, the anodic signal is proportional to the surface coverage (Θ) of the adsorbed analyte. Based on the Langmuir isotherm, for which a plot of I_p vs. C^b is expected to be valid only for $\Theta << 1$ (small C^b), plots of $1/I_p$ vs. $1/C^b$ are predicted to be linear for all Θ. This prediction was verified for thiosulfate, thiocyanate, and sulfide, and linear reciprocal plots were obtained for $0.01 \text{ mM} < C^b < 1.0$ mM.

C. Liquid Chromatography

Interest in the separation and detection of sulfur containing inorganic anions has developed due to the recent emphasis of the effects of these compounds in the environment. In addition to environmental concerns, polysulfides are of interest because of their wide use as intermediates in organic and inorganic synthesis. Thus, PAD was joined with HPLC to learn more about the nature of polysulfides and to determine if separation and detection of sulfur containing inorganic anions is feasible with these combined techniques.

Deoxygenated solutions containing 0.1 mM polysulfide ions (S_x^{2-}, where x = 1 - 5) were injected onto a Dionex AS6 anion-exchange column, with 0.1 M NaOH containing 0.05 M Na_2SO_4 as the eluent. Using PAD, it was determined that S_x^{2-} decomposes to S^{2-} and $S_2O_3^{2-}$ in the time scale of the sample handling and liquid chromatographic separation. It should be noted that no attempt was made to deoxygenate the eluent, as oxygen permeable Teflon tubing was required by the eluent utilized. It is concluded that this dissolved oxygen is responsible for the oxidation of S_x^{2-} during the LC separation. Upon extended exposure to air (many days), $S_2O_3^{2-}$ was the only ion detected in the solution which originally had contained S_x^{2-}. In addition, it was found that oxidation of S_x^{2-} by hydrogen peroxide (H_2O_2) also produces $S_2O_3^{2-}$. Sulfate could not be eliminated as a product of oxidation with O_2 because its presence cannot be determined by PAD. Therefore, it is concluded from these results that $S_2O_3^{2-}$ and/or SO_4^{2-} are the final products formed upon oxidation of S_x^{2-}.

In order to compare the separation ability of eluent systems, a previous separation (117) of S^{2-}, SO_3^{2-} and $S_2O_3^{2-}$

was first duplicated using pulsed amperometric detection. This separation is shown in Figure VI-3. These same ions were then separated using conditions that were optimized for HPLC using PAD. Figure VI-4 illustrates the improved sensitivity of detection and the larger S/N ratio obtained with these optimized conditions. The order of anion elution in Figures VI-3 and VI-4 is not the same due to the different modifying ions which were added to the NaOH. Changing NaOH concentration does not affect the elution order.

Calibration curves for sulfide, sulfite and thiosulfate are shown in Figure VI-5. These curves were obtained using the HPLC/PAD system and over the short range of dilute concentrations examined, the plot of I_p vs. C^b is approximately linear for all three anions ($r^2 = 0.9956$ (S^{2-}), 0.9999 (SO_3^{2-}), 0.9862 ($S_2O_3^{2-}$)). Detection limits (S/N = 2) using this system were determined to be 0.64 ppm for sulfide, 4.0 ppm for sulfite and 2.3 ppm for thiosulfate. The detection is more sensitive than that reported by Story (151) using post-column derivatization and UV detection.

Figure VI-3. Chromatogram of sulfide, sulfite and thiosulfate

Conditions:

Column: Dionex AS6

Eluent: 5 mM NaOH containing 20 mM KNO_3, 1.0 mL min^{-1}

Sample: 50 µL

Waveform: as given in text

Peaks: (1) 0.015 mM S^{2-}
(2) 0.20 mM SO_3^{2-}
(3) 0.10 mM $S_2O_3^{2-}$

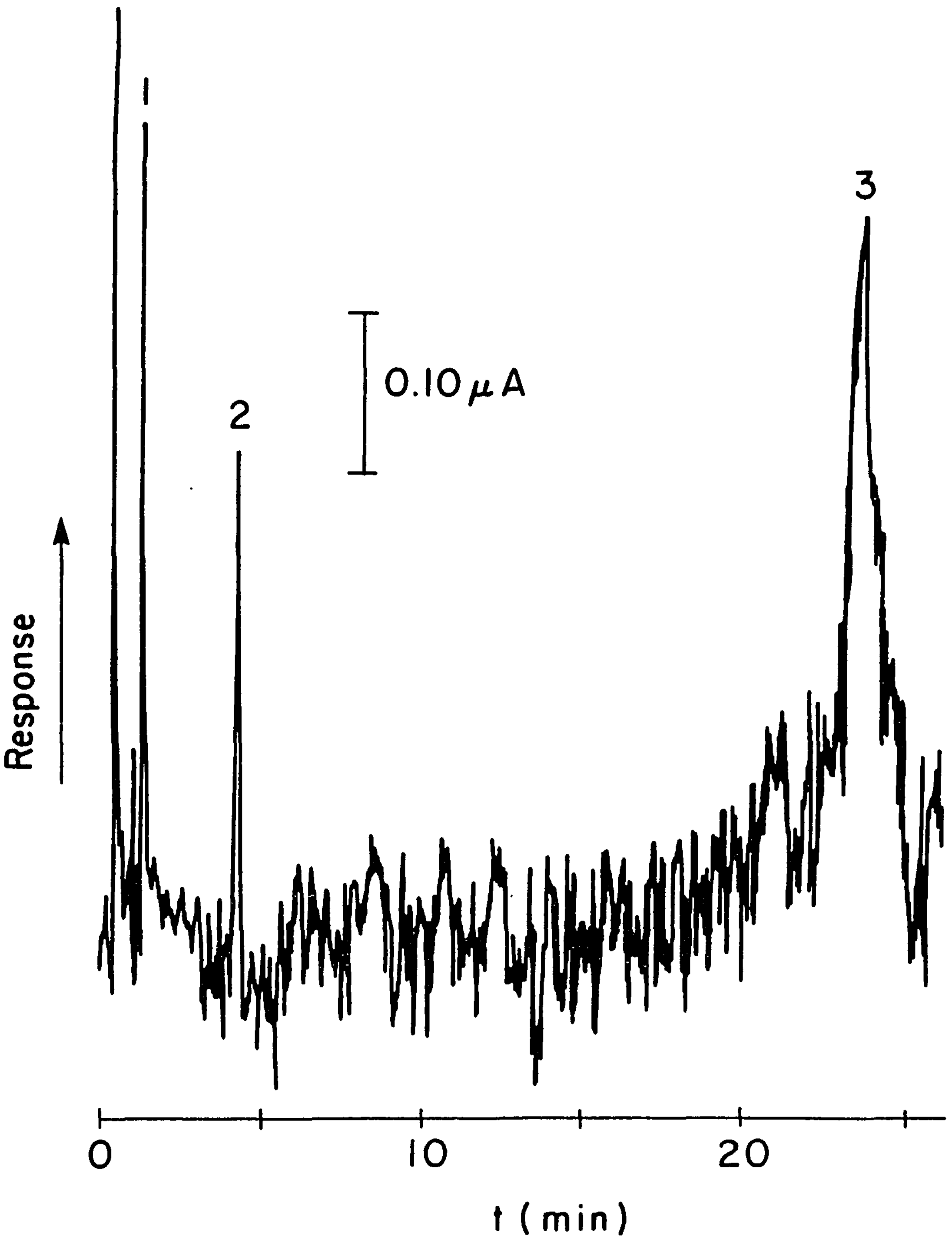
Response
0.10 μA
1
2
3
0
10
20
t (min)

Figure VI-4. Chromatogram of sulfide, sulfite and thiosulfate using PAD

Conditions:

Column: Dionex AS6

Eluent: 0.1 M NaOH containing 50 mM Na_2SO_4, 1.0 mL min^{-1}

Sample: 50 µL

Waveform: as given in text

Peaks: (1) 0.20 mM SO_3^{2-}

(2) 0.015 mM S^{2-}

(3) 0.10 mM $S_2O_3^{2-}$

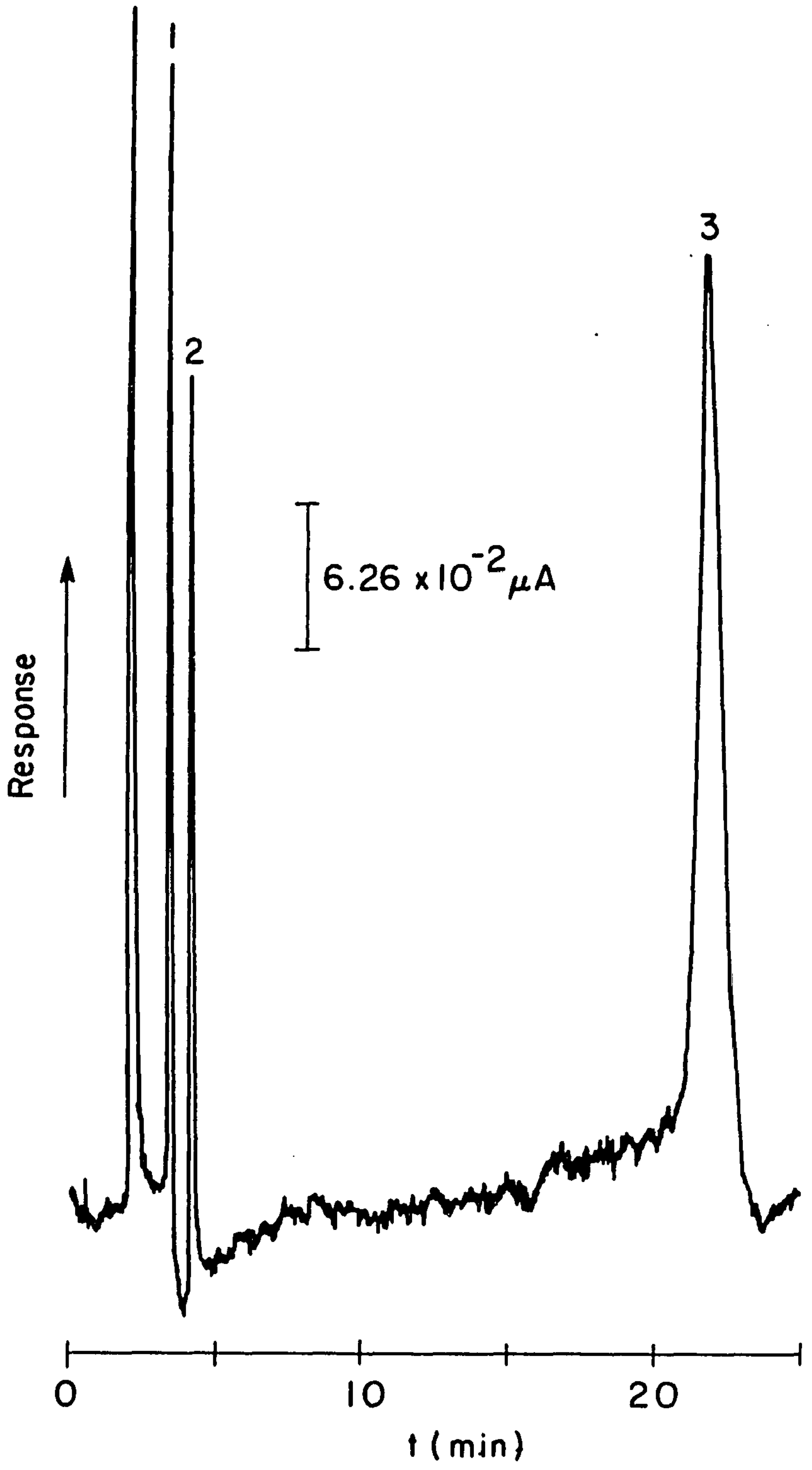
1
2
3
6.26 x 10^{-2} μA
Response
0
10
20
t (min)

Figure VI-5. Calibration curves (I_p vs. C^b) for sulfide, sulfite and thiosulfate by HPLC/PAD

Conditions:

Column: Dionex AS6

Eluent: 0.1 mM NaOH containing 50 mM Na_2SO_4, 1.0 ml min^{-1}

Sample: 50 µL

Waveform: as given in text

Plots: (a) $S_2O_3^{2-}$

$I_p = 0.01 + 10.0\ C^b$

(b) SO_3^{2-}

$I_p = -0.51 + 58.2\ C^b$

(c) S^{2-}

$I_p = 0.11 + 4.4\ C^b$

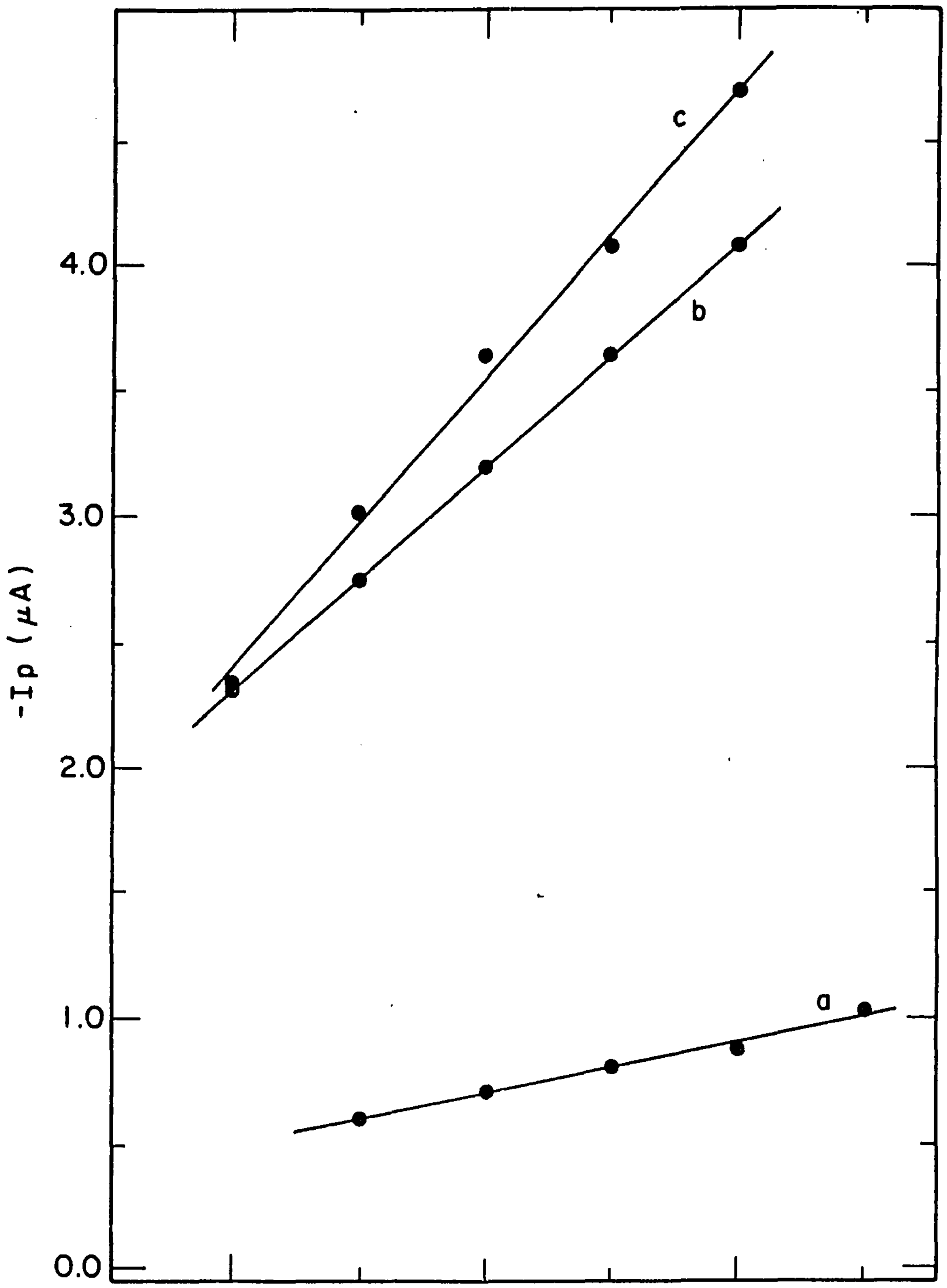
-Ip (μA)
0.0
1.0
2.0
3.0
4.0
5
7
9
C (x10^4 M, b; x10^5 M, a & c)
a
b
c

VII. PULSED AMPEROMETRIC DETECTION OF ORGANIC SULFUR COMPOUNDS AT GOLD ELECTRODES IN AQUEOUS SOLUTIONS

A. Cyclic Voltammetry

The voltammetric response of several sulfur containing organic compounds was obtained for preliminary characterization using cyclic voltammetry in 0.25 M NaOH. Aqueous base was chosen as the electrolyte to minimize the volatility of the compounds studied, and because additional investigations using anion-exchange chromatography with NaOH as the eluent were anticipated. Similar anodic response was observed for the numerous organic sulfur compounds listed in Table VII-1, and thiourea again was chosen as a representative compound for further study. A typical I-E curve for thiourea at a Au RDE is shown in Figure VII-1. The processes which define the residual response (curve a) are adequately described in Chapter VI.

Upon the addition of thiourea (curve b), oxidation of the analyte produces an anodic wave on the positive potential scan in the region -0.15 to 0.8 V. The shape of this anodic wave indicates that the oxidation of thiourea occurs in two steps. The current which is observed in the region -0.15 to 0.1 V on the positive potential scan is concluded to be the formation of the dimer formamidine disulfide, the first oxidation product of thiourea. Continuing the positive scan results in the formation of oxygen containing

Table VII-1. Representative organic sulfur compounds detected by PAD in alkaline media

Class	Structure	Example studied
Thioamide	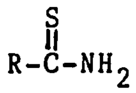 $R\text{-}\overset{S}{\overset{\|}{C}}\text{-}NH_2$	R = NH_2 (thiourea) R = CH_3 R = $NHCH_3$ R = $NHNH_2$ R = 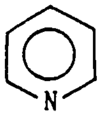
Cyclic thioamide	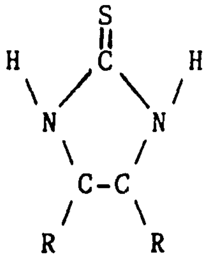	R = H
Thiophene	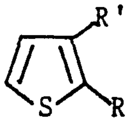	R' = $CH(COOH)_2$, R = H R = COOH, R' = H
Thiocarbamate	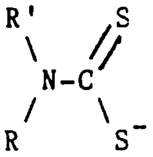	R = R' = C_2H_5 R = R' = CH_3 R = R' = C_2H_5O

Figure VII-1. Current-potential curves for thiourea at a Au RDE by cyclic voltammetry in 0.25 M NaOH

Conditions: Ø = 6.0 V min^{-1}, W = 94 rad s^{-1}

Concentrations: (a) 0.00 mM, (b) 0.10 mM

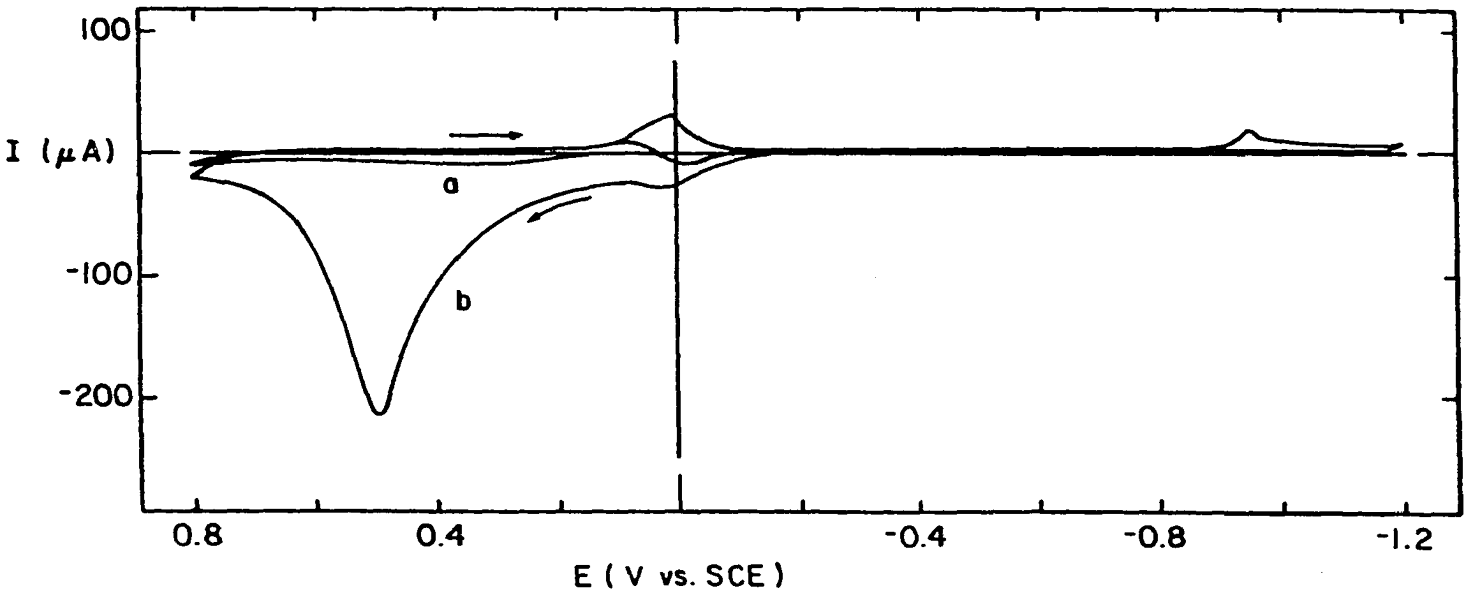
100
I (μA)
-100
-200
a
b
0.8
0.4
-0.4
-0.8
-1.2
E (V vs. SCE)

oxidation products of thiourea in the region 0.1 to 0.8 V. However, this oxidation is severely inhibited by the surface oxide formed during the positive scan, as noted by the dramatic decrease in current upon reversal of the scan at 0.8 V.

During the negative potential scan, no anodic current is observed until $E < 0.05$ V. At potentials greater than this, the electrode is covered with an oxide film, but the reduction of the oxide film beginning at 0.1 V generates bare Au sites upon which oxidation of thiourea to its dimerized product can recommence. Continuing the negative scan is thought to result in the reduction of formamidine disulfide back to thiourea in the region -0.9 to -1.2 V.

The anodic current for thiourea in the region 0.1 to 0.8 V was found to be dependent on the rate of potential scan. A plot of current vs. scan rate was approximately linear with a zero intercept, indicating that the oxidation is a surface-controlled process. An unexpected result was that the current also was found to be a linear function of rotation speed, although the intercept was nonzero. As a comparison, a plot of current vs. rotation speed is linear with a zero intercept for a reaction which is purely mass-transport limited. Thus, it is concluded that mass transport, as well as adsorption, is a factor in determining the anodic response for thiourea. It should be noted, though, that the rate of oxidation of the transported thiourea is controlled by the rate of surface oxide generation and, hence, is a linear function of scan rate. This behavior is identical to that found for the oxidation of thiourea at Pt electrodes.

The anodic current response for thiourea in the region -0.15 to 0.1 V for both the positive and negative potential scans and the cathodic current in the region -0.9 to -1.2 V were found to vary in height only as a function of potential scan rate. Such behavior is consistent with the conclusion that the oxidation and reduction reactions in these regions are surface-controlled. These results also support the earlier conclusion that the dimer of thiourea is the product of the oxidation step at potentials ca. 0.0 V, as this reaction has only been reported to occur at electrode surfaces.

B. Pulsed Amperometric Detection

Amperometric detection of thiourea at a constant electrode potential is not successful for analytical quantitation because of rapid fouling of the electrode surface by the dimerization product, as well as the formation of gold oxides for $E > -0.2$ V. The anodic current response with and without thiourea is shown as a function of time in Figure VII-2 (curves a and b). This type of current decay curve is concluded to result from the oxide-catalyzed oxidative

Figure VII-2. Current-time curves for thiourea at a Au RDE in 0.25 M NaOH

Conditions: W = 377 rad s^{-1}

Concentrations (mM): (a,c) 0.00, (b,d) 0.50

DC detection: (a,b) E = 0.50 V

Pulse detection: (c,d) E_1 = 0.50 V (250 ms)

E_2 = 0.80 V (10 ms)

E_3 = -0.75 V (500 ms)

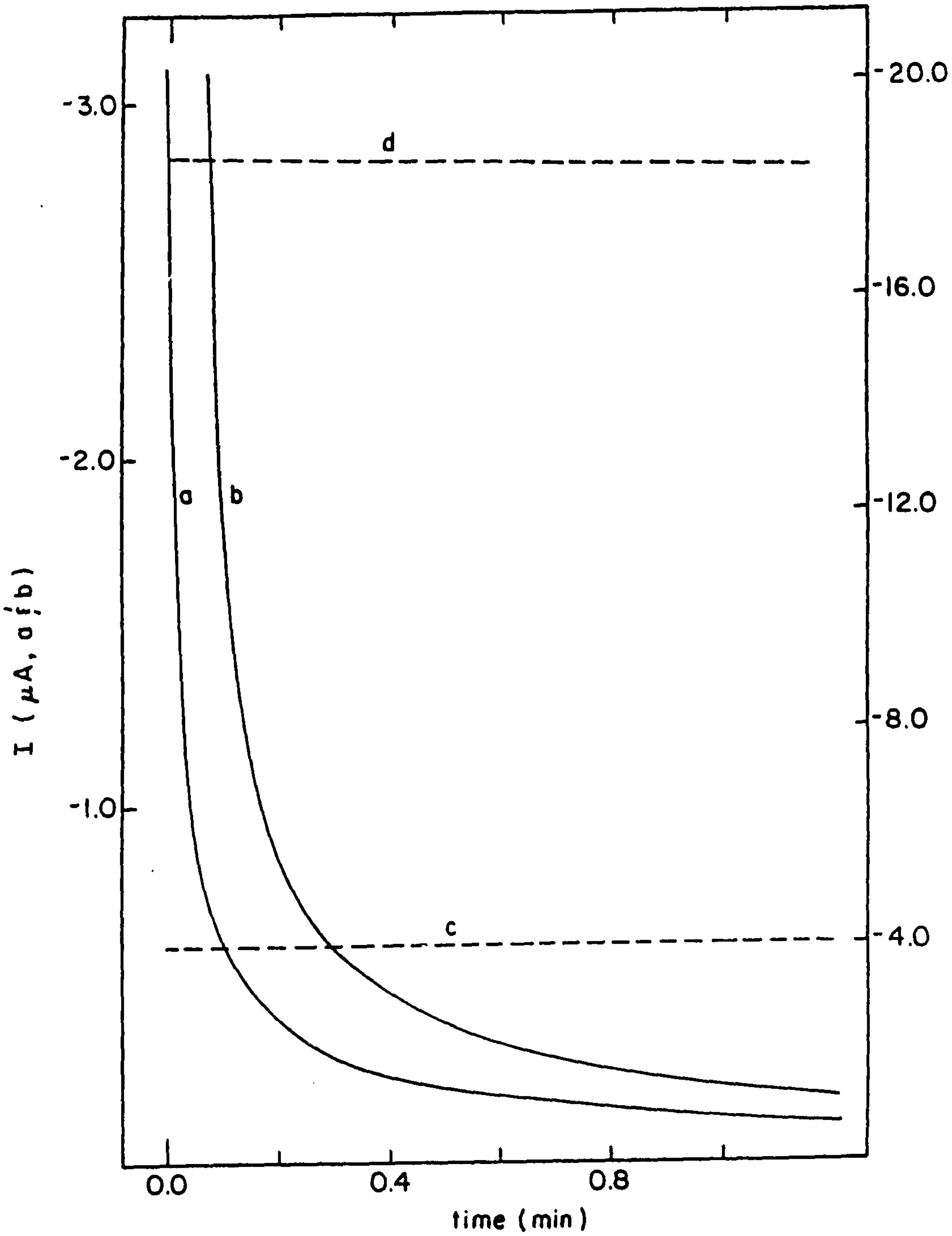
-3.0
-2.0
-1.0
I (μA, a & b)
-20.0
-16.0
-12.0
-8.0
-4.0
I (μA, c & d)
0.0
0.4
0.8
time (min)
a
b
c
d

desorption of thiourea. Also shown in Figure VII-2, is the current response of the electrode upon application of PAD with and without thiourea (curves d and c, respectively). It is readily apparent that the signal response is steady in both cases. The analytical significance of a steady background signal is that it can be electronically offset while amplifying the anodic current signal for the analyte. In addition, it should be noted that in comparison with Pt, the background signal is much smaller on Au, which results in a larger S/N ratio and, hence, lower concentration limits for detection of the analyte.

The selection of an appropriate potential waveform for maximum sensitivity for thiourea with PAD was made on the basis of the I-E curve in Figure VII-1. E_2 was chosen corresponding to the region of rapid oxide reduction and analyte adsorption. E_3 was chosen greater than E_1 to decrease the background current measured at E_1, as the rate of oxide formation at E_3 is greater than at E_1. A suitable value for E_1 was determined from hydrodynamic voltammagrams shown in Figure VII-3. The anodic current is measured 50 ms after a delay period of 300 ms to allow the background currents to decay to a reasonably small value before sampling the faradaic signal for the oxidation of adsorbed thiourea. Upon comparison of the cyclic and pulsed voltammetric curves, it is readily apparent that the shape of the anodic wave

Figure VII-3. Current-potential curves for thiourea at Au by pulsed voltammetry in 0.25 M NaOH

Conditions: E_1 varied (300 ms),
E_2 = -1.15 V (500 ms),
E_3 = 0.90 V (50 ms),
$W = 94$ rad sec^{-1}

Concentrations (mM): (•) 0.0, (X) 0.50

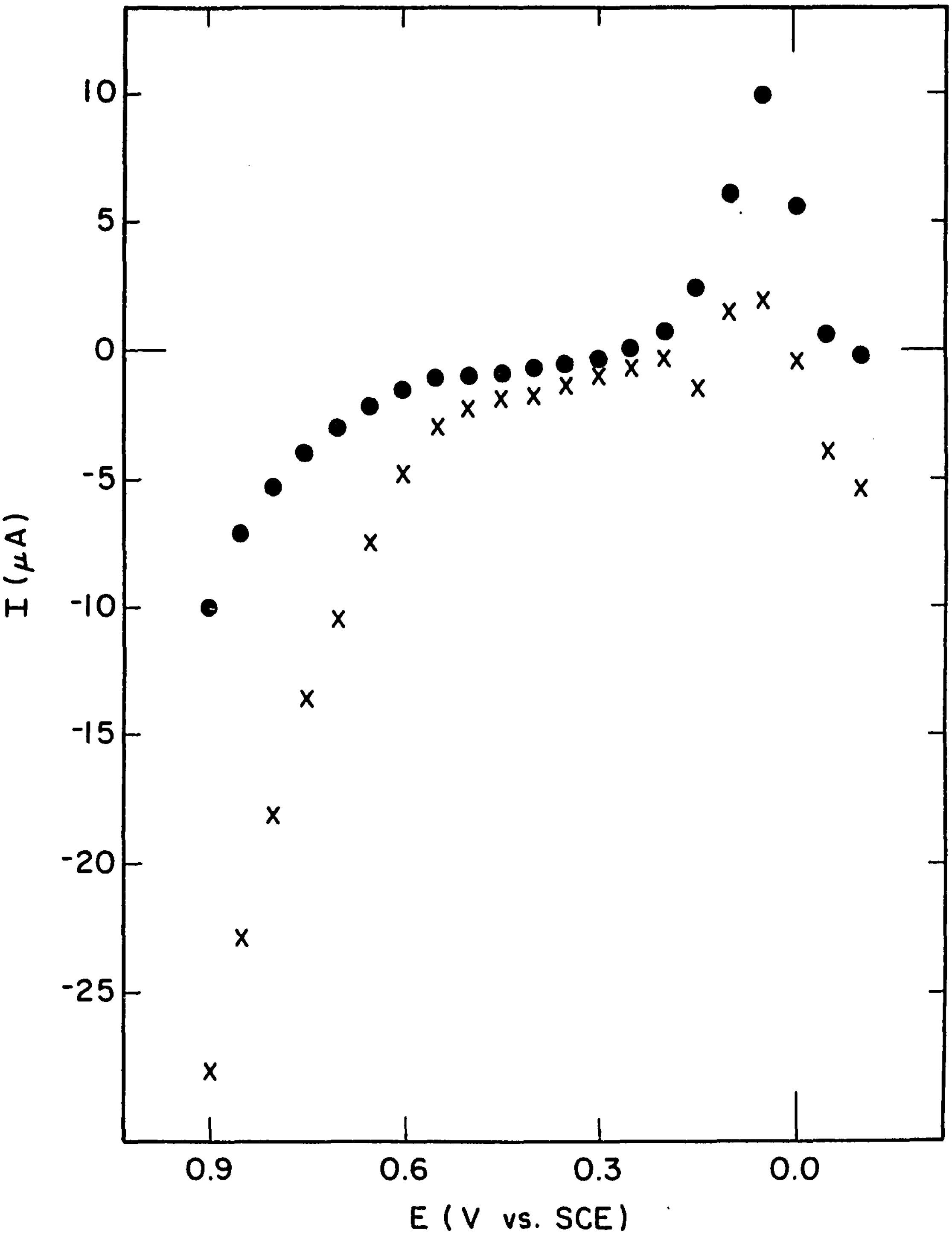
10
5
0
-5
-10
-15
-20
-25
I (μA)
0.9
0.6
0.3
0.0
E (V vs. SCE)

differs for the two experiments. Also, the largest difference between the anodic current signal with and without thiourea occurs at 0.9 V for the pulsed experiment, unlike the cyclic experiment where the maximum occurs at ca. 0.5 V.

An additional study was performed in order to determine the appropriate sequence to apply the waveform potentials to achieve the largest S/N ratio when current is sampled at E_1. It was found that the S/N ratios were larger for detection of thiourea at Au when E_2 was chosen in the vicinity of oxygen evolution and E_3 was in the region of oxide reduction and analyte adsorption. When the waveform was executed in this sequence, it also was found that the time spent to oxidatively clean the electrode surface could be decreased, and reproducible results would still be obtained upon detection at E_1.

C. Dependence of Response on Adsorption Time

To better understand the adsorption behavior of thiourea on Au, values of I_p were obtained as a function of t_{ads} in the range 0 - 1000 ms for $C^b = 1 \times 10^{-4}$ M; the results are shown in Figure VII-4. The data points for $t_{ads} < 300$ ms resemble the adsorption behavior described by Frumkin (173). The Frumkin adsorption isotherm takes into account lateral interaction between adsorbed molecules and can account for multilayer formation on the electrode surface. When graphically represented, the Frumkin adsorption isotherm is

Figure VII-4. Dependence of current response for thiourea in 0.25 M NaOH on t_{ads}

Conditions: $V_f = 0.70$ mL min^{-1}, $V_s = 47$ µL

Waveform: $E_1 = 0.50$ V (250 ms), $E_2 = 0.80$ (10 ms),
$E_3 = -0.75$ V ($t_3 = t_{ads}$)

Concentration: 0.10 mM

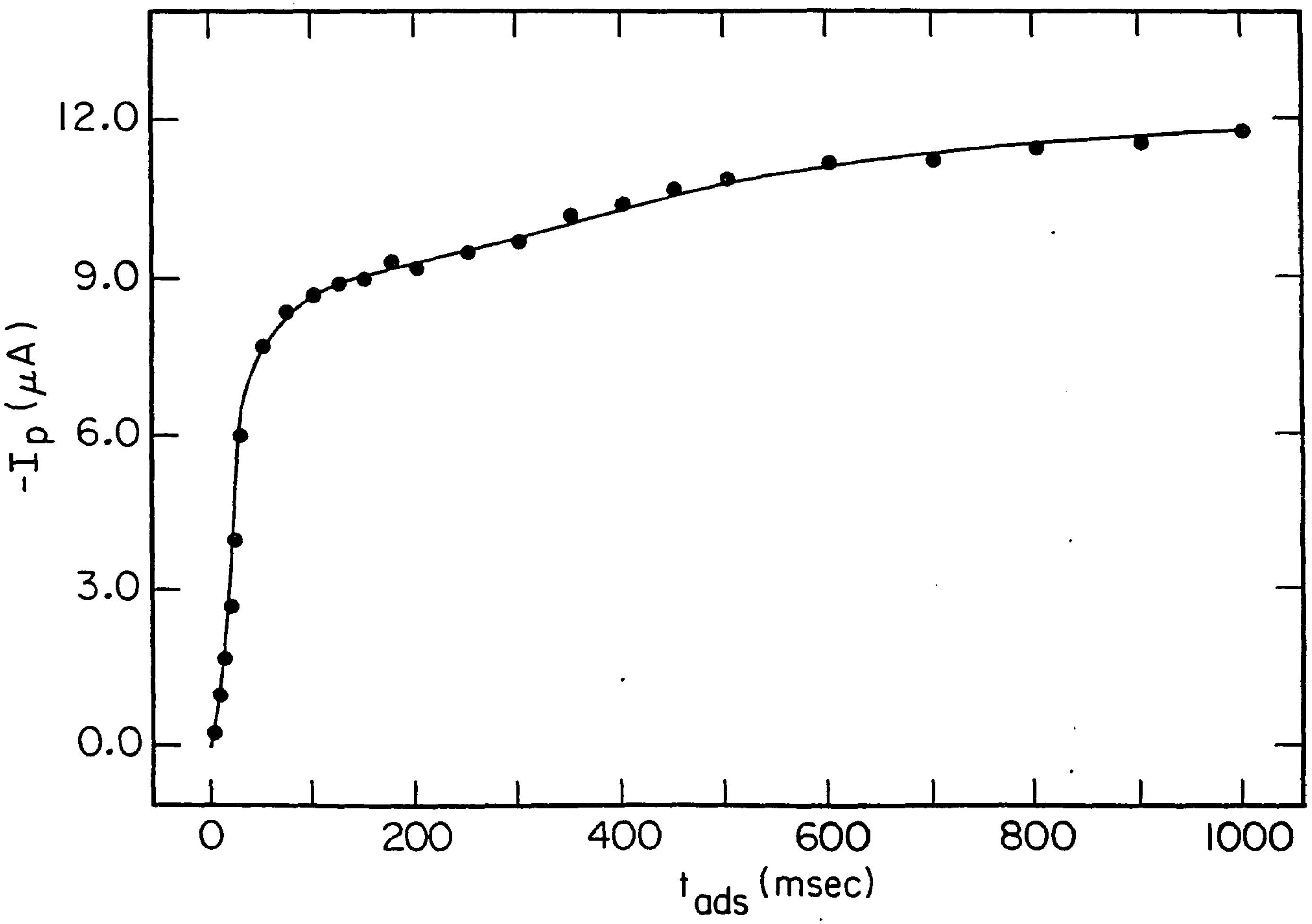
12.0
9.0
6.0
3.0
0.0
$-I_p$ (μA)
0
200
400
600
800
1000
t_{ads} (msec)

characteristically "s-shaped". In order to more clearly visualize the data for $t_{ads} < 50$ ms, the fractional surface coverage by the adsorbate (Θ_A) was estimated using $\Theta_A = I_p/I_{p,max}$. $I_{p,max}$ was determined by averaging the I_p values for $35 < t_{ads} < 100$ ms and was found to be equal to 8.19 μA. The plot of Θ vs. t_{ads} for $t_{ads} < 50$ ms, shown in Figure VII-5, exemplifies the typical "s-shaped" curve associated with the Frumkin isotherm and reveals the knee of the curve, commonly accepted as the point of completion of a monolayer of adsorbate, or some stable fraction thereof. The later data points in Figure VII-4, $t_{ads} > 300$ ms, resemble the isotherm plateau region described by Langmuir. The current response in this region is one-half again as much as the current response obtained for the first plateau region; therfore, it is concluded that an additional one-half of a monolayer, or stable fraction thereof, is adsorbed before surface saturation by the adsorbate is complete.

An intuitive approach was applied to further understand the adsorption phenomena which accounts for the results obtained for $t_{ads} < 35$ ms (Figure VII-5). The reaction which occurs during the adsorption period of the triple-step waveform is represented by

$$S + A \longrightarrow S\text{-}A \qquad [1]$$

where S is a surface adsorption site, A is dissolved analyte at the electrode surface, and S-A is adsorbed analyte. The

Figure VII-5. Dependence of fractional surface coverage for thiourea in 0.25 M NaOH on t_{ads}

Data taken from Figure VII-4

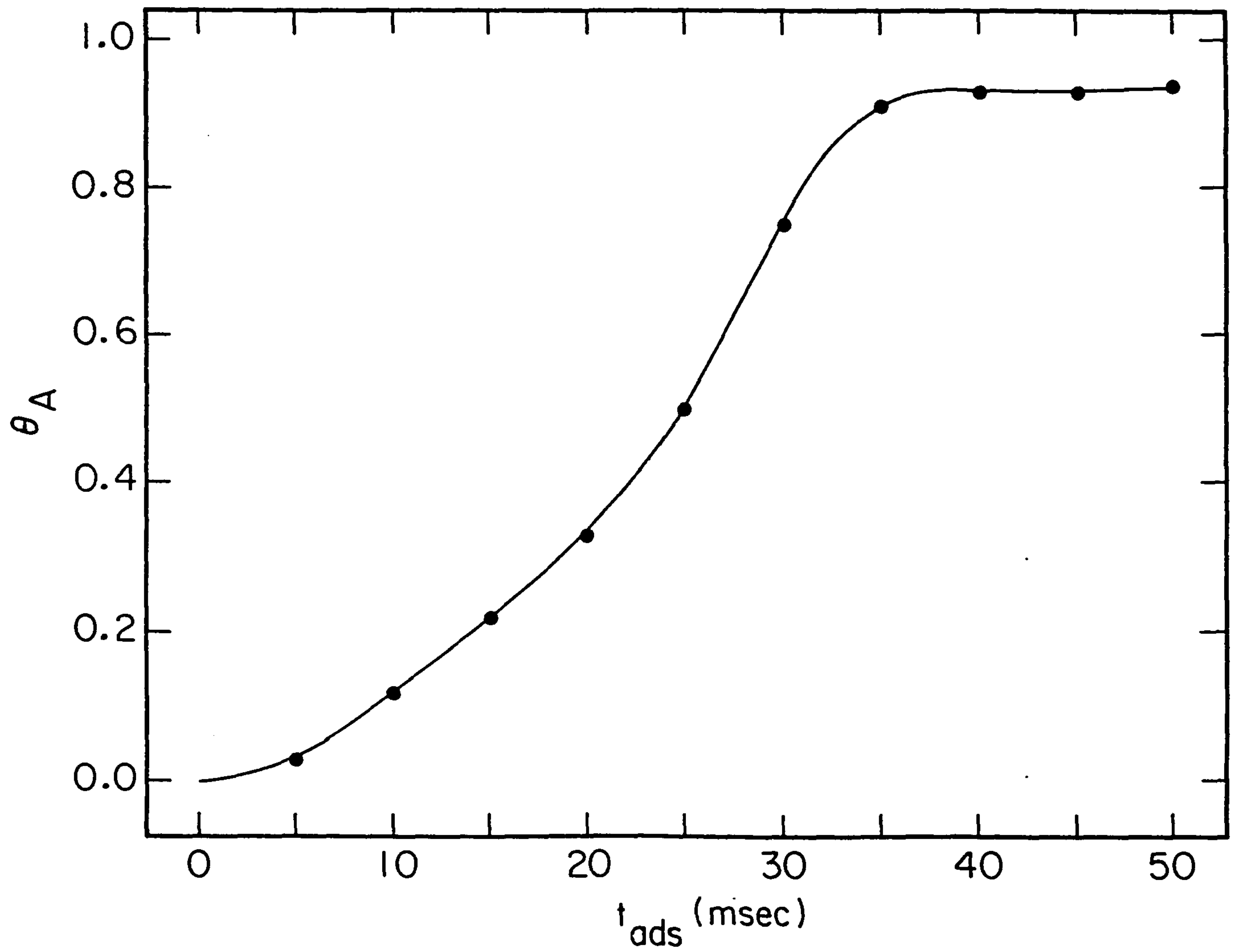
1.0
0.8
0.6
0.4
0.2
0.0
θ_A
0
10
20
30
40
50
t_{ads} (msec)

simplest rate law which can explain the data shown for $t_{ads} <$ 35 ms in Figure VII-5 is given by

$$\dot{\theta}_A = d\theta_A/dt = a + b\theta_A^x \qquad [2]$$

where θ_A is the fractional surface coverage by adsorbed analyte, a and b are rate constants, and x is to be determined. If x = 1, a plot of $\dot{\theta}_A$ vs. θ_A should be linear with a slope equal to b and an intercept equal to a. When plotted, the data proved to be approximately linear ($r^2 = 0.9844$), thus indicating that the assumption x = 1 was well-founded. In addition, the following numerical values were obtained: a = 0.01 and b = 0.05.

The validity of this simple rate law was further tested by rearranging Eq. 2 to give

$$\dot{\theta}_A - a = b\theta_A^x \qquad [3]$$

Therefore, plotting log ($\dot{\theta}_A$ - a) vs. log θ_A should give an experimentally obtained value of x as the slope and log (b) as the intercept. The results of the actual plot gave x = 0.9 and b = 0.04. These values agree closely with the earlier assumption and results, and lead to the conclusion that the rate law given by Eq. 2 adequately describes the adsorption behavior of thiourea on Au for very short adsorption times. No further attempt was made to clarify the adsorption dynamics due to the complexity of the mathematics encountered upon integration of the differential equation of the rate law.

D. Flow-Injection Analysis

Application of the waveform with $E_1 = 0.50$ V (300 ms), $E_2 = 0.80$ V (10 ms) and $E_3 = -0.75$ V (500 ms), for flow-injection detection of thiourea on Au, gave reproducible peaks (rsd < 5% for 30 injections), with representative results shown in Figure VII-6. In addition, calibration plots were obtained for thiourea using FI and PAD. I_p vs. C^b plots were linear for $C^b < 0.10$ mM, but deviated significantly at higher concentrations. As discussed in Chapter IV, for large t_{ads} and large C^b, response must be linearized by plotting $1/I_p$ vs. $1/C^b$. When the data were plotted in this reciprocal manner, linearity of response was obtained over the entire concentration range studied ($0.01 \text{ mM} < C^b < 1.0$ mM). The detection limit for thiourea using this PAD waveform with the FI system is 0.38 ppb (i.e., 17 pg in a 45 -µL sample).

E. Liquid Chromatography

The applicability of PAD for organic sulfur compounds is further demonstrated in the following figures for the chromatographic separation of synthetic mixtures of selected groups of compounds. Included in the discussions on the chromatographic resolution and detection of related compounds

Figure VII-6. Detection peaks for thiourea in 0.25 M NaOH by FI/PAD

Conditions: V_f = 0.60 mL min^{-1}, V_s = 40 µL

Waveform: E_1 = 0.50 V (250 ms),
E_2 = 0.80 (10 ms),
E_3 = -0.75 V (500 ms)

Concentration: 0.10 mM

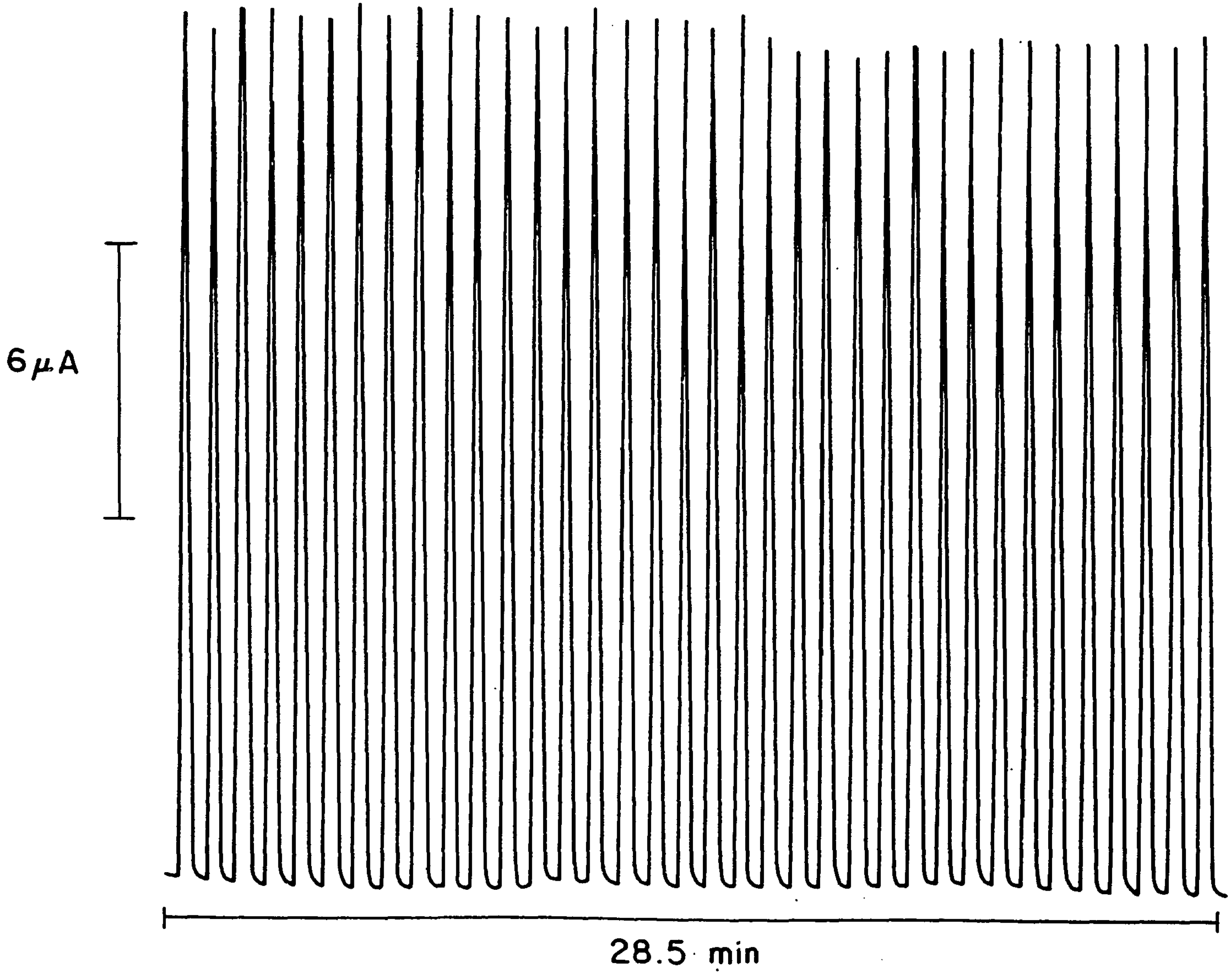
6 μA
28.5 min

will be a brief summary of the principal uses for the specific compounds of interest.

Thiourea and other simple thioamides form an important group of pesticides and are expected to be present in solutions of the pesticides following biological breakdown. Thiourea, one of the most widely used nitrification inhibitors found in common fertilizers, has been shown to be carcinogenic for rats and mice. Ethylenethiourea is a major degradation product of ethylenebisdithiocarbamate fungicides and has been reported to be carcinogenic and teratogenic in rats and mice. The monitoring of these toxic thioureas and related compounds is therefore desirable and a representative chromatogram obtained using anion-exchange chromatography with PAD is shown in Figure VII-7.

Other related thioamides with higher molecular weights are also of interest. Thiosemicarbazide (NH_2-NH-CS-NH_2) is used as an additive in the photographic and textile industries, in galvanic baths and in the manufacture of plastics. In addition, their potent antiviral effect causes thiosemicarbazide and its derivatives to be widely used in pharmacology. Thiosemicarbazide is also an important component in certain agrochemicals which are used as pesticides. These wide practical uses for thiosemicarbazide give reason for trying to develop a simple method for its analytical determination from other similar compounds.

Figure VII-7. Chromatogram of thioureas and thioacetamide using PAD

Conditions:

Column: Dionex AS6

Eluent: 0.1 M NaOH, 1.0 mL min^{-1}

Sample: 50 µL

Waveform: E_1 = 0.65 V (375 ms)
E_2 = 0.80 V (10 ms)
E_3 = -0.75 V (500 ms)

Peaks: 1 - 0.3 mM urea
2 - 0.01 mM ethylene thiourea
3 - 0.02 mM thiourea
4 - 0.02 mM thioacetamide

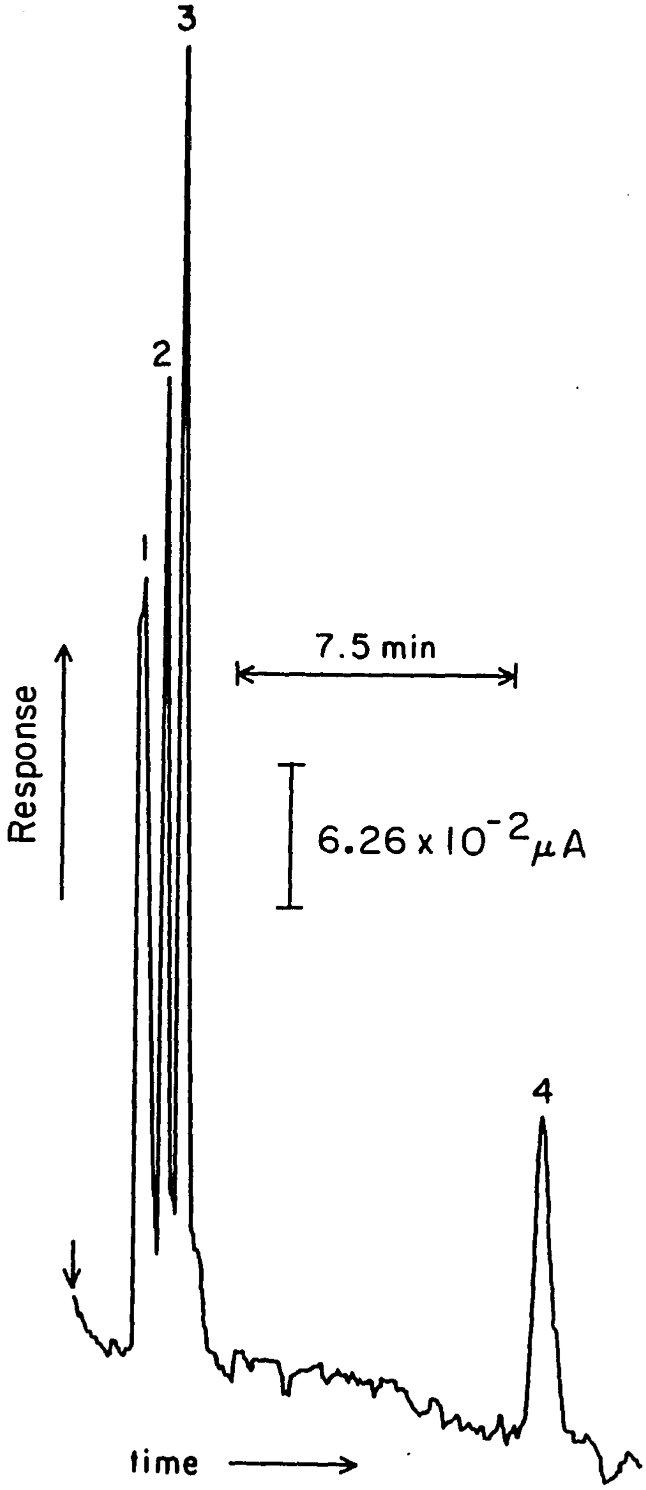
3
2
1
4
Response
7.5 min
$6.26 \times 10^{-2} \mu A$
time

The separation of thiosemicarbazide and thionicotinamide was chosen to demonstrate the usefulness of PAD with HPLC for determining moderate molecular weight thioamides, and a representative chromatogram is shown in Figure VII-8. To affect this separation, a novel chromatographic system was utilized which will be fully explained in the subsequent paragraphs.

HPLC with PAD for organic sulfur compounds is illustrated further in Figure VII-9 for a mixture of 2-thiophenecarboxylic acid and 3-thiophenemalonic acid. These types of compounds are particularly difficult to separate using common ion-exchange chromatography. The large nonspecific interaction of the aromatic portions of these molecules with divinylbenzene makes it nearly impossible to elute them from an anion-exchange column; on the other hand, no retention is observed for cation-exchange columns. What was desired was a very low capacity cation-exchange material which has a capacity that could be varied easily to obtain the appropriate balance between the nonspecific interaction of the analyte with the divinylbenzene and the anion-anion repulsion with cation-exchange sites. For this purpose, a novel chromatographic system was developed using a neutral polystyrene based column (Dionex MPIC) with benzoic acid added to the mobile phase as a modifier. Under the alkaline conditions utilized, a benzoate concentration of 1.0 mM decreased

Figure VII-8. Chromatogram of thiosemicarbazide and thionicotinamide using PAD

Conditions:

Column: Dionex MPIC

Eluent: 0.1 M NaOH containing 1.0 mM Benzoic Acid, 0.5 mL min^{-1}

Sample: 50 µL

Waveform:
E_1 = 0.65 V (375 ms)
E_2 = 0.80 V (10 ms)
E_3 = -0.75 V (500 ms)

Peaks:
1 - 0.25 mM thiosemicarbazide
2 - 0.5 mM thionicotinamide

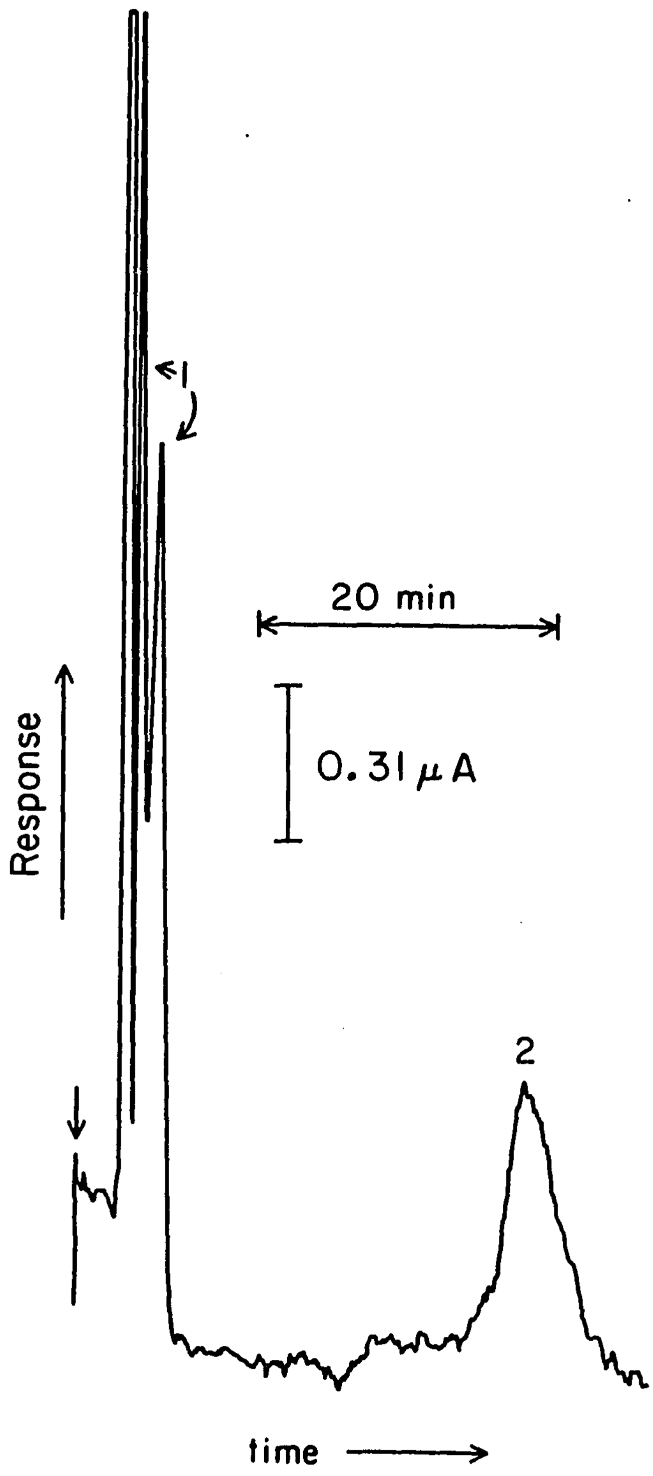
1
20 min
0.31 μA
Response
2
time

Figure VII-9. Chromatogram of thiophenes using PAD

Conditions:

Column: Dionex MPIC

Eluent: 0.1 M NaOH containing 1.0 mM Benzoic Acid, 0.5 mL min^{-1}

Sample: 50 μL

Waveform: E_1 = 0.65 V (375 ms)
E_2 = 0.80 V (10 ms)
E_3 = -0.75 V (500 ms)

Peaks: 1 - 0.4 mM 2-thiophenecarboxylic acid
2 - 0.4 mM 3-thiophenemalonic acid

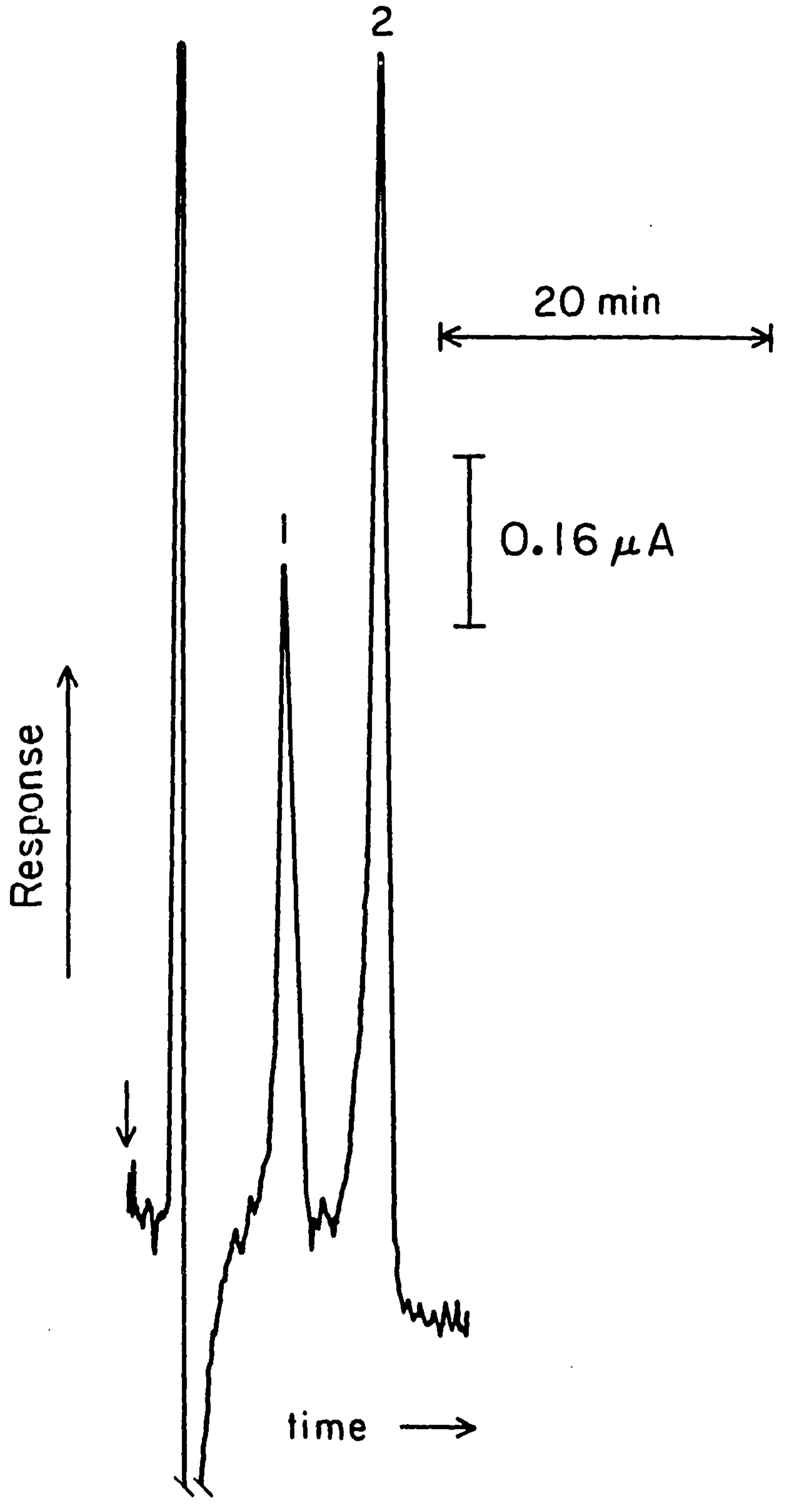
2
20 min
1
0.16 μA
Response
time

the retention times to the practical values shown. In addition, Figure VII-10 illustrates the improved sensitivity obtained upon adding the benzoate modifier for detecting and calibrating these thiophenes, particularly the later eluting 3-thiophenemalonic acid. The detection limits for these compounds using this HPLC system with PAD is 6.4 ppm for 2-thiophenecarboxylic acid and 9.3 ppm for 3-thiophenemalonic acid.

The final class of compounds chosen to demonstrate the suitability of PAD with HPLC is the dithiocarbamates. The salts and disulfides of mono- and dialkyldithiocarbamic acids are widely used as pharmaceuticals, rubber vulcanizers, and fungicides. In fact, the diethyldithiocarbamate anion is one of the most commonly used metal chelating agents in industry today. The planary delocalized electron system of this ligand is known to stabilize all of the metal ions listed in Table VII-2. In addition, other metal ions stabilized by related dithiocarbamates include those listed in Table VII-3. It should, therefore, be obvious why the interest in these compounds has proven to be lasting.

As with most other methods which have been developed for the detection of dithiocarbamates, degradation of the compounds was required prior to detection. The following procedure was found to be satisfactory for the subsequent

Table VII-2. Metal ions complexed by the diethyldithiocarbamate anion

metal ion	reference	metal ion	reference
Cr (III)	174	Ag (I)	176,180-182
Cr (VI)	174	Cd (II)	175,176
Mn (II)	175	In (III)	176
Fe (III)	176	Sb (III)	176
Co (II)	175,176	Au (III)	183
Ni (II)	175,176	Hg (II)	180,184
Cu (II)	175,176	Tl (I)	176
Zn (II)	175,176	Pb (II)	175,176
Mo (VI)	177-179	Bi (III)	175,176
Pd (II)	180		

Table VII-3. Metal ions complexed by dithiocarbamates

metal ion	reference	metal ion	reference
V (V)	185	Os (III)	188
Fe (II)	185	Os (IV)	188
Ga (III)	185	Os (VI)	188
As (III)	185	Os (VIII)	188
Se (IV)	185-187	Pt (IV)	185
Sn (II)	185	Pt (VI)	185
Sn (IV)	185	Tl (III)	185
Te (IV)	185-187	U (VI)	185

Figure VII-10. Calibration curves (I_p vs. C^b) for thiophenes using HPLC with PAD

Conditions:

Column: Dionex MPIC

Eluent: (a,c) 0.1 M NaOH, 0.5 mL min^{-1}
(b,d) 0.1 M NaOH containing
1.0 mM Benzoic Acid, 0.5 mL min^{-1}

Sample: 50 µL

Waveform: E_1 = 0.65 V (375 ms)
E_2 = 0.80 V (10 ms)
E_3 = -0.75 V (500 ms)

Plots: a,b - 2-thiophenecarboxylic acid
c,d - 3-thiophenemalonic acid

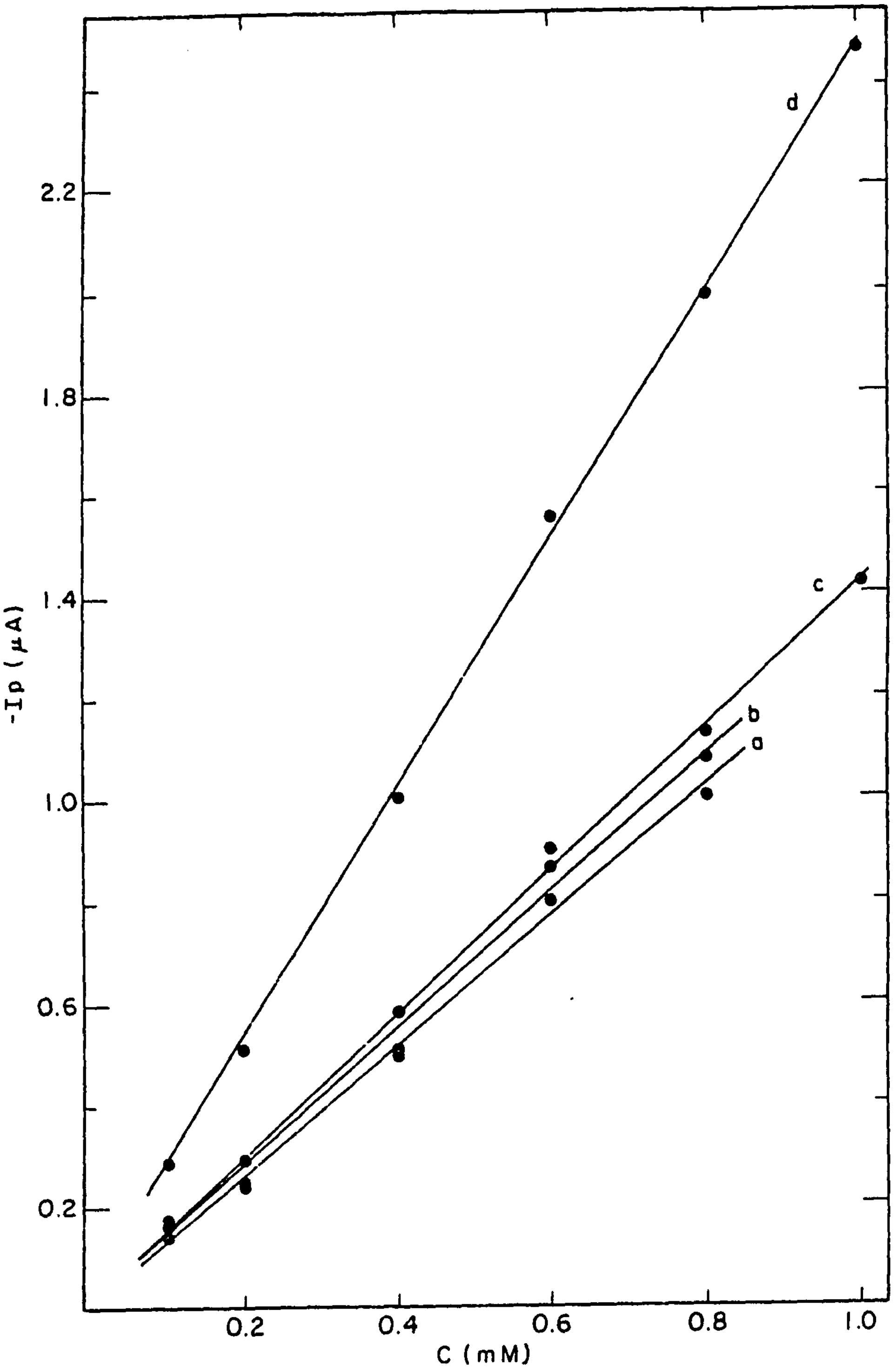
-Ip (μA)
2.2
1.8
1.4
1.0
0.6
0.2
C (mM)
0.2
0.4
0.6
0.8
1.0
a
b
c
d

separation and detection of dithiocarbamates using HPLC with PAD:

1. 100 mL of a synthetic mixture of dithiocarbamate was prepared.
2. a 10 mL aliquot of the above solution was transferred into an appropriate container.
3. 0.05 mL of 30% H_2O_2 was added to the container and the resulting solution was stirred for 1 hr prior to injection into the HPLC system.

A representative chromatogram of the separation of two dithiocarbamates which were subjected to this procedure is shown in Figure VII-11. Calibration plots were also obtained for these compounds and are shown in Figure VII-12. The detection limits using the above procedure with the HPLC system were determined to be 83 ppm for diethyldithiocarbamate and 54 ppm for dimethyldithiocarbamate. It is concluded from these results that this separation and detection scheme is probably not adequate for detection of trace levels of these compounds; however, this scheme could be useful for the monitoring of dithiocarbamate levels in industrial processing effluent streams.

Figure VII-11. Chromatogram of dithiocarbamates using PAD

Conditions:

Column: DEAE weak anion-exchanger

Eluent: 0.5 M KNO_3, 1.1 mL min^{-1}

Sample: 50 µL

Waveform: E_1 = 1.25 V (450 ms)

E_2 = 1.55 V (40 ms)

E_3 = -0.80 V (150 ms)

Peaks: 1 - 0.6 mM dimethyldithiocarbamate

2 - 0.6 mM diethyldithiocarbamate

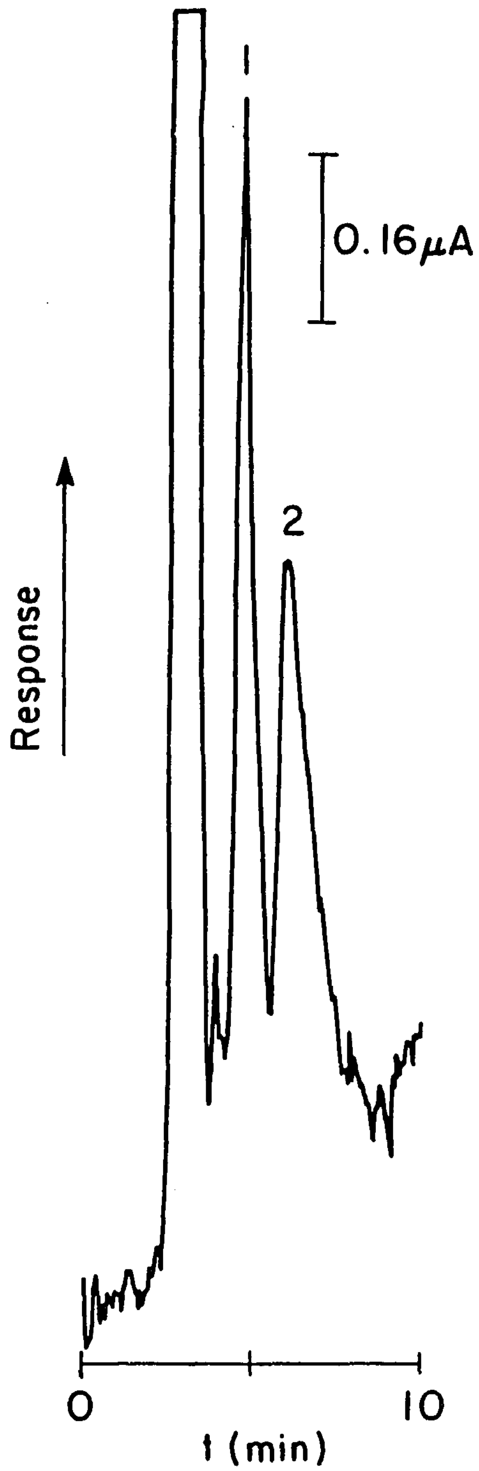
1
2
0.16μA
Response
0
10
t (min)

Figure VII-12. Calibration curves (I_p vs. C^b) for dithiocarbamates using HPLC with PAD

Conditions as in Figure VII-11

Plots: a - diethyldithiocarbamate

$I_p = -0.05 + 0.8\ C^b$

b - dimethyldithiocarbamate

$I_p = -0.39 + 2.1\ C^b$

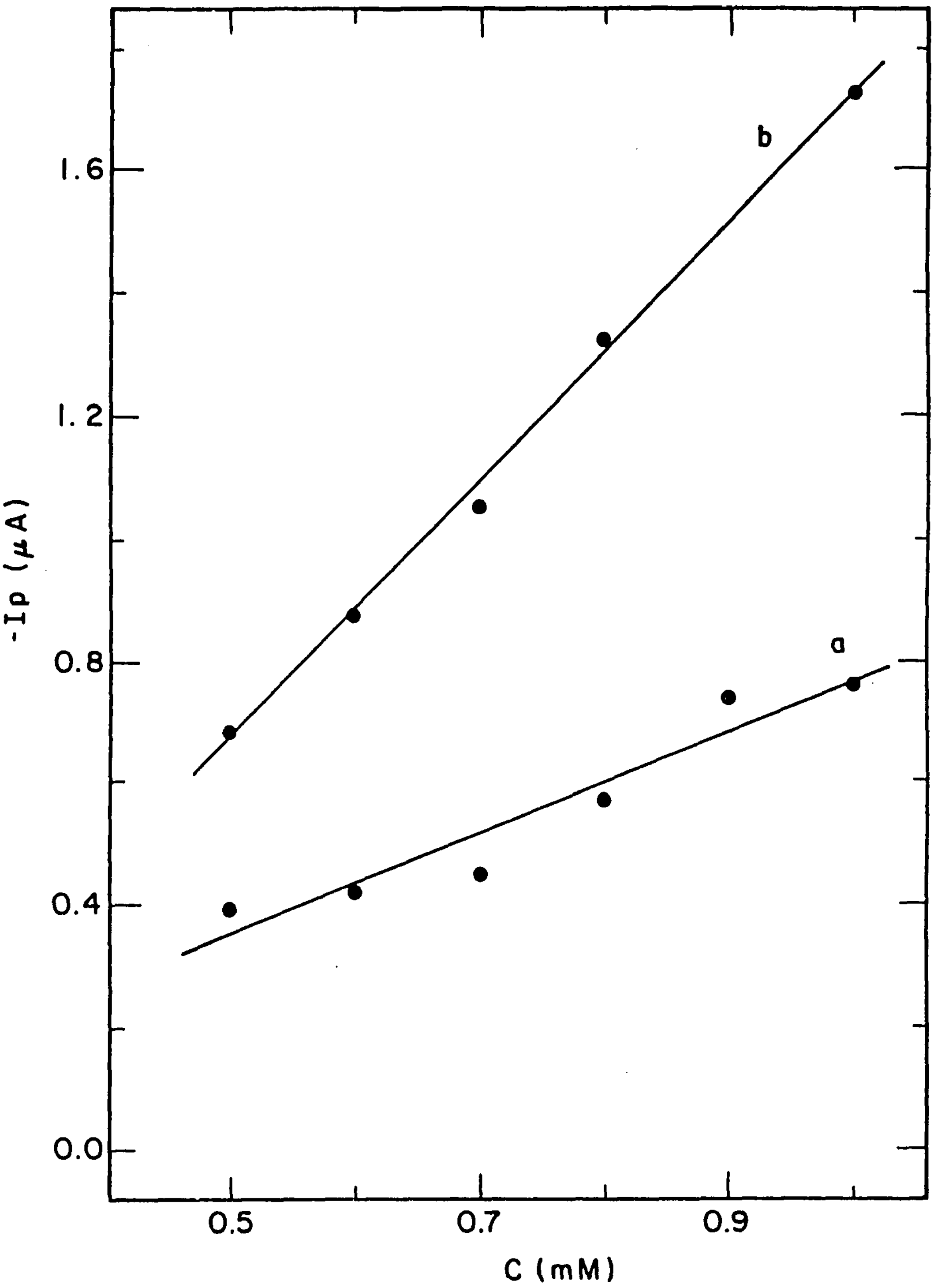
-Ip (μA)
C (mM)
0.0
0.4
0.8
1.2
1.6
0.5
0.7
0.9
a
b

VIII. PULSED AMPEROMETRIC DETECTION OF SULFUR CONTAINING BORON POLYHEDRALS AT GOLD ELECTRODES IN AQUEOUS SOLUTIONS

A. Introduction

Boron Neutron Capture Theory (BNCT) was originally designed to treat a very malignant and invasive form of brain cancer known as "glioblastoma multiforme". These Grade IV astrocystomas are characterized by a central, unencapsulated and often necrotic tumor mass. From this mass, numerous tiny strands of well-vascularized tumor cells can infiltrate the healthy brain.

Glioblastomas are located primarily in the cerebrum, often in deep and surgically inaccessible areas. Only rarely do they occur intraventricularly, in the pons and spinal cord, or in the cerebellum. The rapid growth and extreme size to which these tumors grow severely increases intracranial pressure. The cerebrospinal fluid pathways and blood vessels become restricted, leading to hydroencephalus and secondary infarction. Without treatment, the patient will die within a few months of the initial symptoms.

BCNT is based on the preferred concentration of a boron-10 enriched compound, such as $Na_2B_{12}H_{11}SH$, in a tumor relative to the surrounding tissues. Although the treatment is theoretically useful for all tumors, the intended application, as discussed previously, is for brain tumors.

The therapy is initiated by infusing a boron-10 compound into the patient. The compound is taken up by the brain tumor, but is excluded from the healthy brain by the blood-brain barrier. The patient's head is then irradiated with thermal neutrons from a research reactor port. The neutrons are captured by the boron-10 within the tumor, and emit highly energetic alpha and lithium-7 particles:

$$^{10}B + n \quad \text{---->} \; \alpha + {}^{7}Li + 2.79\ \text{MeV} \qquad [1]$$

Since the range of these particles in tissue is only 10 μm, a very large localized dose of radiation can be delivered to the tumor, while the surrounding nonborated tissues receive only that dose from the transit of the thermal neutrons. Such a dose differential between healthy and cancerous tissues is impossible to achieve with conventional photoradiation therapy.

Recently, $Na_2B_{12}H_{11}SH$ has received Orphan Drug designation for use with BNCT. For further FDA approval of this therapy, proof of the purity and stability of the drug in solution is required. Thus far however, only qualitative data is available via TLC analysis. Quantitation of $B_{12}H_{12}SH^{2-}$ (BSH) and its oxidation products, $B_{12}H_{11}SSH_{11}B_{12}^{4-}$ (BSSB) and $B_{12}H_{11}S(O)SH_{11}B_{12}^{4-}$ (SOS) (see Table VIII-1 for structures), would be most valuable. Two complementary techniques are being developed for this purpose. The first technique, Track Etch/TLC, provides a direct measurement of

Table VIII-1. Structures of sulfur containing boron polyhedrals

Formula	Structure	Abbreviation
$B_{12}H_{11}SH^{2-}$	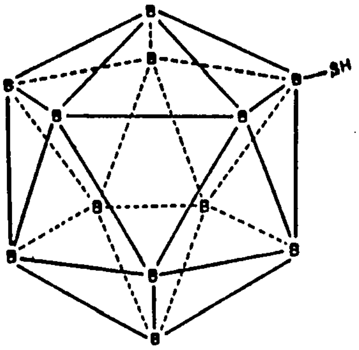	BSH
$B_{12}H_{11}SSH_{11}B_{12}^{4-}$	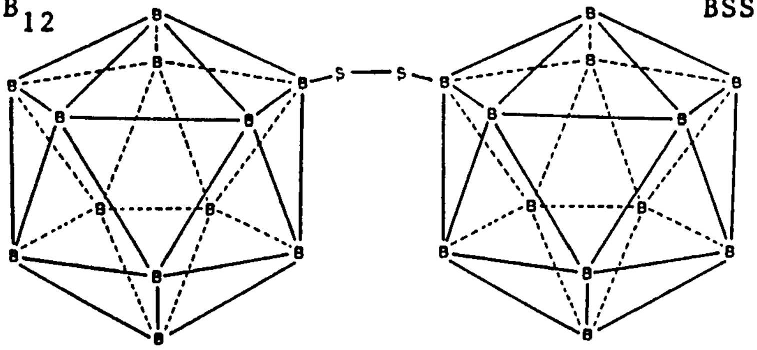	BSSB
$B_{12}H_{11}S(O)SH_{11}B_{12}^{4-}$	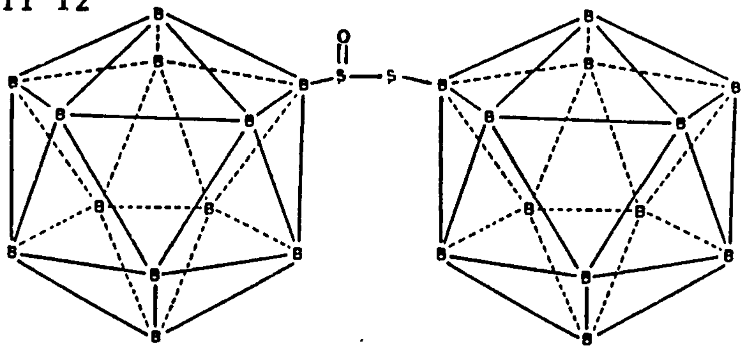	SOS

boron-10 and is being investigated by researchers at Theragenics, Corp. (189). The second method, HPLC/PAD, is the subject of the following studies.

The above information concerning BNCT, its purpose and reaction mechanism, was obtained through personal communications with researchers at Theragenics, Corp., Atlanta, GA.

B. Cyclic Voltammetry

Preliminary investigations into the electrochemical behavior of the sulfur containing boron polyhedrals were made using cyclic voltammetry at Au electrodes in several different solutions. Representative voltammetric results are illustrated in Figures VIII-1, VIII-2, and VIII-3 for these compounds in an ammonium hexaflurophosphate (NH_4PF_6) solution adjusted to neutral pH. The residual response of the electrode in each figure (curves a), obtained in the absense of analyte, is characterized by an anodic wave during the positive potential scan for $E > 0.2$ V which corresponds to the formation of the surface oxide layer. Rapid evolution of $O_2(g)$ occurs for $E > 1.3$ V. The oxide layer is reduced on the negative potential scan to produce the cathodic peak at 0.5 V. Evolution of $H_2(g)$ occurs at $E < -0.8$ V.

Upon addition of the compound of interest (curves b), oxidation of the analyte occurs on the positive potential scan producing an anodic current wave beginning at ca. 0.6 to 0.8 V, depending upon the specific compound added, and

Figure VIII-1. Current-potential curves for $B_{12}H_{11}SH^{2-}$ at a Au RDE by cyclic voltammetry in NH_4PF_6 adjusted to neutral pH

Conditions: $\phi = 6.0$ V min^{-1}, W = 94 rad s^{-1}

Concentration: (a) 0.00 mM, (b) = 0.10 mM

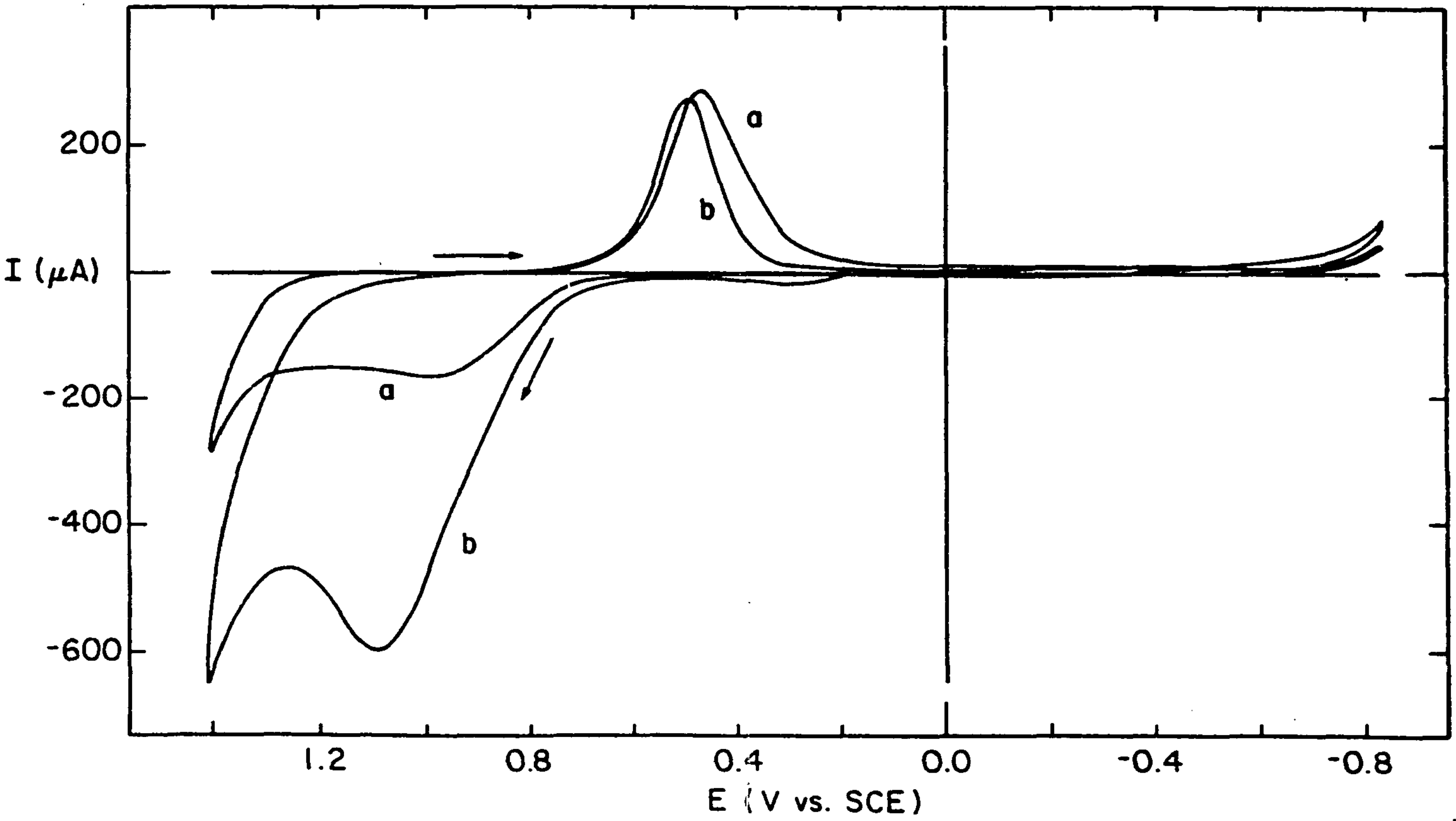
a
b
a
b
200
-200
-400
-600
I (μA)
1.2
0.8
0.4
0.0
-0.4
-0.8
E (V vs. SCE)

Figure VIII-2. Current-potential curves for $B_{12}H_{11}SSH_{11}B_{12}^{4-}$ at a Au RDE by cyclic voltammetry in NH_4PF_6 adjusted to neutral pH

Conditions: ϕ = 6.0 V min^{-1}, W = 94 rad s^{-1}

Concentration: (a) 0.00 mM, (b) = 0.10 mM

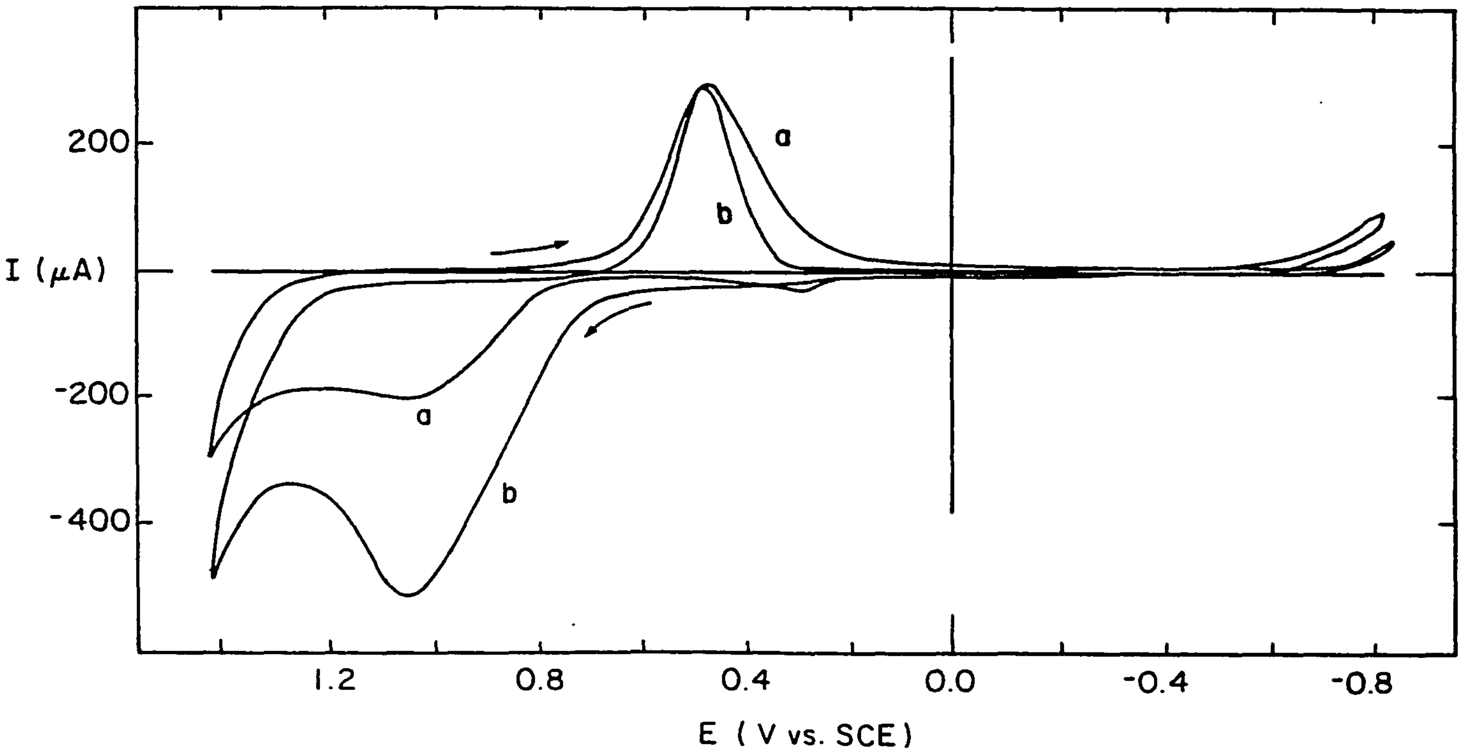
200
I (μA)
-200
-400
1.2
0.8
0.4
0.0
-0.4
-0.8
E (V vs. SCE)
a
b
a
b

Figure VIII-3. Current-potential curves for $B_{12}H_{11}S(O)SH_{11}B_{12}^{4-}$ at a Au RDE by cyclic voltammetry in NH_4PF_6 adjusted to neutral pH

Conditions: ϕ = 6.0 V min^{-1}, W = 94 rad s^{-1}

Concentration: (a) 0.00 mM, (b) = 0.10 mM

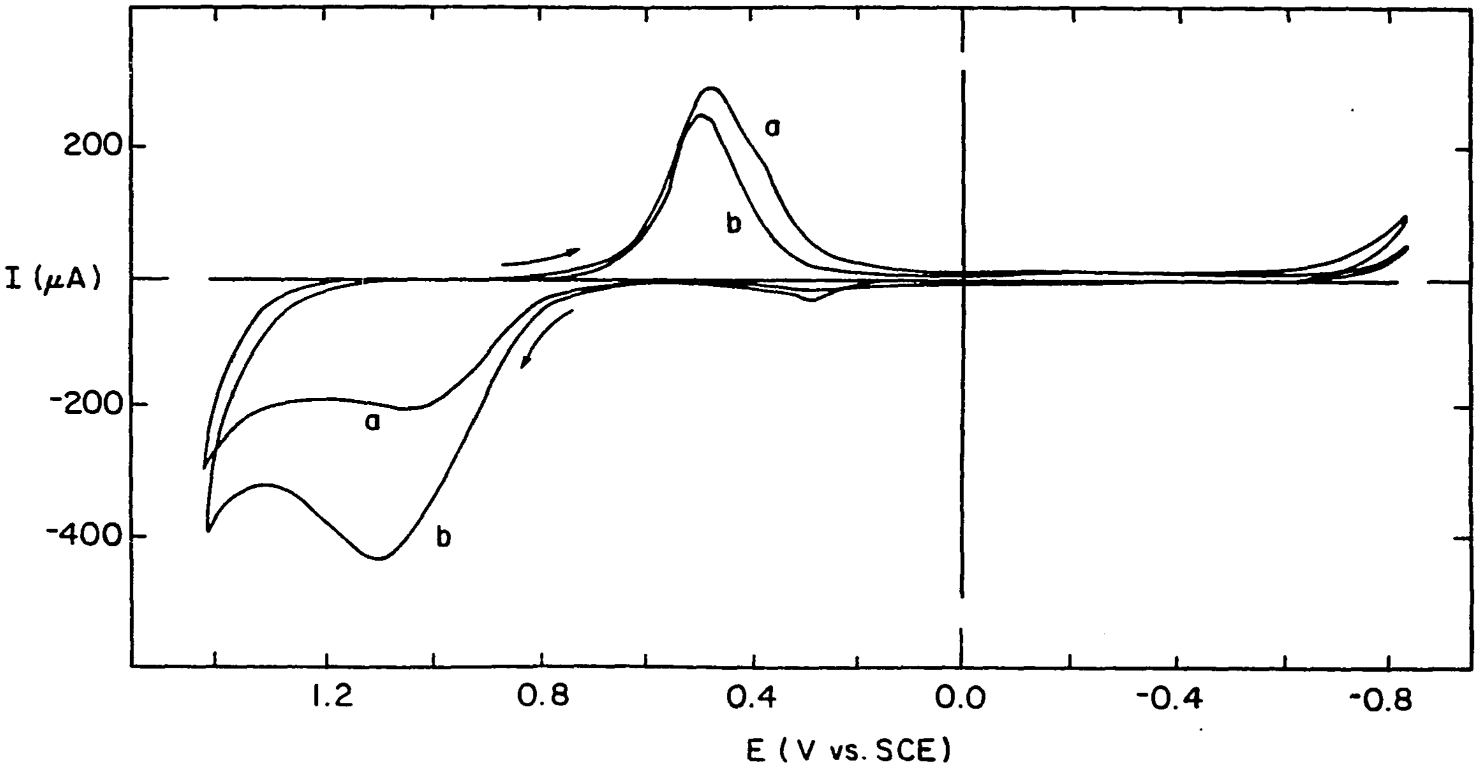
200
I (μA)
-200
-400
1.2
0.8
0.4
0.0
-0.4
-0.8
E (V vs. SCE)
a
b
a
b

extending to E = 1.4 V. As with the organic sulfur compounds discussed in Chapter VII, the anodic current in this region was found to increase as a nonlinear function of the bulk concentration of the analyte (C^b) for each of the compounds. A unique current response was observed for BSSB, in that anodic current also is produced during the negative potential scan for this region. For BSH and SOS, a dramatic decrease in current is observed upon reversal of the potential scan at 1.4 V. This rapid current decay indicates that constant potential amperometric detection is not feasible for these two compounds, as current decay curves similar to those shown in Figures IV-2 and VII-2 would be obtained as a function of time for BSH and SOS upon applying dc detection at Au electrodes.

Continuing the negative potential scan results in the reduction of the surface oxide layer to produce a peak at 0.5 V, as was observed for the residual response. It should be noted that, in the presence of analyte, the oxide reduction peak decreases in area. This implies that adsorption of the analyte occurs at the electrode surface, thereby blocking Au sites upon which surface oxides could form. It is therefore concluded that the analyte adsorbs onto the electrode surface prior to oxidation; this conclusion also is supported by the plots of current vs. scan rate for the positive potential scan, which were approximately linear with zero intercepts for all three compounds.

C. Calibration

Calibration plots were obtained for BSH, BSSB and SOS using FI and PAD, and are shown in Figure VIII-4. The waveform applied at the gold flow-through electrode was such that the detection potential, E_1, was in the region of maximum anodic current, E_2 was in the vicinity of O_2 evolution to oxidatively clean the electrode surface, and E_3 was in the region of rapid oxide reduction and analyte adsoption. Over the short range of dilute concentrations examined (0.01 to 0.1 mM), the plots of I_p vs. C^b are approximately linear for all three compounds (r^2 = 0.9960 (BSH), 0.9886 (BSSH), 0.9996 (SOS)). Detection limits (S/N = 2) using this system were determined to be 0.9 ppm for BSH, 1.8 ppm for BSSB and 5.4 ppm for SOS. These values correspond to sub-nmole quantities for all three compounds.

D. Liquid Chromatography

A chromatographic separation of the sulfur containing boron polyhedrals is particularly difficult in view of the instability of BSSB in the presence of BSH and SOS. Synthetic solutions of the individual compounds in distilled, deionized water are stable for several weeks. Synthetic mixtures of BSSB with either BSH or SOS also are stable

Figure VIII-4. Calibration curves (I_p vs. C^b) for sulfur containing boron polyhedrals in NH_4PF_6, adjusted to neutral pH, by FI/PAD

Conditions: $V_f = 0.5$ mL min^{-1}

$V_s = 50$ μL

Waveform: as given in text

Plots: a - $B_{12}H_{11}S(O)SH_{11}B_{12}^{4-}$

b - $B_{12}H_{11}SH^{2-}$

C - $B_{12}H_{11}SSH_{11}B_{12}^{4-}$

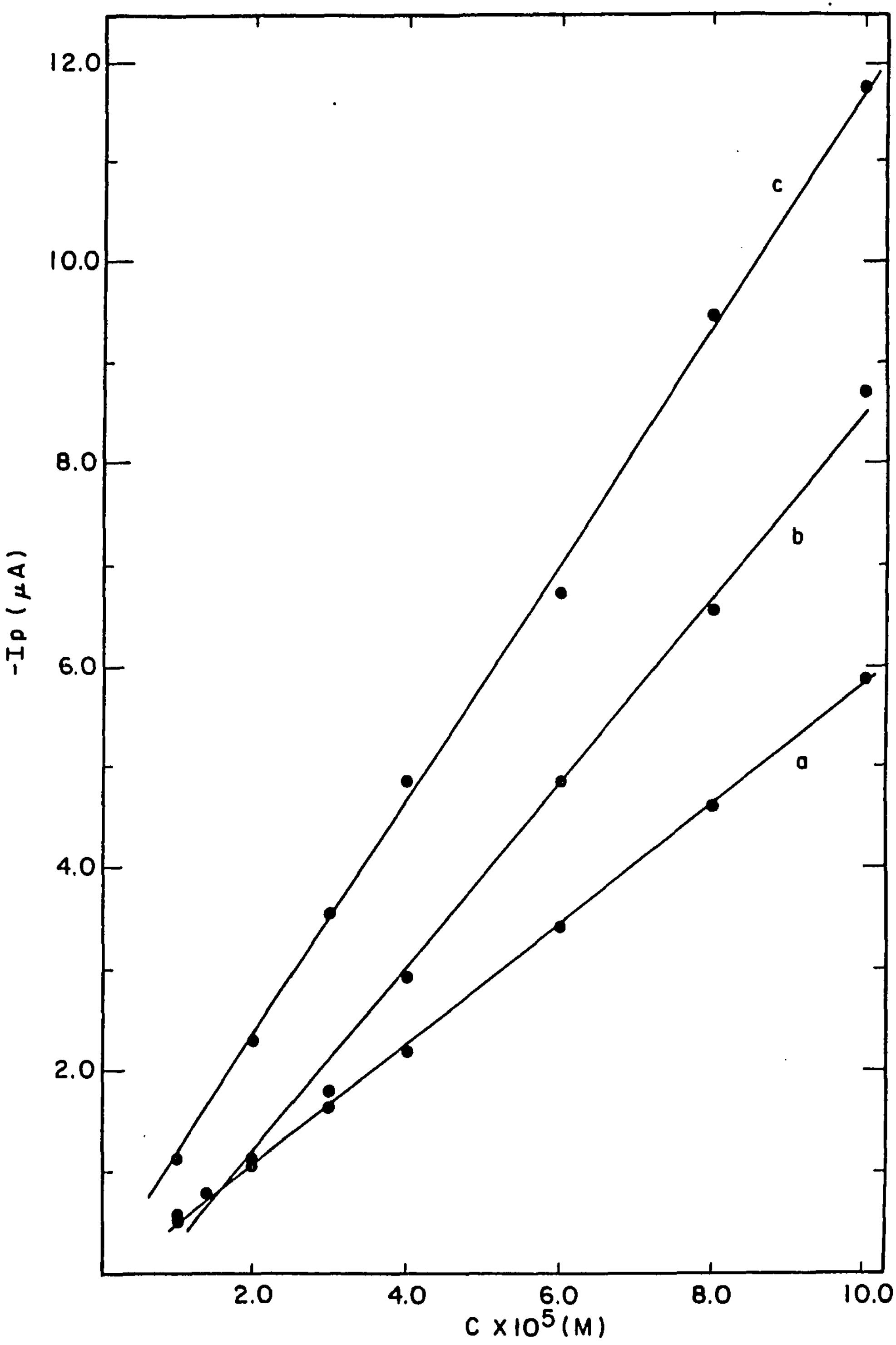
-Ip (μA)
12.0
10.0
8.0
6.0
4.0
2.0
2.0
4.0
6.0
8.0
10.0
C X10⁵(M)
c
b
a

in solution. A solution containing all three compounds, however, is very unstable with respect to BSSB, thereby making it difficult to obtain a chromatogram showing the separation of all three compounds. With this in mind, a representative separation of BSH, BSSB and SOS is shown in Figure VIII-5. The peak labeled "i" is an impurity present in all solutions containing BSSB. The other peaks are as designated in the figure caption. It should be noted that the sited concentrations of the compounds are the bulk values of the individual species calculated prior to dissolution.

It is also emphasized with regard to this separation that the feasibility of direct electrochemical detection of these sulfur containing boron polyhedrals is being stressed and not the quality of the separation. Improved chromatographic conditions are presently being investigated by researchers at and associated with the Theragenics Corporation.

Figure VIII-5. Chromatogram of sulfur containing boron polyhedrals using PAD

Conditions:

Column: DEAE weak anion-exchanger

Eluent: NH_4PF_6 adjusted to neutral pH, 1.1 mL min^{-1}

Sample: 50 µL

Waveform: as given in text

Peaks: 1 - 2.0 mM $B_{12}H_{11}SH^{2-}$

2 - 3.0 mM $B_{12}H_{11}SSH_{11}B_{12}^{4-}$

3 - 1.5 mM $B_{12}H_{11}S(O)SH_{11}B_{12}^{4-}$

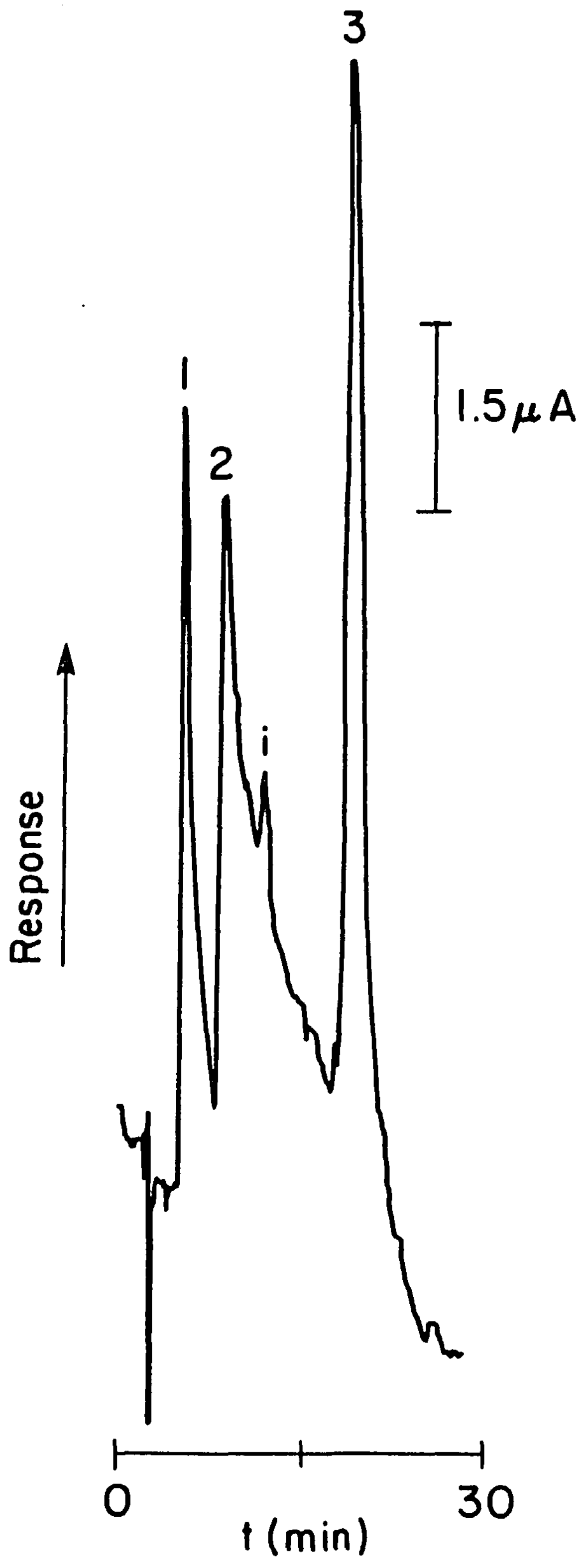
3
1
2
1.5μA
i
Response
0
30
t (min)

IX. CONCLUSIONS

Pulsed Amperometric Detection (PAD) is concluded to be useful for the reproducible anodic detection of numerous sulfur compounds at noble metal electrodes in aqueous solutions. For detection at Pt, the results presented for thiourea are representative of all compounds studied. The response of PAD as a function of adsorption time for thiourea on Pt has been demonstrated to be predictable, and the rate constants governing adsorption and desorption of the analyte have been estimated along with the maximum surface coverage by adsorbed thiourea.

The matter of analytical calibration of PAD has been examined. Linear calibration curves of I_p vs. C^b are obtained only for low concentrations of analyte and short adsorption time. For high analyte concentrations and long adsorption time, linear calibration curves are obtained by plotting $1/I_p$ vs. $1/C^b$. However, based on theoretical and experimental evidence, it is concluded that this expectation of linear plots of $1/I_p$ vs. $1/C^b$ can be defended only for the extreme cases of slow adsorption kinetics, isotherm-limited response, or mass transport-controlled adsorption. For cases of mixed control, plots of $1/I_p$ vs. $1/C^b$ are not expected to be linear. Hence it is recommended that calibration curves as I_p vs. C^b be constructed carefully, using more than one standard over the range of C^b expected for the unknown sample.

The detection of inorganic and organic sulfur compounds at Au electrodes in aqueous solutions using PAD has been demonstrated, and the technique is shown to be well suited for detection of analytes in FI and HPLC effluent streams. Calibration plots of I_p vs. C^b are illustrated for inorganic sulfur compounds and several classes of organic sulfur compounds over short ranges of C^b for HPLC/PAD.

Finally, PAD makes possible the quantitative determination of sulfur containing boron polyhedrals on Au electrodes in aqueous solutions. Calibration and chromatographic separation of $B_{12}H_{11}SH^{2-}$ and its two principal oxidation products are demonstrated. Detection limits of sub-nmole quantities were achieved for all three compounds.

X. FUTURE RESEARCH

The lack of specificity in PAD is apparent. Further work to develop chromatographic conditions suitable for the direct application of PAD is needed. None of the separations illustrated in this work were accomplished using chromatographic columns designed originally to separate molecules containing sulfur atoms. Obviously, LC columns designed for this purpose would be useful. In addition, PAD would be made more applicable to currently existing reverse-phase chromatographic procedures if polystyrene-based columns able to tolerate high pH extremes were developed. This would continue to allow the use of strongly basic electrolytes as the LC eluents to eliminate the requirement of post-column mixing, yet take advantage of the specificity of separation which can be achieved with a binary solvent system.

A more detailed theoretical basis is desired for understanding the adsorption behavior of thiourea and other organic sulfur compounds on Au. To accomplish this, the differential equation of the rate law must be integrated and then solved either numerically or using a cubic spline approximation.

The present understanding of the relationship of adsorption and mass-transport of an analyte to the electrode surface in unclear because it is experimentally difficult to separate the two processes. The technique of Pulsed

Coulometric Detection (PCD), currently being developed in this laboratory, could be applied to help elucidate this problem. PCD is able to eliminate the background current due to surface oxide formation; thus, a true indication of analyte oxidation is obtained upon sampling the anodic current. Coupling PCD with an RDE should enable a distinction to be made between the oxidation of analyte limited by adsorption and the oxidation of analyte limited by mass-transport.

An inherent limitation of PAD is that large quantities of oxidation products are not produced with the technique and, therefore, cannot be identified and quantitated. It also is not possible to experimentally determine "n", the number of electrons participating in the electrochemical oxidation, with PAD in its present state. More research into these problems must be done in order to understand the process of oxidation using this technique. Only then will the full extent of the usefulness of PAD be known.

XI. BIBLIOGRAPHY

1. Weinberg, N. L.; Weinberg, H. R. Chem Rev. 1968, 68, 449.

2. Ross, S. D.; Finkelstein, M.; Rudd, E. J. "Anodic Oxidation"; Academic Press: New York, 1975.

3. Adams, R. N. "Electrochemistry at Solid Electrodes"; Marcel Dekker: New York, 1969; Chapter 10.

4. Tomilov, A. P.; Mairanovskii, S. G.; Fioshin, M. Ya.; Smirnov, V. A. "Electrochemistry of Organic Compounds"; Halsted Press: New York, 1972; Chapter 8.

5. Chambers, J. Q. In "Encyclopedia of Electrochemistry of the Elements"; Bard, A. J.; Lund, H., Eds.; Marcel Dekker: New York, 1978; Volume XII.

6. Svensmark, B. In "Organic Electrochemistry"; Baizer, M. M.; Lund, H., Eds.; Marcel Dekker: New York, 1983; Chapter 17.

7. Brown, O. R. In "Physical Chemistry of Organic Solvent Systems"; Covington, A.; Dickinson, T., Eds.; Plenum Press: New York, 1973; Chapter 7.

8. Nadebaum, P. R.; Fahidy, T. Z. J. Electrochem. Soc. 1975, 122, 1035.

9. Farooque, M.; Fahidy, T. Z. J. Electrochem. Soc. 1977, 124, 1191.

10. Nicholson, M. M. J. Am. Chem. Soc. 1954, 76, 2539.

11. Nicholson, M. M. Anal. Chem. 1955, 27, 1364.

12. Drushel, H. V.; Miller, J. F. Anal. Chim. Acta 1956, 15, 389.

13. Drushel, H. V.; Miller, J. F. Anal. Chem. 1957, 29, 1456.

14. Humffray, A. A.; Houghton, D. S. Electrochim. Acta 1972, 17, 1435.

15. Houghton, D. S.; Humffray, A. A. Electrochim. Acta 1972, 17, 1421.

16. Houghton, D. S.; Humffray, A. A. *Electrochim. Acta* 1972, 17, 2145.

17. Imberger, H. E., Humffray, A. A. *Electrochim. Acta* 1973, 18, 373.

18. Seo, E. T.; Sawyer, D. T. *J. Electroanal. Chem.* 1964, 7, 184.

19. Seo, E. T.; Sawyer, D. T. *Electrochim. Acta* 1965, 10, 239.

20. Binder, H.; Koehling, A.; Sandstede, G. *Advan. Energy Convers.* 1967, 7, 77; *Chem. Abstr.* 1967, 67, 39502y.

21. Binder, H.; Koehling, A.; Sandstede, G. *Advan. Energy Convers.* 1967, 7, 121; *Chem. Abstr.* 1968, 68, 92444c.

22. Binder, H.; Koehling, A.; Sandstede, G. *Amer. Chem. Soc., Div. Fuel Chem., Preprints* 1967, 11, 106; *Chem. Abstr.* 1969, 70, 102355g.

23. Binder, H.; Koehling, A.; Sandstede, G. *Nature* 1967, 214, 268.

24. Binder, H.; Koehling, A.; Sandstede, G. *Angew. Chem. Int. Ed. Engl.*, 1967, 6, 884; *Chem. Abstr.* 1968, 68, 8777h.

25. Binder, H.; Koehling, A.; Sandstede, G. *J. Electroanal. Chem. Interfacial Electrochem.* 1968, 17, 111; *Chem. Abstr.* 1968, 68, 83672y.

26. Binder, H.; Koehling, A.; Sandstede, G. *Advan. Chem. Ser.* 1969, 90, 128; *Chem. Abstr.* 1969, 71, 108415u.

27. Weber, J.; Loucka, T. *Power Sources 3: Res. Develop. Non-Mech. Elec. Power Sources, Proc. Int. Symp., 7th* 1970, 455.

28. Loucka, T. *J. Electroanal. Chem. Interfacial Electrochem.* 1971, 31, 319.

29. Loucka, T. *J. Electroanal. Chem. Interfacial Electrochem.* 1972, 36, 355.

30. Loucka, T. *J. Electroanal. Chem. Interfacial Electrochem.* 1972, 36, 369.

31. Loucka, T. *J. Electroanal. Chem. Interfacial Electrochem.* 1973, 44, 221.

32. Najdeker, E.; Bishop, E. *J. Electroanal. Chem. Interfacial Electrochem.* 1973, 41, 79.

33. Ramasubramanian, N. *J. Electroanal. Chem. Interfacial Electrochem.* 1975, 64, 21.

34. Jayaram, R.; Contractor, A. Q.; Lal, H. *J. Electroanal. Chem. Interfacial Electrochem.* 1978, 87, 225.

35. Contractor, A. Q.; Lal, H. *J. Electroanal. Chem. Interfacial Electrochem.* 1978, 93, 99.

36. Contractor, A. Q.; Lal, H. *J. Electroanal. Chem. Interfacial Electrochem.* 1979, 96, 175.

37. Contractor, A. Q.; Lal, H. *J. Electroanal. Chem. Interfacial Electrochem.* 1979, 103, 103.

38. Comtat, M.; Mahenc, J. *Bull. Soc. Chim. Fr.* 1969, 3862; *Chem. Abstr.* 1970, 72, 62228a.

39. Appleby, A. J.; Pichon, B. *J. Electroanal. Chem. Interfacial Electrochem.* 1979, 95, 59.

40. Audry, C.; Voinov, M. *Electrochim. Acta* 1980, 25, 299.

41. Kazarinov, V. E. *J. Res. Inst. Catal., Hokkaido Univ.* 1982, 30, 127; *Chem. Abstr.* 1983, 98, 187927w.

42. Tarasevich, M. R.; Andreev, V. N.; Kazarinov, V. E.; Levina, O. A.; Radyushkina, K. A. *Elektrokhimiya* 1982, 18, 1569.

43. Szklarczyk, M.; Czerwinski, A.; Sobkowski, J. *J. Electroanal. Chem. Interfacial Electrochem.* 1982, 132, 263.

44. Spotnitz, R. M.; Loeffler, C. E., II; Langer, S. H. *J. Appl. Electrochem.* 1981, 11, 403.

45. Spotnitz, R. M.; Colucci, J. A.; Langer, S. H. *Electrochim. Acta* 1983, 28, 1053.

46. Spotnitz, R. M.; Colucci, J. A.; Langer, S. H. *J. Electrochem. Soc* 1983, 130, 2393.

47. Davis, D. G.; Bianco, E. *J. Electroanal. Chem.* 1966, 12, 254.

48. Pradac, J.; Koryta, J. *J. Electroanal. Chem. Interfacial Electrochem.* 1968, 17, 185.

49. Koryta, J.; Pradac, J. *J. Electroanal. Chem. Interfacial Electrochem.* 1968, 17, 167.

50. Ossendorfova, N.; Pradac, J.; Koryta, J. *J. Electroanal. Chem. Interfacial Electrochem.* 1970, 28, 313.

51. Pradac, J.; Pradacova, J.; Koryta, J. *Biochim. Biophys. Acta* 1971, 237, 450.

52. Samec, Z.; Malysheva, Zh. N.; Koryta, J.; Pradac, J. *J. Electroanal. Chem. Interfacial Electrochem.* 1975, 65, 573.

53. Reddy, S. J.; Krishnan, V. R. *Anal. Chem. Symp. Ser.* 1980, 2, 155; *Chem. Abstr.* 1980, 93, 25166s.

54. Reddy, S. J.; Krishnan, V. R. *Indian Trans. SAEST* 1980, 15, 99; *Chem. Abstr.* 1981, 94, 111508g.

55. Kuz'mina, N. N.; Songina, O. A. *Izv. Vysshikh Uchebn. Zavedenii, Khim. i Khim. Tekhnol.* 1961, 4, 928; *Chem. Abstr.* 1962, 57, 2857b.

56. Santhanam, K. S. V.; Krishnan, V. R. *Z. Physik. Chem.* 1962, 34, 312.

57. Santhanam, K. S. V.; Krishnan, V. R. *Fresenius' Z. Anal. Chem.* 1968, 234, 256.

58. Reddy, S. J.; Krishnan, V. R. *J. Electroanal. Chem. Interfacial Electrochem.* 1970, 27, 473.

59. Reddy, S. J.; Krishnan, V. R. *Trans. SAEST* 1979, 14, 43; *Chem. Abstr.* 1979, 91, 165565e.

60. Reddy, S. J.; Krishnan, V. R. *Indian J. Chem., Sect. A* 1979, 17A, 558.

61. Gorbachev, S. V.; Atanasyants, A. G.; Senatorov, Yu. M. *Zh. Fiz. Khim.* 1972, 46, 2429; *Chem. Abstr.* 1972, 77, 159475y.

62. Maslii, A. I.; Lupenko, G. K. Izv. Sib. Otd. Akad. Nauk SSSR, Ser. Khim. Nauk 1974, 12; Chem. Abstr. 1975, 82, 49119c.

63. Astruc, A.; Astruc, M.; Gonbeau, D.; Pfister-Guillouzo, G. Collect. Czech. Chem. Commun. 1976, 41, 2737; Chem. Abstr. 1977, 86, 80826n.

64. Sorokin, V. I. Ukr. Khim. Zh. 1976, 42, 137.

65. Franklin, T. C.; Iwunze, M. J. Electroanal. Chem. Interfacial Electrochem. 1980, 108, 97.

66. Usatenko, Yu. I.; Tulyupa, F. M. Tr. Dnepropetr. Khim. Tekhonol. Inst. 1959, 12, 25; Chem. Abstr. 1962, 57, 5709b.

67. Bessarabova, I. M.; Zakharov, V. A.; Songina, O. A.; Kufel'd, G. R. Izv. Vysshikh Uchebn. Zavedenii, Khim. i Khim. Tekhnol. 1969, 12, 1202; Chem. Abstr. 1970, 72, 27714j.

68. Usatenko, Yu. I.; Galushko, S. V. Electrokhimiya 1976, 12, 84.

69. Scrimager, C.; DeHayes, L. J. Inorg. Nucl. Chem. Lett. 1978, 14, 125.

70. Labuda, J.; Mocak, J.; Bustin, D. I.; Garaj, J. Proc. Conf. Coord. Chem. 1980, 8, 235; Chem. Abstr. 1981, 94, 111943v.

71. Labuda, J.; Mocak, J.; Bustin, D. I. Chem. Zvesti. 1982, 36, 633.

72. Sobkowski, J.; Szklarczyk, M. Electrochim. Acta 1980, 25, 383.

73. Songina, O. A.; Pavlova, I. M. Izv. Vysshikh Uchebn. Zavedenii, Khim. i Khim. Tekhnol. 1962, 5, 378; Chem. Abstr. 1963, 58, 230g.

74. Calandra, A. J.; Martins, M. E.; Arvia, A. J. Electrochim. Acta 1971, 16, 2057.

75. Arvia, A. J.; Calandra, A. J.; Martins, M. E. Electrochim. Acta 1972, 17, 741.

76. Martinez, C.; Calandra, A. J.; Arvia, A. J. An. Asoc. Quim. Argent. 1972, 60, 413; Chem. Abstr. 1973, 78, 66198n.

77. Pereiro, R.; Arvia, A. J.; Calandra, A. J. Electrochim. Acta 1972, 17, 1723.

78. Martinez, C.; Calandra, A. J.; Arvia, A. J. Electrochim. Acta 1972, 17, 2153.

79. Belyi, O. V.; Belaya, L. M.; Karlovskaya, N. E. Termodin. Neobratimykh Protsessov Ee Primen., Mater. Vses. Konf., 1st 1972, 13; Chem. Abstr. 1975, 82, 49113w.

80. Kuz'mina, N. N.; Songina, O. A. Izv. Vysshikh Uchebn. Zavedenii, Khim. i Khim. Tekhnol. 1963, 6, 201; Chem. Abstr. 1963, 59, 12154a.

81. Yokosuka, F.; Takizawa, M.; Okuwaki, A.; Okabe, T. Chem. Lett. 1974, 319.

82. Yokosuka, F.; Okuwaki, A.; Okabe, T. Nippon Kagaku Kaishi 1975, 1722; Chem. Abstr. 1976, 84, 10445x.

83. Kapusta, S.; Viehbeck, S. M. W.; Hackerman, N. J. Electroanal. Chem. Interfacial Electrochem. 1983, 153, 157.

84. Paris, J.; Plichon, V. Electrochim. Acta 1981, 26, 1823.

85. Paris, J.; Plichon, V. Electrochim. Acta 1982, 27, 1501.

86. Zakharov, V. A.; Bessarabova, I. M.; Barikov, V. G.; Treshchetkina, T. I. Elektrokhimya 1973, 9, 58.

87. Kirchnerova, J.; Purdy, W. C. Anal. Lett. 1980, 13, 1031.

88. Kirchnerova, J.; Purdy, W. C. Anal. Chim. Acta 1981, 123, 83.

89. Lugovoi, S. V.; Chernova, T. N. Nov. Polyarogr., Tezisy Dokl. Vses. Soveshch. Polyarogr., 6th 1975, 132; Chem. Abstr. 1976, 85, 200064r.

90. Hofbauerova, H.; Mocak, J.; Vanickova, M. *Proc. Conf. Coord. Chem.* 1983, 9, 109; *Chem. Abstr.* 1983, 99, *165638w.*

91. Hofbauerova, H.; Mocak, J.; Beinrohr, E. *Chem. Pap.* 1985, 39, 295.

92. Srogl, J.; Janda, M.; Valentova, M. *Collect. Czech. Chem. Commun.* 1970, 35, 148.

93. Janda, M.; Srogl, J.; Janousova, A.; Kubelka, V.; Holik, M. *Collect. Czech. Chem. Commun.* 1970, 35, 2635.

94. Janda, M.; Srogl, J.; Synackova, M. *Collect. Czech. Chem. Commun.* 1972, 37, 2584.

95. Janda, M.; Srogl, J.; Nemec, M.; Janousova, A. *Collect. Czech. Chem. Commun.* 1973, 38, 1221.

96. Srogl, J.; Janda, M.; Stibor, I.; Kos, J.; Vyskocil, V. *Collect. Czech. Chem. Commun.* 1978, 43, 2015.

97. Armstrong, R. D.; Dickinson, T.; Reid, M. *Electrochim. Acta* 1975, 20, 709.

98. Armstrong, R. D.; Dickinson, T.; Reid, M. *Electrochim. Acta* 1976, 21, 935.

99. Armstrong, R. D.; Reid, M. *Electrochim. Acta* 1976, 21, 1105.

100. Armstrong, R. D.; Reid, M. *Electrochim. Acta* 1977, 22, 1329.

101. Stulik, K.; Pacakova, V. *CRC Crit. Reviews in Anal. Chem.* 1984, 14, 297.

102. Stankovich, M. T.; Bard, A. J. *J. Electroanal. Chem. Interfacial Electrochem.* 1977, *75*, 487.

103. Rabenstein, D.; Saetre, R. *Anal. Chem.* 1977, 49, 1036.

104. Saetre, R.; Rabenstein, D. *Anal. Biochem.* 1978, 90, 684.

105. Eggli, R.; Asper, R. *Anal. Chim. Acta* 1978, 101, 253.

106. Demaster, E. G.; Shirota, F. N.; Redfern, B.; Goon, D. J. W.; Nagasawa, H. T. J. Chromatogr. 1984, 308, 83.

107. Allison, L. A.; Shoup, R. E. Anal. Chem. 1983, 55, 8.

108. Allison, L. A.; Keddington, J.; Shoup, R. E. J. Liq. Chromatogr. 1983, 6, 1785.

109. Lunte, S. M.; Kissinger, P. T. Current Separations 1983, 5, 49.

110. Lunte, S. M.; Kissinger, P. T. J. Chromatogr. 1984, 317, 579.

111. Lunte, S. M.; Kissinger, P. T. J. Liq. Chromatogr. 1985, 8, 691.

112. Kolevatova, V. S.; Kuznetsov, V. V. Izv. Vysshikh Uchebn. Zavedenii, Khim. i Khim. Tekhnol. 1976, 19, 496; Chem. Abstr. 1976, 85, 26762e.

113. Hanekamp, H. B.; Bos, P.; Frei, R. W. J. Chromatogr. 1979, 186, 489.

114. Lawrence, J. F.; Iverson, F.; Hanekamp, H. B.; Bos, P.; Frei, R. W. J. Chromatogr. 1981, 212, 245.

115. King, D. M.; Kolby, N. I.; Price, J, W. J. Electroanal. Chem. Interfacial Electrochem. 1972, 40, 295.

116. Kovacova, Z.; Zezula, I. Collect. Czech. Chem. Commun. 1975, 40, 1279; Chem. Abstr. 1975, 83, 123190h.

117. Uddin, Z. Ph. D. Dissertation, Iowa State University, Ames, IA, 1985.

118. Samec, Z.; Weber, J. Electrochim. Acta 1975, 20, 403.

119. Samec, Z.; Weber, J. Electrochim. Acta 1975, 20, 413.

120. Wierse, D. G.; Lohrengel, M. M.; Schultze, J. W. J. Electroanal. Chem. Interfacial Electrochem. 1978, 92, 121.

121. Van Huong, C. N.; Parsons, R.; Marcus, P.; Montes, S.; Oudar, J. J. Electroanal. Chem. Interfacial Electrochem. 1981, 119, 137.

122. Hamilton, I. C.; Woods, R. J. Appl. Electrochem. 1983, 13, 783.

123. Martins, M. E.; Castellano, C.; Calandra, A. J.; Arvia, A. J. J. Electroanal. Chem. Interfacial Electrochem. 1977, 81, 291.

124. Martins, M. E.; Castellano, C.; Calandra, A. J.; Arvia, A. J. J. Electroanal. Chem. Interfacial Electrochem. 1978, 92, 45.

125. Itabashi, E. J. Electroanal. Chem. Interfacial Electrochem. 1984, 177, 311.

126. Moscardo-Levelut, M. N.; Plichon, V. J. Electrochem. Soc. 1984, 131, 1538.

127. Moscardo-Levelut, M. N.; Plichon, V. J. Electrochem. Soc. 1984, 131, 1545.

128. Koryta, J.; Pradac, J. J. Electroanal. Chem. Interfacial Electrochem. 1968, 17, 177.

129. Reynaud, J. A.; Malfoy, B.; Canesson, P. J. Electroanal. Chem. Interfacial Electrochem. 1980, 114, 195.

130. Safronov, A. Yu.; Tarasevich, M. R.; Bogdanovskaya, V. A.; Chernyak, A. S. Elecktrokhimiya 1983, 19, 421.

131. Zakharov, V. A.; Bessarabova, I. M.; Songina, O. A.; Timoshkin, M. A. Elektrokhimiya 1971, 7, 1215.

132. Zakharov, V. A. Nov. Polyarogr., Tezisy Dokl. Vses. Soveshch. Polyarogr., 6th 1975, 119; Chem. Abstr. 1977, 86, 10026c.

133. Muetterties, E. L.; Balthis, J. H.; Chia, Y. T.; Knoth, W. H.; Miller, H. C. Inorganic Chem. 1964, 3, 444.

134. Knoth, W. H.; Sauer, J. C.; England, D. C.; Hertler, W. R.; Muetterties, E. L. J. Am. Chem. Soc. 1964, 86, 3973.

135. Klanberg, F.; Eaton, D. R.; Guggenberger, L. J.; Muetterties, E. L. Inorg. Chem. 1967, 6, 1271.

136. Knoth, W. H.; Miller, H. C.; Sauer, J. C.; Balthis, J. H.; Chia, Y. T.; Muetterties, E. L. Inorg. Chem. 1964, 3, 159.

137. Wiersema, R. J.; Middaugh, R. L. J. Am. Chem. Soc. 1967, 89, 5078.

138. Wiersema, R. J.; Middaugh, R. L. *Inorg. Chem.* 1969, 8, 2074.

139. Morris, J. H.; Gysling, H. J.; Reed, D. *Chem. Rev.* 1985, 85, 51.

140. Karchmer, J. H. "The Analytical Chemistry of Sulfur and Its Compounds, Part I and II"; Wiley-Interscience: New York, 1972.

141. Cox, J. A.; Przyjazny, A. *Anal. Lett.* 1977, 10, 869.

142. Hashimoto, A. *Anal. Chem.* 1979, 51, 385.

143. Kobayashi, H.; Matano, O.; Goto, S. *J. Chromatogr.* 1981, 207, 281.

144. Mockel, H. J.; Freyholdt, T.; Weiss, J.; Molnar, I. In "Practical Aspects of Modern HPLC"; Molnar, I., Ed.; Walter de Gruyter & Co.: New York, 1982.

145. Werkhoven-Goewie, C. E.; Niessen, W. M. A.; Brinkman, U. A. T.; Frei, R. W. *J. Chromatogr.* 1981, 203, 165.

146. Bossle, P. C.; Martin, J. J.; Sarver, E. W.; Sommer, H. Z. *J. Chromatogr.* 1984, 283, 412.

147. Bossle, P. C.; Hallowell, S. F.; Reutter, D. J.; Sarver, E. W. *J. Chromatogr.* 1985, 330, 338.

148. Gustafsson, K. H.; Thompson, R. A. *J. Agric. Food Chem.* 1981, 29, 729.

149. Gustafsson, K. H.; Fahlgren, C. H. *J. Agric. Food Chem.* 1983, 31, 461.

150. Cochrane, W. P. *J. Chromatogr. Sci.* 1979, 17, 124.

151. Story, J. N. *J. Chromatogr. Sci.* 1983, 21, 272.

152. Hughes, S.; Meschi, P. L.; Johnson, D. C. *Anal. Chim. Acta* 1981, 132, 1.

153. Hughes, S.; Johnson, D. C. *Anal. Chim. Acta* 1981, 132, 11.

154. Hughes, S.; Johnson, D. C. *J. Agric. Food Chem.* 1982, 30, 712.

155. Hughes, S.; Johnson, D. C. Anal. Chim. Acta 1983, 149, 1.

156. Edwards, P.; Haak, K. Am. Lab. 1983, 4, 78.

157. Rocklin, R. D.; Pohl, C. A. J. Liq. Chromatogr. 1983, 6, 1577.

158. Neuburger, G. G.; Johnson, D. C. Anal. Chem., in press.

159. Neuburger, G. G.; Johnson, D. C. Anal. Chem., in press.

160. Johnson, D. C. Nature 1986, 321, 451.

161. Polta, J. A.; Johnson, D. C. J. Liq. Chromatogr. 1983, 6, 1727.

162. Polta, J. A.; Johnson, D. C. J. Chromatogr. 1985, 324, 407.

163. Rocklin, R. D. Adv. Chem. Ser., 210 (Formaldehyde) 1985, 13.

164. Polta, J. A.; Johnson, D. C. Anal. Chem. 1985, 57, 1373.

165. Thomas, M. B.; Sturrock, P. E. J. Chromatogr. 1986, 357, 318.

166. Ohsawa, K.; Yoshimura, Y.; Watanabe, S.; Tanaka, H.; Yokato, A.; Tamura, K.; Imaeda, K. Anal. Sci. 1986, 2, 165; Chem. Abstr. 1986, 105, 17715w.

167. Austin, D. S.; Polta, J. A.; Polta, T. Z.; Tang, A. P-C.; Cabelka, T. D.; Johnson, D. C. J. Electroanal. Chem. Interfacial Electrochem. 1984, 168, 227.

168. Johnson, D. C.; Polta, J. A.; Polta, T. Z.; Neuburger, G. G.; Johnson, J.; Tang, A. P-C.; Yeo, I-H.; Baur, J. J. Chem. Soc., Faraday Trans. 1 1986, 82, 1081.

169. Johnson, D. C.; Polta, T. Z. Chromatogr. Forum submitted for publication.

170. Hughes, S. Ph. D. Dissertation, Iowa State University, Ames, IA, 1982.

171. de Boor, C. "A Practical Guide to Splines", Springer-Verlag, New York, 1978.

172. Martins, M. E.; Cordova, O.; Arvia, A. J. *Electrochim. Acta* 11, 26, 1547.

173. Frumkin, A. *Z. Physik. Chem.* 1925, 116, 466.

174. Tulyupa, F. M.; Zheltobryukh, L. P. *Ukr. Khim. Zhr.* 1976, 42, 72.

175. Tulyupa, F. M.; Usatenko, Yu. I.; Barkalov, V. S. *Izv. Vysshikh Uchebn. Zavedenii, Khim. i Khim. Tekhnol.* 1971, 14, 1200; *Chem. Abstr.* 1971, 75, 144356s.

176. Tulyupa, F. M.; Usatenko, Yu. I.; Barkalov, V. S. *Zh. Neorg. Khim.* 1968, 13, 3227; *Chem. Abstr.* 1969, 70, 61750m.

177. Tulyupa, F. M.; Zheltobryukh, L. P. *Koord. Khim.* 1977, 3, 59.

178. Tulyupa, F. M.; Zheltobryukh, L. P. *Deposited Doc.* 1975, 1933; *Chem. Abstr.* 1977, 87, 61963j.

179. Tulyupa, F. M.; Zheltobryukh, L. P. *Vopr. Khim. Khim. Tekhnol.* 1978, 52, 69; *Chem. Abstr.* 1979, 90, 211004a.

180. Tulyupa, F. M.; Usatenko, Yu. I.; Tkacheva, L. M. *Teor. Eksp. Khim.* 1969, 5, 403; *Chem. Abstr.* 1969, 71, 64873k.

181. Tulyupa, F. M.; Tkacheva, L. M.; Usatenko, Yu. I. *Ukr. Khim. Zh.* 1969, 35, 458; *Chem. Abstr.* 1969, 71, 85078v.

182. Baibarova, E. Ya.; Goncharenko, L. V.; Vergun, L. P.; Tulyupa, F. M. *Zh. Neorg. Khim.* 1982, 27, 3202; *Chem. Abstr.* 1983, 98, 41616x.

183. Tulyupa, F. M.; Usatenko, Yu. I.; Garus, Z. F. *Ukr. Khim. Zh.* 1970, 36, 1269; *Chem. Abstr.* 1971, 74, 150590j.

184. Tulyupa, F. M.; Tkacheva, L. M.; Usatenko, Yu. I. *Zh. Neorg. Khim.* 1968, 13, 2058; *Chem. Abstr.* 1968, 69, 60988r.

185. Tulyupa, F. M.; Usatenko, Yu. I.; Barkalov, V. S. *Zh. Anal. Khim.* 1968, 23, 1844; *Chem. Abstr.* 1969, 70, 61702x.

186. Tulyupa, F. M.; Barkalov, V. S.; Usatenko, Yu. I. *Khim. Tekhnol. (Kharkov)* 1971, 17, 166; *Chem. Abstr.* 1972, 76, 67830h.

187. Tulyupa, F. M.; Barkalov, V. S.; Usatenko, Yu. I. *Zh. Anal. Khim.* 1967, 22, 399; *Chem. Abstr.* 1967, 67, 39877z.

188. Tulyupa, F. M.; Usatenko, Yu. I.; Shvydka, L. F. *Zh. Neorg. Khim.* 1972, 17, 1411; *Chem. Abstr.* 1972, 77, 39796d.

189. Schremmer, J.; Noonen, D. *J. Med. Phys.*, to be submitted for publication.

XII. ACKNOWLEDGEMENTS

I would like to thank Dr. Dennis Johnson for his guidance and support throughout my graduate studies. His ability to motivate and give direction when "nothing worked" proved to be invaluble.

I also thank Dr. Glenn Luecke of the Mathematics Department at Iowa State University. Without his assistance, guidance and patience, the mathematical derivations presented in this work would not be nearly as precise or detailed.

The financial and instrumental support of the Dionex Corporation is gratefully recognized. In addition, I thank Theragenics Corporation for providing me with an interesting and practical application for PAD of sulfur compounds. I wish to specifically acknowledge Jacalyn Schremmer, who guided my research effort.

I wish to acknowledge the past and present members of the electrochemistry group for the exchange of ideas. A special thanks to Jodi Johnson for her time, patience, excellent experimental technique in collecting data and, most especially, her friendship.

I thank the chemistry faculty of the College of St. Benedict/St. John's University for providing enthusiasm and the desire to understand the world around us to all of its graduates.

My deepest gratitude is expressed to my parents, Mary and Lloyd Zieske. They taught me that it is possible to achieve anything with hard work and desire, and supported me in every way possible while I reached for my goal.

I thank John, my constant companion, for the loving support that only he can provide. Also I wish to acknowledge his skill as a typist, without which this document would not exist in its present form. And lastly, I wish to recognize Alex, who loved me only as "Mommy", no matter what else happened around us.

XIII. APPENDIX

The solution to Eq. 16 is derived here. The notation is simplified by letting $A = \Gamma_o k_1/k_{mt}$ and $B = k_1 C_A{}^b$ and Eq. 16 becomes

$$(1 + A)\dot{\theta}_A + (B + k_{-1} - A\dot{\theta}_A)\theta_A - B = 0 \qquad [A1]$$

or

$$(1 + A - A\theta_A)\dot{\theta}_A = B - (B + k_{-1})\theta_A \qquad [A2]$$

or

$$\int[(1 + A - A\theta_A)/[B - (B + K_{-1})\theta_A]]d\theta_A = \int dt + C_1 \qquad [A3]$$

where C_1 is a constant to be determined. To integrate the left side of Eq. A3, let $U = B - (B + k_{-1})\theta_A$, so that $\theta_A = (B-U)/(B + k_{-1})$ and $d\theta_A = -dU/B + k_{-1})$. Then

$$(1 + A - A\theta_A)/[B - (B + k_{-1})\theta_A]$$

$$= [1 + A - A(B - U)/(B + k_{-1})]/U \qquad [A4]$$

$$= \{[B + (1 + A)k_{-1}]/(B + k_{-1})\}/U + A/(B + k_{-1}) \qquad [A5]$$

Equation A3 becomes

$$-(B + k_{-1})^{-2}[\int(B + (1 + A)K_{-1})dU/U + \int AdU] = t + C_1 \qquad [A6]$$

Integration of Eq. A6 yields

$$[B + (1 + A)k_{-1}]\cdot\ln|U| + AU = -(B + k_{-1})^2(t + C_1) \qquad [A7]$$

To evaluate C_1, recall the initial condition for $\theta_A(t)$ in the adsorption region is $\theta_A(0) = 0$; therefore, $U = B$ and

$$C_1 = -[(B + (1 + A)k_{-1})\cdot\ln(B) + AB]/(B + k_{-1})^2 \qquad [A8]$$

Equations A7 and A8 are combined to give

$$\begin{aligned} &(B + (1 + A)k_{-1})\cdot\ln|U| + AU \\ &= -(B + k_{-1})^2\{t - [(B + (1 + A)k_{-1})\cdot\ln(B) + AB]/(B + k_{-1})^2\} \qquad [A9] \\ &= (B + (1 + A)k_{-1})\cdot\ln(B) + AB - (B + k_{-1})^2 t \qquad [A10] \end{aligned}$$

Remember that $U = B - (B + k_{-1})\theta_A$; thus,

$$\begin{aligned} &(B + (1 + A)k_{-1})\cdot\ln|B - (B + k_{-1})\theta_A| + AB - A(B + k_{-1})\theta_A \\ &\quad = (B + (1 + A)k_{-1})\cdot\ln(B) + AB - (B + k_{-1})^2 t \qquad [A11] \end{aligned}$$

Simplification and division by $(B + k_{-1})$ yields

$$\begin{aligned} &[1 + Ak_{-1}/(B + k_{-1})]\cdot\ln|1 - (1 + k_{-1}/B)\theta_A| - A\theta_A \\ &\qquad = -(B + k_{-1})t \qquad [A12] \end{aligned}$$

Recall that $A = \Gamma_o k_1/k_{mt}$ and $B = k_1 C_A{}^b$. Therefore, the exact solution to Eq. 16 is

$$\begin{aligned} &\{1+[k_1 k_{-1}\Gamma_o/k_{mt}(k_1 C_A{}^b+k_{-1})]\}\cdot\ln|1-[1+(k_{-1}/k_1 C_A{}^b)]\theta_A| \\ &\qquad\qquad -\Gamma_o k_1\theta_A/k_{mt} = -(k_1 C_A{}^b+k_{-1})t \qquad [17] \end{aligned}$$

It should be noted that k_{mt} is assumed to be constant in this derivation; hence, the diffusion layer is presumed to be of constant thickness for all values of t in Eq. 17.